Title
Neural substrates of the perceptual awareness of sound in the cerebral cortex

Author
DeCharms, R. Christopher

Publication Date
1998

Peer reviewed|Thesis/dissertation

Neural Substrates of the Perceptual Awareness of Sound in the Cerebral Cortex

by

R. Christopher deCharms

DISSERTATION

Submitted in partial satisfaction of the requirements for the degree of

DOCTOR OF PHILOSOPHY

in

Neuroscience

in the

GRADUATE DIVISION

of the

UNIVERSITY OF CALIFORNIA

San Francisco

This PhD dissertation is dedicated to my parents (all three), who have been dedicated to me for so long , and made it possible for this to come about.

Acknowledgments

I would like to acknowledge the help of many people who have provided education, help and support to me during the process of my graduate studies. Most importantly, I would like to thank my thesis advisor Dr. Michael M. Merzenich who has served as an outstanding mentor to me, and unparalleled source of inspiration, and a good man. In addition to his considerable scientific wisdom, Mike has shown me tremendous trust and support.

I would also like to thank the members of "the implant team", David Blake, Virginia deSa and Karen McLeod, for tireless help in the technical aspects of these experiments. They have given more long nights and dedicated work to this project than I can express here. I would also like to thank all of the previous workers who have conducted experiments setting the groundwork in this area, particularly Purvis Bedenbaugh and Ralph Beitel.

I would like to thank my thesis committee, chaired by Steve Lisberger and including Michael Stryker, Howard Fields and William Newsome (from Stanford). I would like to thank a number of scientific colleages including all members of the Keck Center for Integrative Studies and UCSF during my tenure there, but particularly Mike Kilgard, Henry Mahncke, Steve Rebscher, Christoph Schreiner, Russ Snyder, and Xiaoqin Wang,

Finally, I would like to thank my many teachers and friends and my family members who have supported me through this time in my life.

Abstract

In this dissertation, I present work investigating how the perceptual awareness of sounds is mediated by neural activity, focusing on how sounds are represented by the activity of neurons in the cerebral cortex. To understand how neural processes can mediate our ongoing perceptual experience, we must understand the coding scheme that the brain uses for representing external objects. This code is comprised of the activity of large populations of neurons, and this dissertation explores the coding of sounds by individual neurons and populations of neurons in the primary auditory cortex. The representational code makes use of the temporal relationships between activity from many different neurons. It is shown here that the relative timing of action potential activity from pairs of cortical neurons in the anesthetized animal carries ongoing information about long tonal stimuli, that this information is stimulus specific, that it is mapped, and that this relative timing information follows the time course of the stimulus even when the average firing rates of individual neurons do not. To explore how the awareness of sounds is represented in the awake animal, a new method was developed for simultaneously recording responses from populations of neurons to either sounds presented passively, or to sounds presented during performance of an active auditory discrimination task. This method has allowed an extensive characterization of the responses of neurons in the primary auditory cortex, particularly using stimuli which allow us to estimate the feature selectivity of a neuron in terms of its combined spectral and temporal selectivity (the spectrotemporal receptive field). Auditory cortical neurons are selective for precise sound feature patterns within their preferred frequency range, and can be driven to high rates of activity by stimuli designed to match these feature patterns.

Stephen G. Lisberger

Table of Contents

Chapter 1. A View of Cortical Neurophysiology

Reprinted with permission from Merzenich, M. M., & deCharms, R. C. (1996). Experience, change, and plasticity. *In* R. Llinas, & P. Churchland (Eds.), *The Mind-Brain Continuum*. Boston: MIT Press.

Introduction

We support the view that the mind is expressed in physical form as the brain, that it can in principle be studied to any level of detail, and that ultimately this study will lead to the solutions of many of its great unsolved mysteries. In this paper we would like to convey something of our vision of how this study program might unfold and what it might mean. Our view is that the nervous system and particularly the cerebral cortex is best understood in terms of ensembles of neurons that are used to represent the perceived world -- ensembles that are continually formed, reformed, and maintained by simple competitive rules operating on inputs throughout life and that function dynamically and in relation to one another, providing both the content and the context of our experiences. We believe that the rules that govern the changes in the brain that account for learning can be understood, and that these rules underlie the creation of cognitive functions, experiences, and human behaviors. We shall discuss several aspects of functional brain processes that have been little studied, and that are crucial to explore to relate brain mechanisms to cognitive functions and behaviors. Finally, we shall consider some aspects of what these principles mean for our limited understanding of the functioning of the mind in terms of the brain.

There are five themes that are largely missing from contemporary neurophysiology -- themes that most people would agree with at least in part, but which do not yet hold a central position in currently predominant views of functional brain operations, and in some cases have been almost entirely neglected. a) The cerebral cortex is always changing, so its most fundamental functions will only be fully understood by models and experiments that seek to explain how specific properties develop and maintain capacities over time, rather than by attempting to explain functions presumed to be innate and static. b) The cerebral cortex is not a passive machine that waits for inputs, but an ever-

active dynamic system that constructs and maintains our complex internal world. All perceptions, choices, actions, and representations take place against the backdrop of an internal context which is formed from past experience and is intrinsic to the system. c) A key element in cortical processing is temporal structure, meaning both the use of temporal information by the nervous system as a representational strategy, and the fact that most of the percepts and actions that we experience throughout life proceed moment by moment through time, as opposed to being discrete events. d) The cortex represents the world through the use of interconnected networks of neurons, or 'neuronal ensembles', and these ensembles can only be fully understood when observed as such, and not by observing individual neurons in isolation. e) Coding in the cortex is probably relational rather than strictly combinatorial, meaning that the system uses relations between elements and ensembles to establish reliable representations.

CORTICAL REPRESENTATIONS ARE CONSTANTLY CHANGING

It is now clear to all that the brain is malleable throughout life, but the implications of this have not yet permeated very deeply into experimental neuroscience. There is an artificial separation between 'plasticity studies', which show that cortical neurons have great capacities to perform different functions depending upon how a given cortical system has been created and shaped through use, and 'functional studies', which commonly explore what a particular element or region of the cortex 'does', usually ignoring the fact that what it does may be almost entirely determined by what it has been asked to do during its life history. Plasticity studies often do not take into account the specific roles of activity accounting for complex functions that the cortex is performing, while functional studies rarely take into account the complex evolution of the behavioral capabilities that are being assessed.

Many functional studies of cortical neurons assume or demand an artificial stasis of function so that change doesn't complicate the assessment of functional representation, then assess the function of one member of the population of responding neurons at a time, and draw conclusions about how the entire population might function. This is akin to trying to learn how a team of people function to perform a task without taking into account that some of the people may be professionals at the task and others newcomers, what effect prior experience and training of the team may have on the team

members' performance, or how the team as a whole can interact to complete the task even though the individuals could not do it alone. One common approach is to study functional representation in a cortical field without any direct behavioral assessment of the cortical area's capacities. This is akin to studying the performances of team members one at a time, with no knowledge of how any individuals or the team as a whole can actually perform the task, and with no knowledge of their prior experiences that might affect their performance at the task in any event. Another approach is to overtrain the team at the task until an asymptotic performance level is achieved. Overtraining in a strictly contextually controlled behavior creates a highly artificial picture of functional representation in any cortical area under study, reflecting circumstances that scarcely ever occur in real life.

Our general approach has been to try to control what prior practice our hypothetical team has had, comparing the performance of the individuals in a presumed naive state with that in a trained state, concluding that a given ability or function can be created and shaped by experience in the ways that the data show. We believe that the ideal approach, which has still not been accomplished in more than a limited sense, is to record the progress of many individuals and preferably much of the whole team simultaneously at various stages of practice, to try to figure out what they can do individually and as a team, and how they came to be able to do it through practice. We believe this will ultimately explain what cortical elements do in the context of how they came to be able to do it. Short of this approach, we will keep missing major elements of cortical function and plasticity.

THE CORTEX IS A DYNAMIC SYSTEM IN WHICH ALL REPRESENTATIONS OCCUR AGAINST A BACKDROP OF ON-GOING, INTERNALLY GENERATED CONTEXT

We all know that our perceptions, decisions, actions, and so on take place against a backdrop of what is going on in our minds at the time -- for example the extent to which we see what we are looking for while we ignore much of the rest of incoming information. The effects of what we have experienced and learned in the past are often expressed through these processes of attention and expectation. In a parallel fashion, the brain also operates with incoming and outgoing information existing within an ever-changing context of internal representations, which are rarely studied. Since there is a whole psychological literature dedicated to this subject(Desimone & Duncan, 1995; Desimone, Wessinger,

Thomas, & Schneider, 1990; Farah, 1989a; Farah, 1989b; Kinchla, 1992; Naatanen, 1988; Posner & Petersen, 1990; Shepard & Metzler, 1971), it is clearly worthy of our experimental time.

Traditionally this territory has been put off-limits by behaviorism, which said that mental states did not exist if they could not be perceived by an outside observer, and more recently by what we call "'neurobehaviorism", which similarly suggests that subjective mental phenomena are too hard to measure with current techniques, or even that they are impossible to measure, as the behaviorists thought. The studies that have begun to address this issue have already shown that this is not true(Benson & Hienz, 1978; Colby, 1991; Desimone & Duncan, 1995; Desimone et al., 1990; Farah, 1988; Farah, Peronnet, Gonon, & Giard, 1988; Fuster, 1973; Fuster, 1990; Goldberg & Wurtz, 1972; Haenny, Maunsell, & Schiller, 1988; Hsiao, DM, & Johnson, 1993; Hubel, Henson, Rupert, & Galambos, 1959; Motter, 1993; Posner & Petersen, 1990; Wurtz & Mohler, 1976), that there is no absolute barrier which prevents us from gaining significant insights into subjective mental phenomena, and that the techniques to continue this pursuit are already in hand. For example, if traditional experiments can systematically hold the behavioral context of an observer constant and present different stimuli, then parallel experiments can hold the stimuli constant while systematically changing the behavioral context, and thereby their meaning to the observer.

The internal context supplied by the nervous system includes such things as attention, expectancy, mental semblancy, planning, emotion and motivation, and it determines the qualities of our awareness of an object, our choices of how to act, and our actions themselves. It is our belief that object and context hold equally important causal roles that lead to perception and onward through action, that each is represented by ongoing activity patterns in the brain, that mentation can only be fully understood as the interaction of these two processes, and that the tools to begin to rigorously test this view are now available.

THE NERVOUS SYSTEM FUNCTIONS OVER TIME

Serial order is typical of the problems raised by cerebral activity... We can, perhaps, postpone the fatal day when we must face them, by saying that they are too complex for present analysis, but there is a danger here of constructing a false picture of those processes that we believe to be simpler.

-Karl Lashley, 1951(Lashley, 1960)

In the early 1950's, Lashley made a point that most everyone agreed with in principal, but that has still not been embraced by the field of neuroscience as a whole. He contended that a real understanding of the neural basis of the mind will depend critically on how neural processes take place in context *and through time*. He made these comments against the prevailing behaviorist winds of his time, which almost entirely ignored dynamic temporal questions such as motor control or language, or the context within which perception and action take place. He stressed that behavior is an ongoing process, not a discrete series of responses to isolated stimuli, and that it takes place against an ongoing background of activity. The neurobehaviorist version of this wind still blows, and it is that discrete, rapid onset stimuli produce the most robust neural firing rate responses -- in other words, that they are the observables -- and that these are therefore the most important types of phenomena for us to study. For whatever reasons, there has been very little exploration of how neural responses progress through time during perceptual streams. Even the most basic issues of representation in the time domain, such as how one stimulus conditions the cortical representation of a following stimulus, have yet to be systematically explored.

One of the central questions to be answered here is how streams of perception are held together through time and held separate from one another. Another is whether temporal coding is time-locked to external events and so can be averaged across instances or is commonly locked to internal events and so would be completely lost by averaging. We know there are powerful neural mechanisms for temporal smoothing, completion, and conditioning of responses across time, but their mechanistic origins are not yet clearly understood, and it has still to be determined how they can account for time-continuous percepts.

STIMULUS REPRESENTATION IS BY NEURONAL ENSEMBLES

Many convincing arguments contend that individual neurons in the cortex are not the units of representation: there are not enough of them to code stimuli individually (the grandmother cell argument); their activity patterns show broad tuning and maps of coordinated activity (the argument of

inadequate specificity); individual events, like percepts, activate cortical systems widely and focal lesions do not knock out focal functions but diminish overall performance (the distributed representation argument); cortical connectivity is sufficiently dense and synapses sufficiently weak that most cortical neurons probably cannot activate other neurons when they fire individually (the argument of weak connectivity); and so on. An assessment of these findings and our own cortical plasticity results lead to an obvious conclusion: the cortex needs to be investigated by measuring the neural structures that it creates and then uses for representation, distributed neuronal ensembles. Several classes of studies have already shown that important aspects of neural representation take place only through the combined actions or interactions of parts of neuronal ensembles, and are not understandable by the activities of the individual neurons alone(Abeles, Bergman, Margalit, & Vaadia, 1993; deCharms & Merzenich, 1996a; Vaadia, Haalman, Abeles, Bergman, Prut, Slovin, & Aertsen, 1995).

Further, representational ensembles clearly span cortical and subcortical systems, with objects represented simultaneously across broadly separated cortical areas. There have been only a few direct attempts thus far to learn about how single representations simultaneously span multiple brain areas, and no direct study of how dramatic plasticity can occur within these representations with the maintenance of appropriately associated linkages between them.

REPRESENTATIONS ARE IN PART RELATIONAL

There are a number of reasons to believe that an important aspect of neural representation consists of the relationships between neural elements and ensembles, rather than merely the combinations of population activities. We would like to make clear that by relational representation we mean something conceptually separate from ensemble representation, the combining of the activities of a large ensemble of neurons to generate a single representational construct. In principle, relational representation and combinatorial representation could even exist independently of one another, although in practice the two almost certainly operate together. We would like to stress that combinatorial processing does occur. However, we believe that a combinatorial view needs to be expanded in order to explain cortical representational operations and human perceptual capacities.

In a relational representation, information is carried in the relations between elements and ensembles. For a spatial metaphor of this, if all of the people in a football stadium hold up red and yellow cards to form a pattern that spells out the word 'MIND', then each person passes his or her card three people to the left and then all hold up their new cards, the same word is still be represented, although the individuals might all be doing something different than they had been. It is heuristically more useful to consider the information borne by the relations in the group, and not merely the combination of all the members' activities. For a temporal metaphor, imagine that all of the people in the crowd are clapping about 4 times per second. Now imagine that all of the people near the midline of the field continue clapping at the same rate but that all begin to clap in unison, or that each person claps just after the person to his or her left, so that there are moving waves of clapping and silence. Again, the activity of each individual and even the combined activity of the population do not adequately represent what is happening. What is going on might only be clear by a reconstruction of relationships. The representation of such an event certainly requires a population to take place, but it requires a relational reconstruction of that population to be understood.

We believe that relational coding must apply in a dynamically changing cortex because only the representational relations among a group of neural elements are isomorphic across changing patterns of activity and effective connectivity, and thereby can accomplish representational 'constancy' -- and because a relational schema is hypothetically a powerful one for creating novel complex representational combinations that have not been directly experienced or practiced. Neural representation is virtually certain to make use of the relations between elements of ensembles, for example, distributed temporal synchrony and other timing relations. These relations will only be understood when significant parts of ensembles are sampled together(Abeles et al., 1993; deCharms & Merzenich, 1996a; Vaadia et al., 1995). To understand the principles of network self-organization and learning and the distributed representations of learned stimuli and behaviors in general, we believe that we must use multiple-site recording methods that probe the instantaneous relations across and between engaged ensembles. In our view, while relational coding may indeed be involved in solving the binding

problem, a presently important idea, it is likely to have a fundamental role in all cortical representation, a role which goes well beyond the issue of how local features are grouped together into objects.

SUMMARY AND CONCLUDING REMARKS

These five themes suggest a study program of neurophysiology that we believe will have to be met, sooner or later, before a full understanding of cortical processing can be reached. They point to new areas of research that should bear easy fruit once they are addressed in earnest. This perspective in expanded form represents our attempt to put forward testable ideas of how experience and neural representation might be brought together into a unified and empirical understanding of awareness and action.

Functional activity and plasticity are inseparable, and can only be fully understood when explored together. Many current approaches treat these processes as largely autonomous, and conduct experiments accordingly. We believe that questions of change and of function are so closely related that they cannot be dissociated one from the other. Connectivity leads to activity and activity to connectivity. Fortunately, modern approaches are integrating these two questions more and more.

We believe that mind is the product of an environment expressed in the nervous system and manifested by it through actions; it is a circular and relational interaction between an incoming world, an experiential context, and outgoing activity. To a large extent we choose what our experience will be of, then we choose the details that we will pay attention to, then we choose how we will react based on our expectations, plans and feelings, and then we choose what we will do as a result. This element of choice, and the relational nature of awareness in general, have almost never been considered in neurophysiological experiments. We realize now that experience coupled with attention leads to physical change in the structure and future functioning of the nervous system. This leaves us with a clear physiological fact, a fact that is really just a mechanistic confirmation of what we already know experientially: moment by moment we choose and sculpt how our ever-changing minds will work -- we choose who we will be the next moment in a very real sense -- and these choices are left embossed in physical form on our material selves.

We have reached the point in experimental neuroscience at which we should bring this experiential aspect of our minds more directly into our studies of brain operations. We must begin to explore more specifically how the brain operates in real life, with fewer of the artificial behavioral restraints that are applied in almost all neurophysiological experiments, but rarely in our own human existence.

Chapter 2. Primary cortical representation of sounds by the coordination of action-potential timing

Reprinted, with permission, from deCharms, R. C., & Merzenich, M. M., "Primary cortical representation of sounds by the coordination of action-potential timing," Nature 381(1996): 610-3.

Primary cortical representation of sounds by the coordination of action-potential timing

R. Christopher deCharms & Michael M. Merzenich

Keck Center for Integrative Neuroscience, 828-HSE, University of California, San Francisco, California 94143, USA

Cortical population coding could in principle rely on either the mean rate of neuronal action potentials, or the relative timing of action potentials, or both. When a single sensory stimulus drives many neurons to fire at elevated rates, the spikes of these neurons become tightly synchronized[1,2], which could be involved in 'binding' together individual firing-rate feature representations into a unified object percept[3]. Here we demonstrate that the relative timing of cortical action potentials can signal stimulus features themselves, a function even more basic than feature grouping. Populations of neurons in the primary auditory cortex can coordinate the relative timing of their action potentials such that spikes occur closer together in time during continuous stimuli. In this way cortical neurons can signal stimuli even when their firing rates do not change. Population coding based on relative spike timing can systematically signal stimulus features, it is topographically mapped, and it follows the stimulus time course even where mean firing rate does not.

Although the timing[4–6] and correlations[7–10] of action potentials have been studied for over three decades, the fundamental logic of cortical population coding is still not understood. The firing rates of the majority of individual neurons in the primary auditory[11–13], somatosensory[14–19] and visual cortices[20–22] are changed most markedly only at the onset, offset, change or motion of a stimulus, and they typically habituate to nearer their background levels if the stimulus persists, with only a subgroup showing a markedly phasic–tonic profile. Further, it has recently been shown that sensorimotor neurons in the frontal cortex can change their relative timing during behaviour even when their mean firing rates are unchanged[23]. Are cortical neurons that fire at low rates uninvolved in signalling, or might they be signalling by some other mechanism at the level of the cortical population? Figure 1*f*,*g* shows the rate of individual action potentials recorded simultaneously from multiple neurons at each of two locations in the primary auditory cortex of an adult marmoset monkey, which were driven by a pure tone stimulus with the amplitude envelope shown in Fig. 1*e*, at a frequency appropriate to drive these two locations (4 kHz). Soon after the onset burst, the neurons returned to near their background firing rates, so the firing-rate response to a brief tone pulse (50 ms) was quite similar to that for an ongoing stimulus, although the two stimuli sound dramatically different.

The change in the pattern of relative timing between spikes from these same two locations during these stimuli is shown in Fig. 1*a*–*d*. We define the coordination of a population of neurons as the entire pattern of relative action-potential timing within that population, driven by both stimuli and internal dynamics, as this is the signal received by target populations. We define the coordinated rate of a single neuron or group of neurons as the rate of spikes that occur within a fixed time interval from a spike produced by a separate reference neuron or population of neurons. This is computed by making an average peristimulus time histogram of the rate of spikes from one location triggered on spikes from the other (Fig. 1*a*–*d*), and measuring the rate in a given bin. This measure reflects both relative timing and relative rate, which both affect postsynaptic targets. Each of the locations shown in Fig. 1 tended to fire more spikes that were close in time to a spike from the other location during the stimuli, even though the overall rate of spikes from each location was not increased, and the neurons were not phase locked to the stimulus (in cycle histograms, interval distributions, or shift predictors). In both cases, the change in coordinated rate was highly statistically significant ($P < 1 \times 10^{-5}$ for *b*, $P > 3 \times 10^{-4}$ for *c*; permutation test). As a control for changes in relative spike timing or short-term synaptic plasticity that might remain after a stimulus tran-

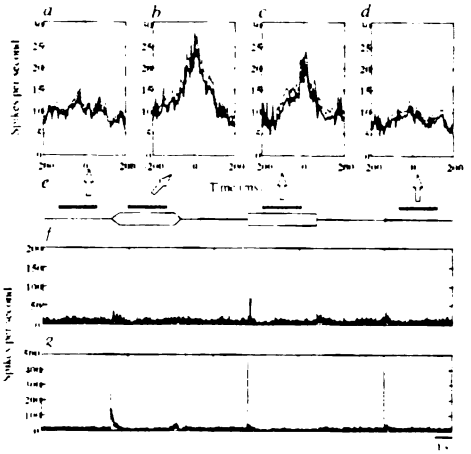

FIG. 1 Changes in mean firing rate and neuronal coordination in the primary auditory cortex during continuous pure-tone stimuli. A 4-kHz pure-tone stimulus with the amplitude envelope shown in *e* (maximum intensity 70 dB sound pressure level) was presented binaurally, during multisite neuronal recording. Histograms of mean neuronal firing rates for two cortical locations are shown in *f* and *g*, and average cross-correlations between the two locations are shown in *a*–*d*, all constructed from 100 repetitions of the stimulus sequence *a*–*d*. Rate of coordinated discharge (mean, thick line; mean plus standard error, thin lines) between the two locations *a*, during an initial silent period; *b*, during the 3-s constant phase of a ramped-onset pure tone; *c*, during the same 3-s constant phase of a rapid-onset pure tone; and *d*, during the silent period following the presentation of a 50-ms pure tone burst. *e*, Time periods for cross-correlation. The mean half-width at half-height of the central correlation peak in our sample was 11.2 ms; this example is particularly broad. Calculations excluded initial 500 ms after stimulus onsets, and were computed for individual trials by making a spike-triggered average of the action-potential rate from the lower cortical location triggered on each action potential from the upper location, using 5-ms bins.

METHODS. We recorded neurons from pairs of locations in the supragranular primary auditory cortex of 3 marmoset monkeys (anaesthetized using Nembutal), with electrode pairs separated by 75–1,000 μm. We used conventional sharp extracellular microelectrodes, standard electrophysiological amplification with filtering from 300 Hz to 10 kHz, computer storage of spike waveforms sampled at 20 kHz and computer spike sorting. Data are from neuronal signals that were thresholded and sorted to remove non-neuronal waveforms, giving spike times from 54 pairs of single units with well-differentiated action potentials throughout Fig. 2, and 369 pairs of multiunit groups, which consist of the times of all individual action-potential waveforms recorded from each location. Auditory stimuli were generated by a DSP chip and presented binaurally using a closed speaker system. Values of statistical significance of differences between cross-correlograms were derived by comparing the cross-correlation for individual trials (using 25-ms bins) at the typical (central) peak, and comparing the values at the zero-phase-shift bin between different conditions using the permutation test, a Monte Carlo simulation that does not assume normal distribution[24]. They were confirmed using the Mann–Whitney *U* test or joint peristimulus time histogram (JPST) analysis. Mean and s.e. values were derived from all trials, typically 100, and confidence limits were also computed using the point-wise bootstrap method[24]. We tested our results using the other normalization methods for correlograms: the raw number of coincidences, no normalization, or coincidences normalized by the autocorrelation of the spike trains interpolated to zero phase-shift.

sient, we measured the coordinated rate immediately after a brief tone pulse that mimicked the stimulus onset (shown in *d*), and found it to be unchanged. Cortical neurons can thus maintain signals about ongoing stimuli by temporally coordinating the few action potentials present even at low firing rates.

To compare the patterns of coordination found between distinct pairs of individual neurons and within larger neuronal populations, we simultaneously recorded multiple isolated single neurons, multiunit clusters, and local field potentials. The coordinated rate histogram between two single neurons during silence and during a stimulus is shown in Fig. 2*a*. There appeared to be a stimulus-induced change, but there were far too few coordinated spikes at these low firing rates to have sufficient statistical power to measure the effect; this was true of nearly all single unit pairs. A pair of single neurons that did show a statistically significant increase in coordinated rate during the stimulus is shown in Fig. 2*b*, but the effect was still comparatively weak ($P < 0.04$). When we measured the change in average coordinated rate between all of the action potentials taken from two very small groups of neurons (each group containing one of the neurons shown in Fig. 2*b* and one additional cell), we found that the effect was very similar in form but was much more robust ($P < 0.018$). When we added all of the action potentials measured from these same two locations that were above a fixed size, the effect was stronger still ($P < 0.005$). The coordination between one of these single neurons and the local field potential, a measure of the global activity of all surrounding neurons, also showed a similar profile and a significant change ($P < 0.01$). The coordination between nearby pairs of neurons are often similar in form, so their effects can therefore summate and become much more robust in large populations than in single pairs.

Figure 3*a*–*h* illustrates the frequency tuning of spike time coordination from groups of neurons at two cortical locations that had traditional onset burst tuning to frequencies between 2 and 6 kHz. Groups of neurons from different locations were typically somewhat coordinated even during silence (Fig. 3*a*). Following a brief and frequency-tuned coordinated burst at stimulus onset, the neurons showed an enduring frequency-tuned change in coordinated rate throughout the stimulus (Fig. 3*b*–*h*). The coordinated rate of action potentials was significantly increased by a 4-kHz stimulus ($P < 0.05$; Fig. 3*e*), but significantly decreased by a 6.35-kHz stimulus ($P < 0.01$; Fig. 3*g*). The coordinated rate can increase even in cases where the overall mean firing rate is decreased (Fig. 3*e*; firing rate less than background, $P < 0.0001$). Where firing rate and relative timing both change, the absolute number of coordinated events reflects both effects.

A particular sound increases the coordinated rate within a restricted and tonotopically mapped sector of the cortical surface (Fig. 3, bottom; the spatial positions of pairs of cortical locations that increased their coordinated rate during the stimulus are connected by red lines, and those that decreased are connected by blue lines). The population response to a 4-kHz tone at 70 dB is shown in Fig. 3*i*, demonstrating that within a discrete subregion of the auditory cortex (containing about 10^6 neurons[21]), cells from almost all locations maintain a temporally coordinated pattern of spike timing after a widespread coordinated onset burst; this region may also be decorrelated from surrounding regions. A similar spatial pattern of spike-time coordination is maintained during a stimulus of the same frequency but 30 dB lower intensity (Fig. 3*j*). A stimulus with a nearby but different frequency (2.52 kHz), sampled at fewer points, coordinated a distinct but partly overlapping region (Fig. 3*k*). The centre frequency of coordinated spike tuning versus spatial location for pairs of locations from which we collected full coordination tuning curves is shown in Fig. 3*l*. Coordination tuning forms an organized topographic map across the cortical surface, commensurate with the map for traditional onset burst tuning.

Neuronal coordination could also mimic the time course of the stimulus for locations at which the firing rate did not. Two locations are shown in Fig. 4*b*, *c* that did not have any statistically significant change in firing rate in response to a long tonal stimulus, not even transients (because the stimulus rose so slowly; Fig. 4*d*), but still showed a tonic time course of coordinated discharge rate (Fig. 4*a*) that lasted throughout the stimulus. Figure 4*f* shows the sum of all of the firing-rate histograms for this stimulus from the population mapped in Fig. 3. Most of these locations produced a transient discharge, and some also showed smaller sustained changes in firing rate, but the mean of the individual firing rates was unchanged during the constant phase of the stimulus. In contrast, the mean of the coordinated firing-rate profiles from all of the pairs (Fig. 4*e*) showed an increase that lasted throughout the stimulus (Fig. 4*g*). This suggests that a target

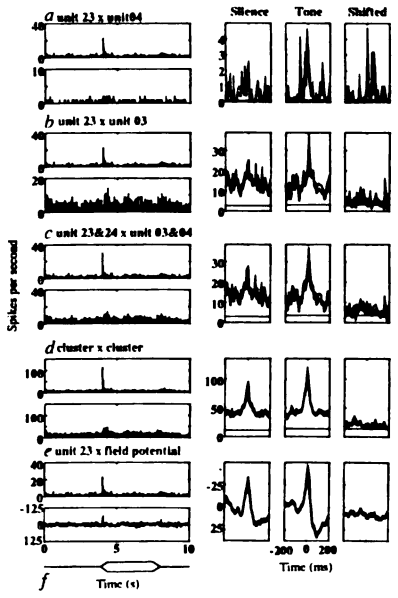

FIG. 2 Neuronal coordination is a population effect. Firing-rate responses from two locations (left: top, reference unit; bottom, target) and the coordination between the two (right) during the silence preceding a stimulus, and during the tonic phase of the stimulus. Far right, the 'shift predictor', a measure of the coordination between two locations that is locked to the timing of the stimulus, computed by making correlations between trial number *n* for the reference unit and trial *n* + 1 for the target unit. As we are interested in the total coordinated signal to a downstream target, whatever its source, we have not excluded stimulus-locked components using shift predictors of JPST analysis[29,30]. However, stimulus locking does not contribute to our measured correlation because we chose stimuli during which these neurons do not stimulus lock. None of the shift predictors showed significant stimulus-locked correlation. *a*, Two neurons that appear to increase their cross-correlation during a stimulus, but have too great a variability for the change to be reliably observed. *b*, Two neurons that did show a statistically significant change in cross-correlation due to the stimulus, but had little or no tonic change in firing rate. *c*, Correlation between two groups of well-isolated units, each comprising two neurons and including one of the units shown in *b*, which shows a very similar but more statistically robust effect. *d*, Correlation between two thresholded multiunit groups, which show a similar effect. *e*, Increase in correlation between a single unit and the local field potential recorded form an adjacent electrode (the voltage waveform filtered from 10 to 300 Hz to remove individual action potentials). *f*, Envelope of the presented 4-kHz, 70-dB stimulus. Field potentials are in μV. Mean, thick line; mean plus s.e., thin line.

location which samples across a broad and non-homogeneous population of neurons that are firing on average near background rate can nonetheless extract the time course of an ongoing stimulus by using temporal coincidence information from that population.

Coordinated relative spike timing could in principle be created by mechanisms of recurrent neural circuitry, by divergent temporal input to many neurons from a common internal source (possibly the thalamus in this case), or by divergent temporal input from a common external stimulus. All of these sources contribute to the signal received by a postsynaptic cell. Because neurons are temporal integrators, the synchronization and temporal pattern of

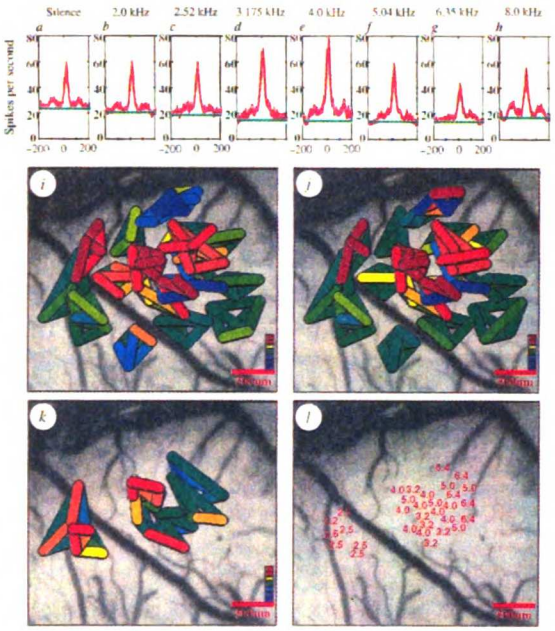

FIG. 3 Neuronal coordination is stimulus specific, and can be either increased or decreased relative to background by particular stimuli. *a–h*, Changes in cross-correlation between two locations during silence or 4-s, 70-dB, continuous pure-tone stimuli at different frequencies; mean, thick line; mean plus s.e., thin line. The green lines indicate the mean target-location firing rate during each period. All cross-correlations were computed (as described for Fig. 1) during the tonic phase of the stimulus, excluding onset and offset transient responses. Of 48 pairs of locations for which we constructed full coordination tuning curves using multiple stimuli, 90% showed a stimulus-dependent and frequency-tuned change in coordinated rate ($P < 0.05$ permutation test on central 25-ms bin: of these, 64% tuned increase, 15% tuned increase with surround decrease, 21% tuned decrease), and 10% showed no change. In every case the frequency tuning of ongoing spike coordination was commensurate with that observed for onset bursts, and in some cases was accompanied by changes in firing rate. Of 197 pairs for which we presented only a single stimulus frequency of 4 kHz, which was not the tuned frequency for some neurons, 39.3% showed a significant change in coordinated rate ($P < 0.05$, permutation test). Changes in neuronal coordination also generate an organized topographic map of sound frequency across the cortical surface. We recorded 96 locations in the primary auditory cortex of one monkey in groups of four, each group yielding six measures of cross-correlation, plotted as lines between the corresponding surface locations in *i–k*, with surface vasculature shown for spatial reference. Increases in coordinated rate during the stimulus are shown in red, decreases in blue. *i*, Cortical area that responded with a change in sustained coordination to a 4-kHz tone at 70 kB; *j*, responses of the same locations during presentation of the same tone at 40 dB; *k*, responses of a smaller number of locations during a 2.52-kHz tone at 40 dB; *l*, centre frequency of tonic phase coordinated discharge rate tuning for pairs of locations where a full tuning curve was computed, plotted near the midpoint of the line joining the two locations. Changes in coordination in *i–k* are plotted as the change in coordinated spike rate driven by the stimulus, divided by the background coordinated spike rate, $(C_{stim} - C_{back})/C_{back}$, with the order of overlaying of lines reflecting the magnitude of this index. The colour bar corresponds to index values of <-1, -1, -0.5, 0.05, 1, >1 from blue to red.

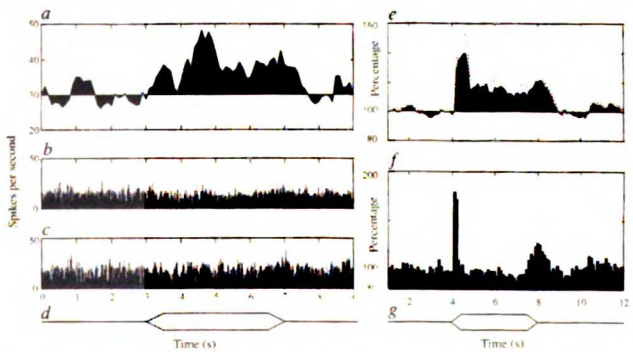

FIG. 4 Cortical sensory neurons can represent a stimulus and its time course through their coordination without any change in mean firing rate. *a*, Time course of the mean coordinated rate in a 500-ms time window ending at the time plotted; *b*, *c*, histograms (binned to 5 ms) of the evoked firing rates of the neurons at the two cortical locations summed over 100 stimulus presentations; *d*, time course of the stimulus envelope of the 4-kHz, 70-dB tonal stimulus. The coordinated spike rate was computed by calculating the average rate of target-location spikes in a 25-ms bin centred on all reference location spikes during a 500-ms segment of the trial (using the spike-triggered average method as before). Subsequent points in *a* are shifted by 100 ms, leading to 5 × 'oversampling', and shading is centred around the background period mean. The time courses of firing rate and coordinated firing rate were computed for all pairs of locations for this stimulus, and each was normalized to its own background rate. *e*, Mean plus standard error of all coordinated spike-rate time courses, each expressed as a percentage of its own baseline rate. The dotted line indicates the mean plus standard error of all of the curves. *f*, Average of all of the individual firing rates for the same locations, also expressed as a percentage of baseline rate and binned a 100 ms. The population mean of the coordinated discharge rate remains elevated throughout the time course of a long stimulus (in *g*), while the population mean of individual firing rates marks only the stimulus transients.

inputs arriving at a target cell can, in principle, be used to increase or decrease its output according to basic properties of synaptic integration[24–26]. At stimulus transients, spikes are necessarily coordinated, so population firing rate and coordinated firing rate reflect essentially the same phenomenon, and these two sides of population signalling presumably work together to provide robust cortical signals in many circumstances. Our results demonstrate that the relative spike timing of cortical action potentials may be a fundamental mechanism for signalling basic object features, one that goes well beyond neuronal grouping. They suggest that a basic cortical signal may be the number of temporally coordinated action potentials in a large neuronal population, which could converge to drive target neurons. Our data can also be understood as a reflection of the temporal patterns of activity that evolve moment by moment in cortical circuitry.

Note added in proof: We have recently observed similar phenomena both in the awake animal and in the primary somatosensory cortex. □

Received 5 September 1995; accepted 16 April 1996.

1. Gray, C. M., Konig, P., Engel, A. K. & Singer, W. *Nature* **338,** 334–337 (1989).
2. Singer, W. & Gray, C. M. A. *Rev. Neurosci.* **18,** 555–586 (1995).
3. von der Malsburg, C. Internal report, Max Planck Institute for Biophysical Chemistry, Gottingen, Germany (1981).
4. Adrian, E. D. *Electroenceph. clin. Neurophysiol.* **2,** 377–388 (1950).
5. Perkel, D. H., Gerstein, G. L. & Moore, L. *Biophys. J.* **7,** 391–418 (1967).
6. Middlebrooks, J. C., Clock, A. E., Xu, L. & Green, D. M. *Science* **264,** 842–844 (1994).
7. Abeles, M., Bergman, H., Margalit, E. & Vaadia, E. *J. Neurophysiol.* **70,** 1629–1638 (1993).
8. Abeles, M. *Corticonics: Neural Circuits of the Cerebral Cortex* (Cambridge Univ. Press, New York, 1991).
9. Dickson, J. W. & Gerstein, G. L. *J. Neurophysiol.* **37,** 1239–1261 (1974).
10. Eggermont, J. J. *J. Neurophysiol.* **73,** 246–270 (1994).
11. Ts'o, D. Y., Gilbert, C. D. & Wiesel, T. N. *J. Neurosci.* **6**(4), 1160–1170 (1986).
12. Ahissar, M. *et al. J. Neurophysiol.* **67,** 203–215 (1992).
13. Nicolelis, M. A. L., Baccala, L. A., Lin, R. C. S. & Chapin, J. K. *Science* **268,** 1353–1358 (1995).
14. Brugge, J. F. & Merzenich, M. M. *J. Neurophysiol.* **36,** 1138–1158 (1973).
15. Creutzfeldt, O., Hellweg, F. C. & Schreiner, C. *Expl Brain Res.* **39,** 87–104 (1980).
16. Pfingst, B. E. & O'Connor, T. A. *J. Neurophysiol.* **45,** 16–34 (1981).
17. Mountcastle, V. B., Davies, P. W. & Berman, A. L. *J. Neurophysiol.* **20,** 374–407 (1957).
18. Mountcastle, V. B. *J. Neurophysiol.* **20,** 408–434 (1957).
19. Mountcastle, V. B., Talbot, W. H., Sakata, H. & Hyvarinen, J. *J. Neurophysiol.* **32,** 452–484 (1969).
20. Hubel, D. H. & Wiesel, T. N. *J. Physiol. Lond.* **160,** 106–154 (1962).
21. Maunsell, J. H. R. & Gibson, J. R. N. *J. Neurophysiol.* **60,** 1332–1344 (1992).
22. Vaadia, E. *et al. Nature* **373,** 515–518 (1995).
23. Gabbott, P. L. A. & Stewart, M. G. *Neuroscience* **21,** 833–845 (1987).
24. Grannam, E. R., Kleinfeld, D. & Sompolinsky, H. *Neural. Computat.* **5,** 550–569 (1993).
25. Murthy, V. N. & Fetz, E. E. *Neural Comput.* **6,** 1111–1126 (1994).
26. Bernander, O., Koch, C. & Usher, M. *Neural Computat.* **6,** 622–641 (1994).
27. Lehmann, E. L. *Nonparametrics: Statistical Methods Based on Ranks* (Holden-Day, San Francisco 1975).
28. Efron, B. *The Jackknife, The Bootstrap, and Other Resampling Plans* 75–87 (Society for Industrial and Applied Mathematics, Philadelphia, 1982).
29. Perkel, D. H., Gerstein, G. L. & Moore, G. P. *Biophys. J.* **7,** 419–440 (1967).
30. Aertsen, A. M., Gerstein, G. L., Habib, M. K. & Palm, G. *J. Neurophysiol* **61,** 900–917 (1989).

ACKNOWLEDGEMENTS. We thank M. Fong, X. Wang, P. Bedenbaugh and D. Buonomano for technical and experimental assistance; E. Ahissar, W. Bialek, D. Ferster, D. Kleinfeld, W. Newsome, W. Singer and others for comments on the manuscript; and K. Parker and J. Stevens for outstanding scientific training. This work was supported by the NIH and by an NSF graduate fellowship to C.d.C.

CORRESPONDENCE and requests for materials should be addressed to M.M.M. (e-mail: merz@phy.ucsf.edu).

The cover art appearing on this article has been enhanced from the original by including a high resolution digital image that was not previously available.

Chapter 3: Design, Fabrication, and Implantation of a 49 Electrode Chronic Neuronal Recording Array

ABSTRACT

To simultaneously record neurons from many densely sampled locations in the auditory cortex of the awake, behaving primate, producing the minimum of tissue damage and allowing the best possible individual neuronal recordings, we designed and built a device that allows the individual placement and positioning of 48 fine, metal microelectrodes, with 350 micron center-to-center spacing. A recording chamber carrying the electrode array is mounted to the skull. A high-pressure seal was employed to hermetically seal this skull perforation to prevent the entry of pathogens. Recording electrodes were ultra-thin, etched Iridium probes, coated with paralene-C, and ending in a 5-15micron long sharp tip which was anodized with an ultramicroscopic layer of iridium oxide. This procedure substantially lowered electrode impedences while maintaining original tip size and recording volume, resulting in very low noise recordings with excellent neuron isolation. Electrodes make frictional contact with individual guide tubes which are soldered to a printed circuit board that connects each electrode to one contact of a 51 pin micro connector. The 45 electrode and 4 ground outputs of this connector are attached to the inputs of high input impedence voltage follower JFTs, that are attached to the device during recording. These JFTs are connected in turn to a custom-built 48 channel amplifier system, and ultimately to second stage amplifiers, filters, and digitization hardware. The device is made from lightweight, biocompatible materials, weighing only 14 grams in its entirety, making it suitable for use on species as small as rats, marmoset monkeys and owl monkeys. The device is completely reusable.

INTRODUCTION

For many years, it has been clear that it would be very desirable to be able to record simultaneously from a large number of neurons in the cerebral cortex simultaneously, but the technology to accomplish

this adequately has been lacking. For this reason, the great majority of work on cortical neurons has focused on recordings of responses from individual neurons, which provides limited information about the relationships between the activity of different cells, and is a comparatively time-intensive method for data acquisition.

There have been a number of attempts to develop multi-channel cortical recording arrays, that have met with varying degrees of success(Bach & Kruger, 1986; Buzsaki, Horvath, Urioste, Hetke, & Wise, 1992; Gray, Maldonado, Wilson, & McNaughton, 1995; Jones, Campbell, & Normann, 1992; Kruger & Bach, 1981; Najafi & Hetke, 1990; Najafi, Ji, & Wise, 1990; Nicolelis, Baccala, Lin, & Chapin, 1995; Nicolelis, Ghazanfar, Faggin, Votaw, & Oliveira, 1997; Nicolelis, Lin, Woodward, & Chapin, 1993; Rousche & Normann, 1992; Wilson & McNaughton, 1993; Wilson & McNaughton, 1994). Existing methods suffer a number of difficulties, particularly relating to the quality of recording that has been achieved, the tissue damage that is caused by the recording device, and the ability to accurately, individually position the electrodes spatially. The method described here allows for the best possible combination of recording characteristics with a dense, penetrating array of electrodes designed to minimize tissue damage. Each electrode is individually placed and precisely spatially localized. Decades of neurophysiological research in many laboratories have shown that sharp, fine extracellular electrodes produce by far the best recording characteristics, and iridium oxide coated electrodes provide the best known single neuron recording characteristics among these(Loeb, Peck, & Martyniuk, 1995). Iridium is the stiffest of the practically utilizable noble metals, and using an ultrafine shank linearly tapered over 2 millimeters and a 3 micron coating of the insulation polymer paralene-c, these electrodes penetrate the dura and pia arachnoid while producing the minimum of local tissue damage. This device also allows for the positioning of electrodes only in locations that do not compromise the cortical vasculature. By contrast, other high density recording methods do not allow the sparing of the extensive network of surface cortical vessels. Finally, this recording device is sufficiently light-weight that it can be used successfully in small species such as the rat or marmoset monkey, mammals with a total body weight of less than 400 grams.

METHODS

Overview of Implant Function

Mounting

An overview of the implant is presented in figure 3.1. The recording array is mounted to the skull as a central appliance loaded in a small, round, titanium chamber. This cylindrical chamber is connected to the skull using slotted screws and methyl-methacrylate adhesive. The remainder of the device casing is connected to this skull-mounted chamber by several small screws. The device casing includes an outer protective shell with cover, and an electrode guide tube appliance that can be advanced down into the base cylinder. This inner guide tube appliance can be advanced up to 2mm within the outer casing by four perimeter screws. The electrode guide tubes fill the body of this structure; a printed circuit board is mounted on top of it. This guide tube appliance serves as a 'plunger' to pressurize a polysulfone/silastic 'sandwich' below it, through which the recording electrodes pass. When the polysulfone layer is brought under high pressure, it hermetically seals the path through the device along the chamber walls, and seals the paths of the 49 penetrating electrodes.

Electrode Path

Each recording electrode enters into a stainless steel guide tube at the top of the device, passes down through a metal guide tube, passes through a channel in a sealing layer of silastic rubber, passes through a hole the polysulfone wafer on the bottom of the device, and then passes down into the brain. The electrode is not fastened at any point along this length, but is held rigidly in place by the friction of the sealing silastic layer. With the sandwich depressurized, electrodes can be individually advanced or withdrawn using a single hydraulic microdrive. The electrodes make frictional contact with their individual guide tubes through their length.

Electrical Connectivity

Electrical connectivity is achieved by kinking the uninsulated shanks of the electrodes to ensure good frictional contact with the guide tubes. The guide tubes are then soldered to the printed circuit board on top of the guide tube appliance, which in turn establishes connections to JFT voltage followers and

external amplifiers. The electrodes are insulated with Paralene-C from above the point that they exit from the guide tubes to within about 5-15 microns of their tips within the brain.

Seal

The device is ultimately sealed by using the guide tube appliance to compress the silastic layer against the bottom (polysulfone) plate of the device, which rests upon a lip at the bottom of the titanium chamber. The silastic layer pressure level is adjusted using the screws which hold the guide tube appliance within the casing, with the casing in turn connected to the titanium chamber. The silastic is therefore compressed over a very small compression distance to a very high pressure, and an effective and reliable hermetic seal is formed around each electrode shank, and against the inside wall of the Titanium chamber.

Implant Hardware

Design schematics for implant parts are shown in figures 3.1- 3.5. The titanium chamber and casing parts are made from lightweight, biocompatible materials, including Ultem, a biocompatible plastic, and tianium, as described on schematics.

Implant Assembly

All assembly stages beyond the fabrication of the parts are conducted in a microparticulate-free clean room. This both ensures ultimate biocompatibility and prevents blockage of the microscopic channels in the device with small particulate matter.

Guide Tubes, Printed Circuit Board

Guide tubes are made from 220um diameter thin-walled stainless steel tubing with 110 micron inner diameter (K-Tube, San Diego, CA 619-453-0052). This tubing is cut to approximately 40mm length, de-burred with a diamond hone, and gold plated inside and out using Orotemp 24 plating solution (Technic Inc., Cranston, RI). Guide tubes are inserted into matching holes cut on 350 micron center-to-center spacing into an ultem disk with a pattern exactly matching that of the polysulfone plate of the poslysulfone/silastic sandwich. Guide tube ends extend 500microns through this ultem disk and into the silastic layer. This disk is cemented into a retaining ring that fits into the bottom of the guide tube appliance.

The guide tubes are then each cut to a different length, by row and column, so that they can easily be fed into the matching holes in the printed circuit board, after they pass as a group through the pressure tube. With all guide tubes passing through their appropriate holes in the circuit board, the guide tubes are cemented into the pressure tube using Epoxy resin, and the circuit board is attached to the top of the pressure tube with its mounting screws. The guide tubes are cut to protrude about 4mm above the circuit board; each one is soldered into place on the circuit board. Since these tubes are stainless steel and do not solder adequately on this size scale, fine gauge wires are inserted into the via hole before soldering to ensure the establishment of good electrical contact. Finally, guide tube ends are filed to within 500microns of the circuit board top, and the tubes cleaned of any fine particulate matter using 100micron Tungsten wire.

Silastic Sandwich

The 100 micron holes in the polysulfone plate are de-burred with a diamond hone. They are opened further using the sharp tip of ultrafine forceps. The polysulfone plate is then placed against the bottom of the pressure tube, with its holes matching the holes of the corresponding guide tubes, and 100 micron tungsten blanks are inserted through the plate and into the guide tubes. The plate is pulled away from the bottom of the pressure tube, taking care to maintain the electrodes parallel. Silastic (Med4210, NuSil Inc., 805-684-8780) is made up according to manufacturers instructions, vacuum-centrifuged to remove dissolved gases, and pressure-injected into a cylindrical mold holding the pressure tube and polysulfone plate so that it forms a cylindrical layer between them, surrounding all of the electrode blanks, and free from air cavities or bubbles. This structure is cured at 60 degrees C for 4-6 hours. After removing the joined part from the mold and cutting away excess material, the tungsten blanks are removed, and each hole is again cleared of any debris with a 100micron Tungsten wire, first from the bottom, then from the top.

Electrodes and Electrode Insertion

Electrodes are 75 micron pure Iridium wires, linearly tapered to a sharp point over the last 2 mm of their length by electrolytic etching (Microprobe, Inc, 301 972-7100). Electrodes are insulated with a 3 micron coating of Paralene-C, then tips formed by a current arc, to produce a desired impedence and

uninsulated region(Loeb et al., 1995). Electrode tips are 'activated' using cyclic voltammetry. Electrodes with a starting impedence of 2-5MOhm, with a tip size of 5-15 microns, yield a final impedence of 20-200KOhm after the deposition of a complex oxide layer on the surface and identical tip size and shape.

Electrodes are inserted through the top of the device using a micromanipulator under manual or automatic control under a binocular microscope. After inserting the electrode tip and about 6 mm of the electrode shaft into the top of the guide tube, the remainder of the electrode is de-insulated by burning off the Paralene-C coating using an adjustable electrocautery. The uninsulated electrode shaft is then kinked in a number of locations to ensure good frictional contact with the inner surface of the guide tube. The electrode is inserted down just through the bottom of the polysulfone plate under visual guidance, and cut to length 4 mm above the surface of the printed circuit board using an 18 gauge tube cut to this length, which serves as a spacer and supports surgical scissors at the correct height, which then make the precise cut. The four corner locations are ground electrodes, and are de-insulated for their entire length, and coated with poly-L-Lysine to promote tissue adhesion to the electrodes and thus recording stability.

Surgical Procedure

The entire device is autoclaved prior to surgery, and electrodes should be activated under sterile conditions immediately preceding implantation. Surgery is conducted using standard sterile procedures and anesthesia. Monkeys were anesthetized at a deep surgical level using Sodium Pentobarbital anesthesia. Other anesthetics, including isofluorane, were found to interfere with recording.

After exposing the cranial surface, initial recordings using single glass-coated Tungsten microelectrodes and standard electrophysiological techniques were made through small burr holes in the skull sited stereotaxically over the area of interest, to accurately site the chronic recording device chamber. When the location of the area of interest was confirmed, a precisely cut 9mm circular skull penetration with three slots radiating out at 120 degree angles was made. The cortical vasculature was photographed, and a siting device with the same pattern as the bottom plate of the device was used that accurately positions where the electrodes will lie with respect to cortical vessels. This insures that the blood supply is not compromised and prevents sub-dural bleeding. The device is inserted flush against

the dura mater, and held in place using Titanium slotted screws in the skull slots which fit into the flanges on the chamber sides. Additional mechanical support for the implant is provided by small skull screws surrounding the device at about 3 mm from the outer edge, and finally by methyl-methacrylate bone cement. After suturing the skin opening closed and photographing the cortical vasculature, the electrode carrying appliance is inserted into the chamber, and sealed.

In a second surgical procedure no more than two or three days after the first (to minimize the impact of dural thickening), under light anesthesia, after loosening the Silastic seal, electrodes were individually inserted through the dura during recording using a hydraulic microdrive (Kopf Instruments) mounted on a micromanipulator on a stereotaxic frame (Narashige, Japan). After all electrodes had entered the dura, the sandwich was again pressurized, and individual electrodes advanced to the desired depth while monitoring neuronal response signals with appropriate stimuli.

RESULTS

Recording Quality and Stability

This method has been successfully employed to record from the primary auditory cortex of several adult new world monkeys, achieving isolated single neuron recordings, and recordings that show well defined action-potentials that cannot be resolved from one another (multiple-unit recordings). Recordings is typically very stable within sessions, but different neurons are often recorded on successive days. This is clear from changes in action-potential waveforms, which are occasionally constant across days but more often variable. For example, in many instances we have observed clearly isolated single units one day, no clear spikes the next, and well isolated spikes again the following day. Examples of some well-isolated action potentials recorded with this device are shown in figure 3.6. Using oxidized Iridium electrodes, recording quality can rival any other cortical recording method presently available, acute or chronic. Unfortunately, the yield of electrodes per implant has been lower than we had anticipated. Thus far, we have been able to record good quality signals from a maximum of slightly less than half of our 45 implanted channels in each monkey on any given recording day.

After repositioning, the active channels can change. We hypothesize that the inability to record from a larger percentage of channels thus far is primarily due to the difficulty of adequately positioning all of the electrodes at the same time.

Recording Longevity

Several animals have been studied using this device, each for a period of several months. Using slotted screws and additional supporting skull screws, implants were very stably attached to the skull. The animals have at times exerted considerable torque against these devices, either by impact with the side of a cage or by pulling the device against parts of our behavioral training apparatus. The device appears to be very robustly protected against these forces.

Discussion

A method for the simultaneous recording of a large number of neurons from the cerebral cortex of the awake animal has been described. This technique has several notable advantages over existing methods.

Electrode Placement

Using this device, it is possible to record from each electrode individually while it is being introduced into the cortical tissue. This makes it possible to optimize the recording position of the electrode, as well as to individually select the recording depth of different electrodes. During the implantation procedure the cortical vasculature was visualized and photographed, and electrodes were positioned to insure that the local cortical blood supply was not compromised.

A principle limitation of this method is that the exact position of the cortical surface with respect to the base of the device was not determinable. While the relative depths of electrodes can be known precisely, the depth with respect to the pial surface must be estimated from physiological measures. In practice, there was a pattern of activity consistent across electrodes after penetrating the dura, with strong responsiveness in the middle cortical layers. These physiological responses properties

allow the electrode tips to be placed with respect to the pial surface to an accuracy of only about 300-500 microns, within the upper, middle, or lower cortical layers.

Recording Quality

Outstanding signal to noise ratios have been acheived with this device, often 3:1 or better and more than 10:1 in many examples. These recordings rival those obtained with acutely placed single electrodes.

General Utility of the Method

Once a monkey was implanted using this method, we are able to bring the animal to our electrophysiological recording laboratory, plug in our hardware, begin the behavior or stimulus delivery, and start recording action potentials from multiple channels almost immediately, typically in less than ten minutes total. It is possible to record simultaneously from a large number of neurons, and thereby perform a large number of experiments very efficiently. In addition, data about the relationships among populations of neurons that are precisely spatially localized across the cortical surface can be easily reconstructed. This method has led to a dramatic advance in our ability to record data from the awake animal, and in our ability to analyze the activity of large neuronal populations.

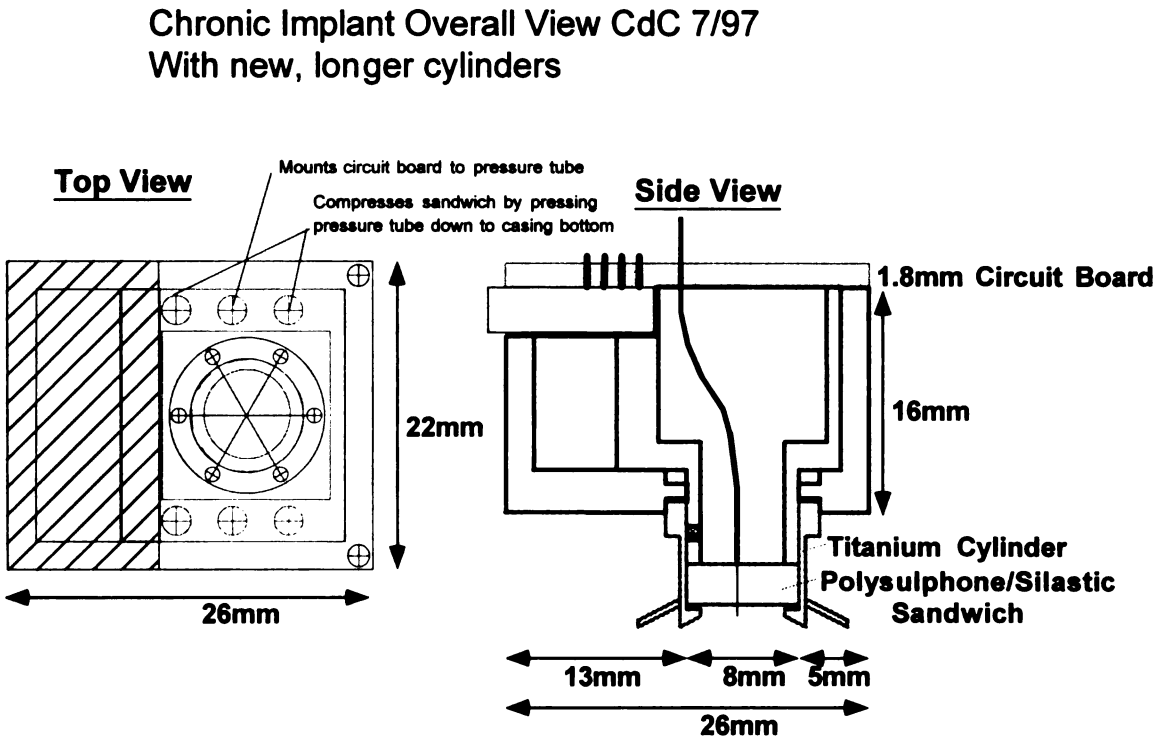

Figure 3.1: Overview schematic of chronic neuronal recording array.

Chronic Implant Casing Design v1.5 CdC 7/97
This version built to fit the new, longer cylinders

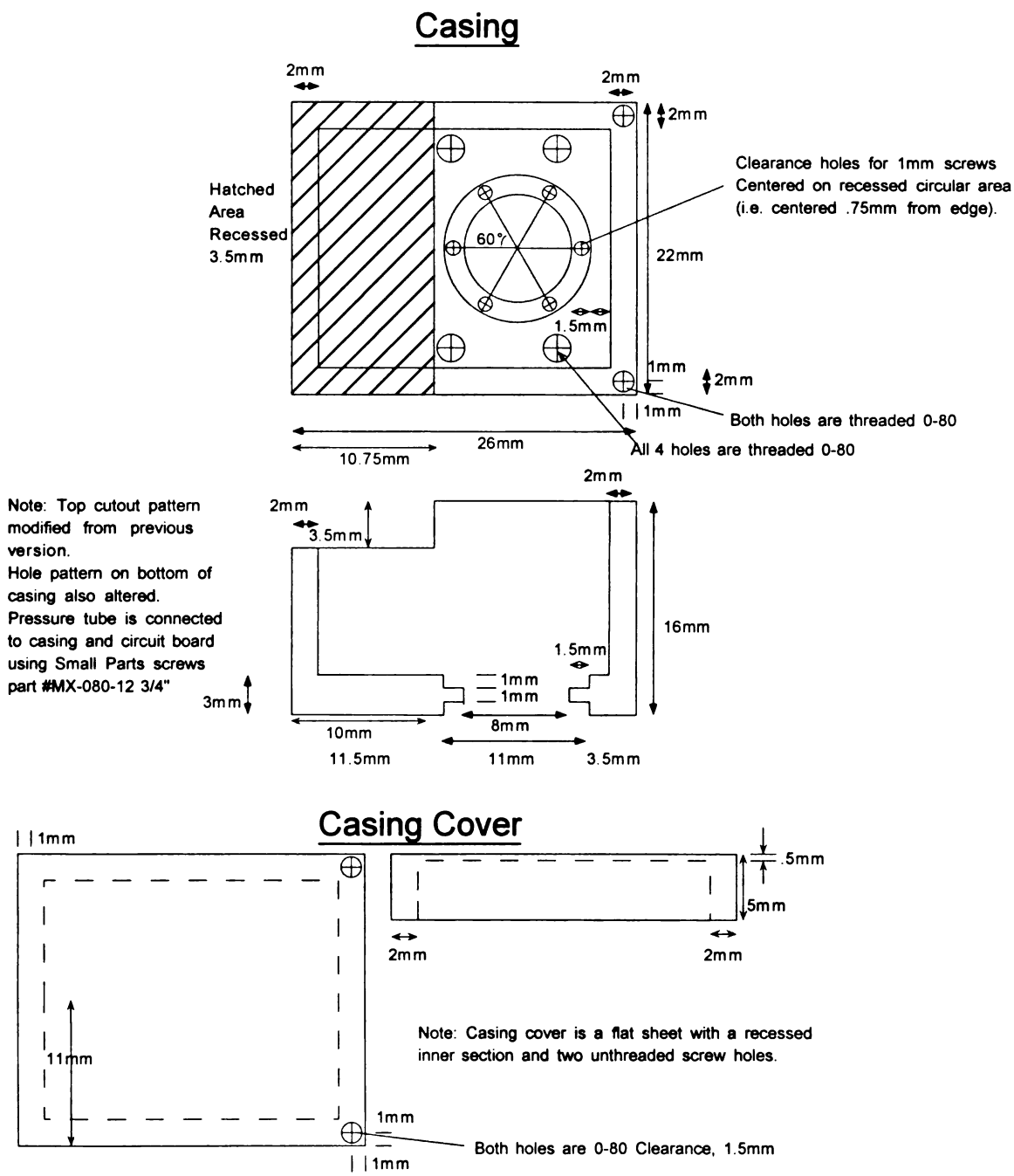

Figure 3.2: Schematic of implant casing and cover, made of Ultem biocompatible plastic.

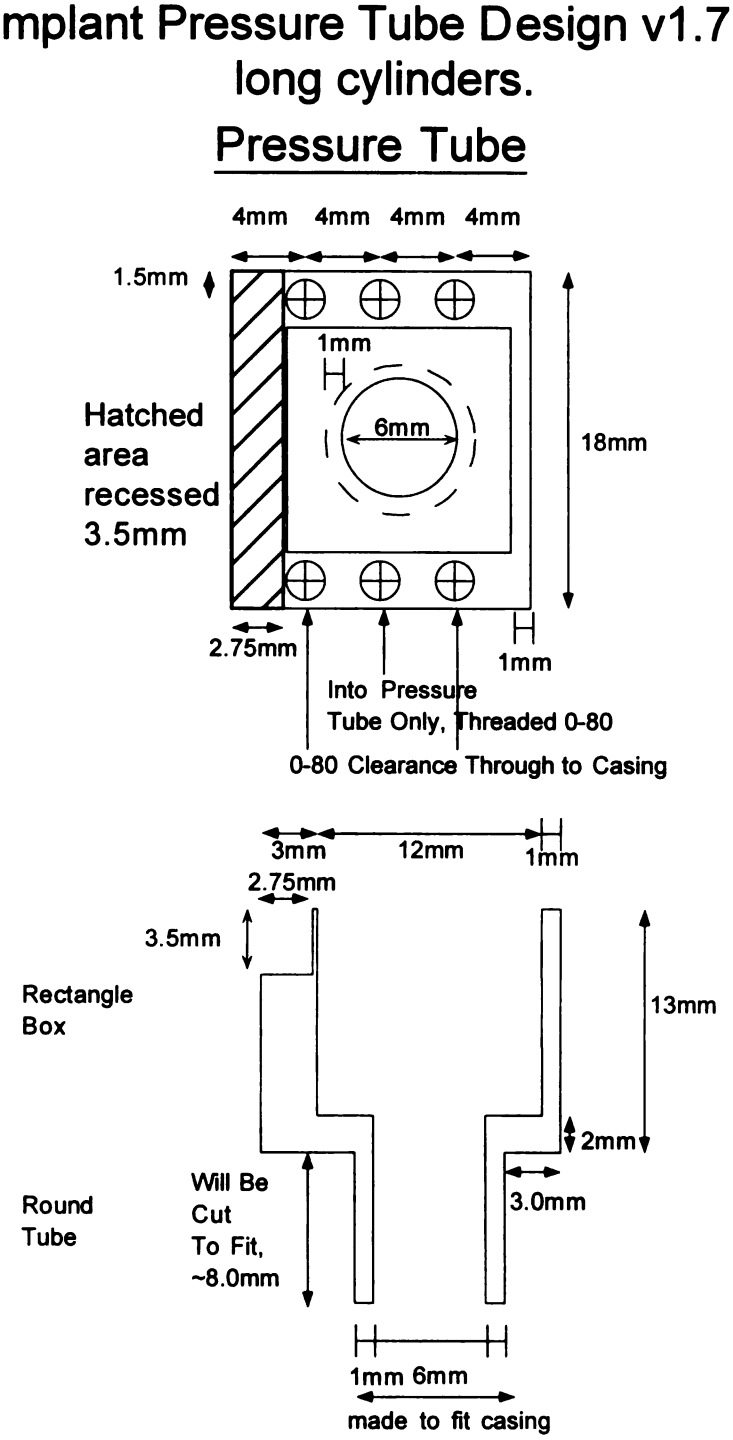

Figure 3.3: Schematic of implant pressure tube.

Chronic Implant Titanium Cylinder Design v1.5 CdC 7/97 and Polysulfone/Silastic Sandwich Design

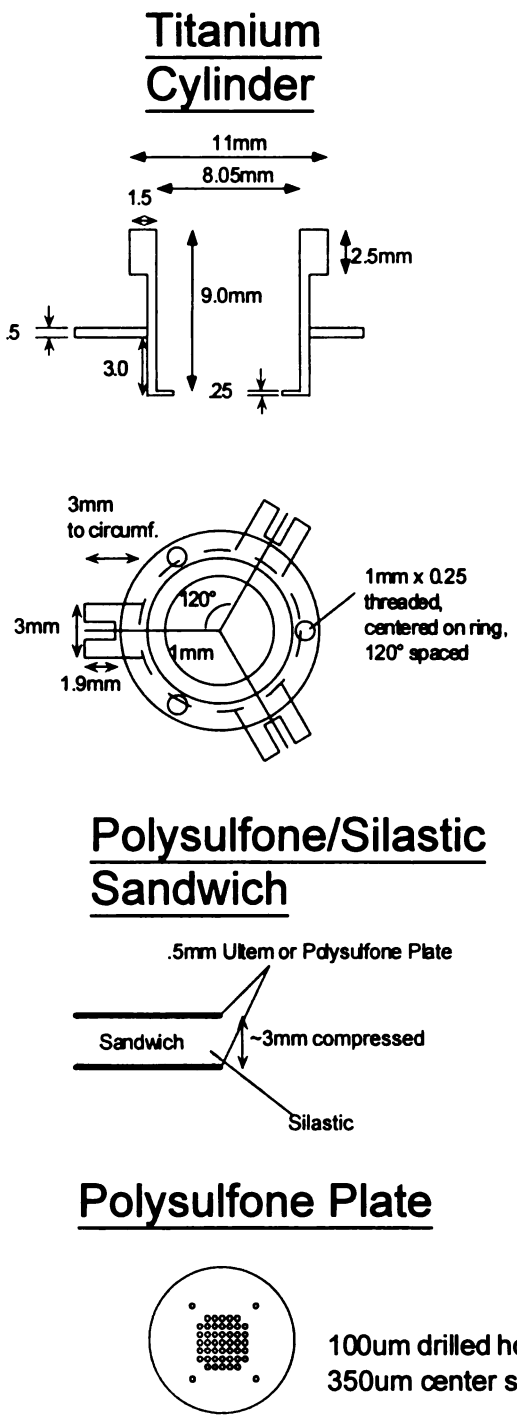

Figure 3.4: Schematic of polysulfone/silastic sandwich.

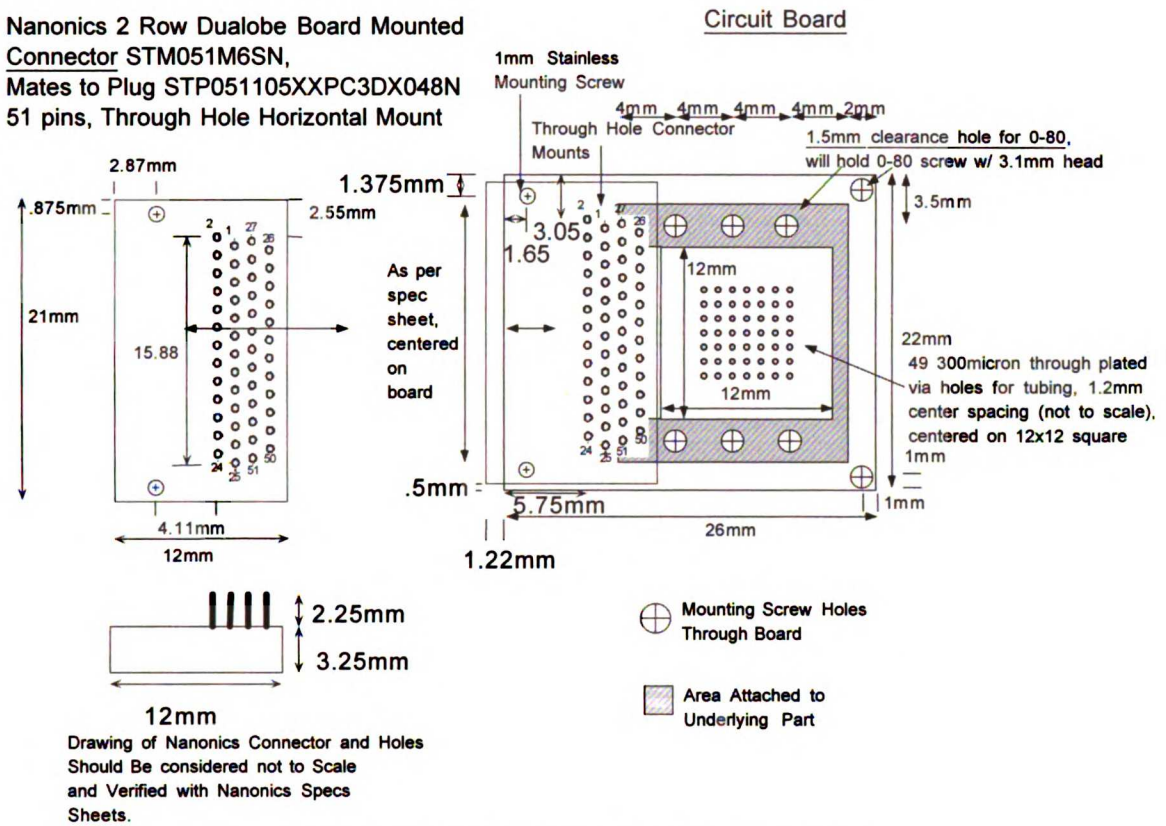

Board is simply a connection between 49 through plated via holes which will have tubes soldered into them and a 51 pin Nanonics connector. Each of the 49 holes must be connected to one of the pins on the connector, and the pin-to-pin connectivity can be arbitrary to suit routing convenience. In addition, the two mounting screws on Nanonics connector must be connected to pins on the connector. Connector is on board bottom. The board will be mounted onto a square, hollow piece by its bottom, with hatched contact area shown. The screw holes to the underlying piece are shown. The board must meet the dimensions shown (22x26mm) and the contact area and mounting screws to the underlying piece must be obeyed. Other details should be considered approximate and the Nanonics connector layout should be checked to ensure that it will fit properly on the bottom side of the board. The tubes will be soldered into place last from the top. Entire part must withstand 250degrees F autoclave, 20 minutes.

Figure 3.5: Schematic of printed circuit board and connector.

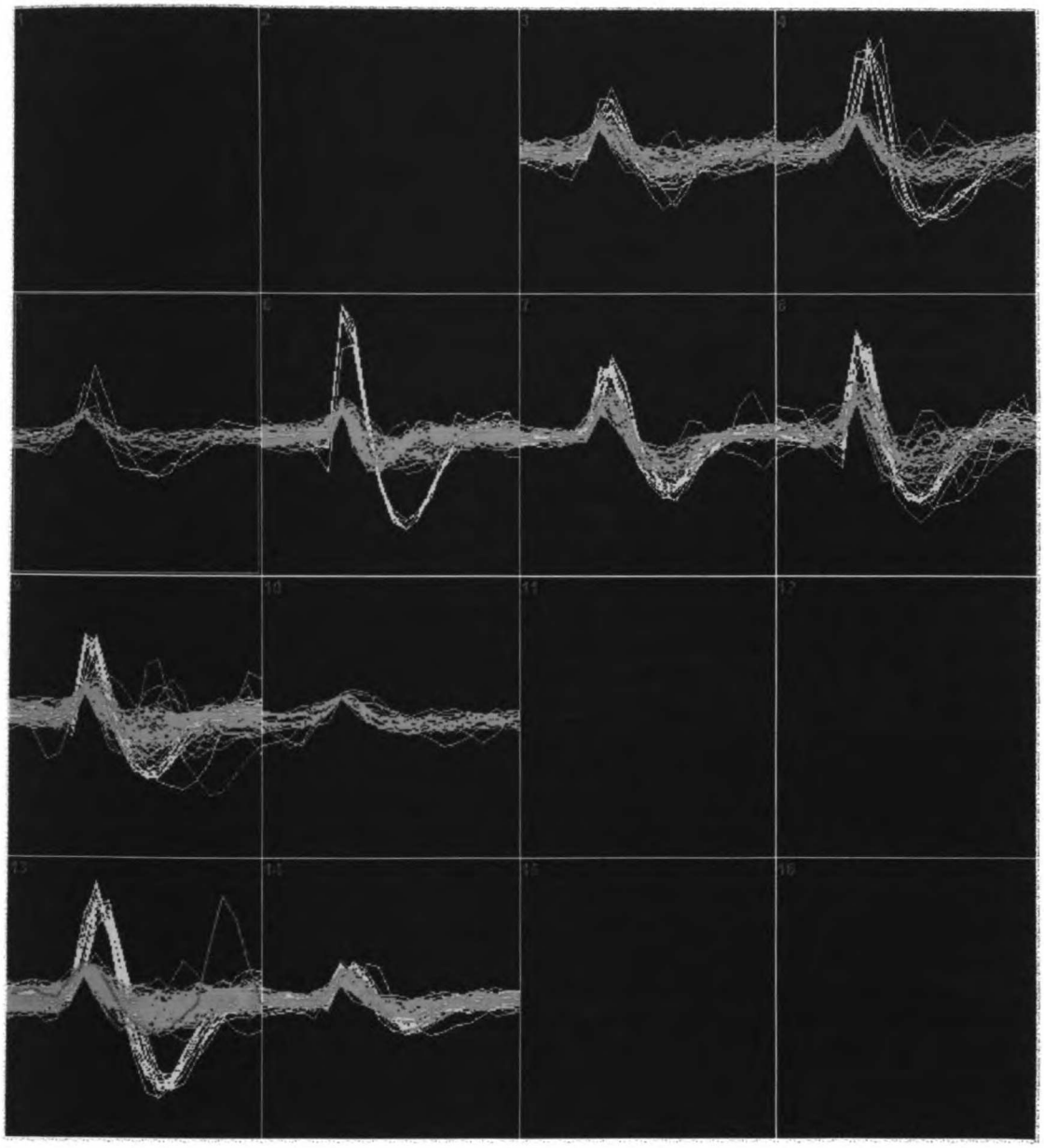

Figure 3.6. Activity recorded from one of three banks of sixteen electrodes. Colors show the online classifications of spike shapes. Yellow waveforms are attributed to an isolated neuron, blue waveforms represent unclassified spikes. In this example, single units had signal to noise ratios up to approximately 10:1, unclassified waveforms had signal to noise ratios of from 2:1 to 5:1.

Chapter 4. Sound Feature Processing in the Awake Primary Auditory Cortex

ABSTRACT

The cerebral cortex decomposes visual images into oriented edges, direction and velocity information, and color. Does the cortex use a similar coding strategy to decompose the features of sounds? We used a novel reverse correlation technique to compute linearly estimated optimal stimuli for neurons in the awake primate auditory cortex, and found that neurons are selective for acoustic feature patterns. Auditory feature selectivity often included multiple excitatory and inhibitory regions documenting particular modes of complex stimulus decomposition, including sensitivity to stimulus edges in frequency space or in time, sensitivity to stimulus transitions such as sweeps in frequency or intensity, or sensitivity to feature conjunctions. Stimuli optimized for a particular neuron's full spectrotemporal feature selectivity profile can drive that neuron with higher sustained firing rates than have typically been recorded previously. Data are presented on the excitatory and inhibitory spectral and temporal extents of response areas from neurons in the primary auditory cortex, as well as response area sizes and volumes. These data indicate that cortical neurons may decompose an auditory scene into component parts and represent it using a logic and coding scheme that is similar to that used for the cortical decomposition of a visual image.

INTRODUCTION

Feature processing by neurons in the primary visual cortex has been studied extensively since the time that Hubel and Wiesel, discovered that the 'right' kinds of stimuli for visual cortical neurons are moving, oriented bars within a spatial receptive field (Hubel & Wiesel, 1962) -- a finding later confirmed and extended in detail using reverse correlation methods (Jones & Palmer, 1987b; Reid & Alonso, 1995; Reid, Soodak, & Shapley, 1991). The fundamental feature processing modes within the spectral receptive fields of neurons in the awake primate auditory cortex are still much less completely resolved.

A comparatively rich understanding of central auditory processing has been derived for well-studied specialist species such as bats,(Riquimaroux, Gaioni, & Suga, 1991) owls, (Knudsen & Brainard, 1995) and song-birds(Konishi, 1994), while our understanding of feature processing in non-specialist species is less fully developed.

Our understanding of auditory cortical physiology in species where auditory ethology is not so well understood results very largely from work conducted in anesthetized animals. (Brugge & Merzenich, 1973a; Eggermont, 1994; Kowalski, Depireux, & Shamma, 1996a; Kowalski, Depireux, & Shamma, 1996b; Mendelson, Schreiner, Sutter, & Grasse, 1992; Middlebrooks, Clock, Xu, & Green, 1994; Schreiner & Mendelson, 1990; Wang, Merzenich, Beitel, & Schreiner, 1995) Moreover, most studies have used individual simple stimuli, typically pure tones, to characterize neuronal responsiveness along a single continuum, such as pure tone frequency(Brugge & Merzenich, 1973b; Merzenich, Knight, & Roth, 1973; Phillips, Semple, Calford, & Kitzes, 1994), amplitude(Pfingst, TA, & Miller, 1977b; Sutter & Schreiner, 1995), amplitude modulation (Eggermont, 1994; Schreiner & Urbas, 1988b), onset rate onset rate (Heil, 1997a; Heil, 1997b), or binaural structure (Brugge, Dubrovsky, Aitkin, & Anderson, 1969; Semple & Kitzes, 1993a; Semple & Kitzes, 1993b). Therefore, while it is known that auditory cortical neurons are sharply frequency selective, that responses to two stimuli can enhance or suppress one another in a time dependent fashion, (Brosch & Schreiner, 1997; Shamma & Symmes, 1985) and that these neurons show selectivity for complex natural vocalizations, it is not yet known whether auditory cortical neurons are selective for an underlying pattern of features within their responsive range which accounts for these more complex responses. This pattern of feature selectivity might be analogous to the detailed combinations of features selected for by visual neurons within their spatial response area, such as orientation and velocity. Since sustained firing rate responses in the auditory cortex to tonal stimuli are typically much lower than visual responses to drifting bars, (deCharms & Merzenich, 1996b) it has often been suggested that the preferred type of auditory stimulus may still be unknown. (Nelken, Prut, Vaadia, & Abeles, 1994a; Nelken, Prut, Vaadia, & Abeles, 1994b; Nelken, Prut, Vaddia, & Abeles, 1994c)

METHODS

Implantation Procedure

Two new world monkeys (*Aotus trivirgatus*, the South American owl monkey) were implanted with chronically placed arrays of cortical extracellular neuronal recording electrodes, as described above. Briefly, under strictly sterile conditions using Nembutal anesthesia, a 9mm diameter Titanium chamber was mounted to the skull above the exposed dura covering the primary auditory cortex, and attached with slotted screws, bone screws, and methyl-methacrylate cement. The location of the device was based on stereotaxic coordinates, skull landmarks, and initial mapping recordings of neural activity using a single electrode to confirm auditory driven neural activity. In each case, we made at least 20 mapping penetrations with a high impedance (1-3 megohm) glass coated tungsten microelectrode in order to confirm the tonotopic gradient of the primary auditory cortex, and the adjacent rostral field. At each location tonal stimuli produced by an anolog function generator were presented through a free field speaker, and the approximate best frequency response of neurons was determined by viewing stimulus-locked activity on an oscilloscope, and listening to action potentials on an audio monitor.

The surface vasculature was digitally photographed, and the chronic recording device was positioned to avoid major vessels on the cortical surface. When the location of the area of interest was confirmed, a precisely cut 9mm circular skull penetration with three slots radiating out at 120 degree angles was made. In addition, a sterile siting device was used to line up the ultimate position of each electrode with the surface vasculature in order to avoid inserting electrodes through vessels. The chronic array device was inserted into the titanium chamber to the level of the dura, but electrodes were not inserted into the brain, and the animal was allowed to recover. In a second procedure, under Ketamine/Valium anesthesia, each electrode was independently advanced through the dura with concurrent electrical monitoring until electrical contact was made with the brain and neural activity was heard, and then advanced approximately 500microns further, and finally positioned precisely to achieve maximal responsiveness in the middle cortical layers. This latter procedure was repeated on successive occasions to reposition the electrodes, or to improve response quality on some electrodes.

Neuronal Recording

Neuronal activity was recorded from up to 20 channels at once, using JFT voltage followers on the animal's head, and two stages of amplification to yield a total gain of 10000, with bandpass filtering from 300Hz-10kHz. These signals were digitized, and waveforms that crossed a predefined threshold well above the background noise level were stored to disk using a computerized data acquisition system (Biographics). Responses were sorted either online or offline into well isolated single units. Data were either collected during free field stimulation in silence, or during the performance of a frequency discrimination task. All behavioral and spike time data were merged for later analysis either using the program Stranger (Biographics), or Matlab (The Mathworks).

Stimuli

Noise stimuli used to characterize responses in the primary auditory cortex were made up of random selections of pure tones taken from 84 possible discrete frequencies spanning the range 110Hz-14080Hz in even octave spacing at 12 steps per octave (see figure 4.1). In direct analogy with stimuli used in the visual system, stimuli were chosen to contain isolated components randomly spanning the auditory range of interest, using a density of stimuli that was constant on average within all frequency ranges. Stimuli were presented as a randomly chosen sequence of 20msec long tone 'chords', with 5 msec cosine onset and offset ramps to each chord. Each chord was made up of a random selection of pure tones, averaging 1 tone per octave. Alternatively, stimuli were created with asynchronous onsets of the tonal components in each independent frequency band, such that each frequency band was a Poisson process convolved with a ramped sinusoidal function. Stimuli were presented from compact disk (sampled at 44.1kHz) at 70dBSPL in the free sound field enclosed within a double-walled acoustic isolation chamber. The animal sat in a specially designed primate chair and received occasional juice reward between stimulation periods for sessions of from 1-3h per day.

For single tone response areas, stimuli were 100msec long pure tone pips, presented at a rate of .5 Hz. Stimuli included the same 84 frequencies from 110Hz to 14080Hz in logarithmic steps with 12 increments per octave, and were presented at 8 intensities from 10 to 80dBSPL. The number of spikes

evoked during each stimulus was counted to generate traditional neuronal response areas according to established methods. (Schreiner & Mendelson, 1990)

Stimuli were also created to match spectral or temporal properties to those recorded for individual neurons, as shown in figure 4.5. These stimuli were comparable to the inverse Fourier transform of the spectrogram corresponding to the spectrotemporal receptive field of a neuron. Optimized stimuli, created to match both the spectral and temporal selectivity of individual neurons, were computed by multiplying the average spectrotemporal selectivity of the cell with identical sin wave components to those used to generate our noise stimuli, as shown in the top two panels of figure 4.5. The intensity at each pixel of the spectrotemporal receptive field was computed in units of average sound intensity preceding each neuronal action potential in 5 msec bins, and these intensity values were convolved at 44.1kHz sampling rate with an envelope identical to that used for our stimulus set (i.e. 5 msec cosine onset and offset ramps), and the values were multiplied frequency by frequency with individual sinusoidal components at each corresponding frequency band and time point. Finally, the matched stimulus was concatenated end on end to produce a stimulus of one second total duration.

Stimuli corresponding to perturbations from this matched stimulus were also generated. Perturbation stimuli with matched spectral content but random temporal structure were created by shuffling the frequency positions of each tonal component across frequency bins, and computing the resulting waveform using the same method, as shown in the central two panels of figure 4.5. Stimuli with matched envelopes but differing frequency composition were created by shuffling the frequency positions of each tonal component across time bins, and computing the resulting waveform, as shown in the bottom two panels of figure 4.5.

Reverse Correlation Methods

Spike trains were simultaneously collected from multiple sites in the primary auditory cortex during the presentation of our characterization stimulus set, and spike trains recorded from separate channels were individually reverse correlated with the times of occurrence of each of the tonal stimuli. The reverse correlation method computes the number of spikes from a neuron that were detected, on average, during a given time preceding, during, or following each tonal stimulus component onset, generating a

standard peri-stimulus time histogram of the neuron's response to each stimulus component, with the mean background response to all components subtracted. This method is somewhat similar to a much earlier method developed for characterizing auditory midbrain neurons in the grass frog. (Eggermont, Aertsen, & Johannesma, 1983a; Eggermont, Johannesma, & Aertsen, 1983b; Hermes, Aertsen, Johannesma, & Eggermont, 1981; Hermes, Eggermont, Aertsen, & Johannesma, 1982)

RESULTS

Data analyzed here come from 206 isolated single units recorded in the primary auditory cortex of two owl monkeys. Neurons from all of these locations were analyzed using our reverse correlation technique, and the majority were additionally analyzed using a number of other parametric stimulus sets (data not presented here).

Spectrotemporal Receptive Field Structure

Figure 4.2 shows the feature selectivity of seven neurons from the primary auditory cortex plotted in the form of spectrotemporal receptive fields. Panel *a* presents the frequency tuning of a typical AI neuron, showing the selectivity for tones near 440Hz. (Schreiner & Mendelson, 1990) Single tone response areas were generated according to established methods (deCharms & Merzenich, 1996b; Schreiner & Mendelson, 1990). Individual tonal stimuli were presented in silence, and the number of spikes elicited by each stimulus is presented as the color of the pixel at the corresponding frequency and intensity location in the response area, with brighter colored pixels indicating a stronger response to a stimulus. This neuron had a predominantly monotonically increasing response to increasing stimulus intensities up to 70dBSPL, and responded to stimuli spanning slightly more than one octave at 70dBSPL.

Panel *b* presents the full feature selectivity for this same cell in frequency and time in the form of a spectrotemporal receptive field at 70dBSPL, similar to a sonogram of the estimated optimal stimulus that was computed from the same amount of recording time (ten minutes). The spectrotemporal receptive fields presented in panels *b-i* show the average firing rate effect on the neuron driven by each individual component of the complex stimulus as the pixel's color (spikes/second). This is a stimulus triggered spike rate average (analogous to a standard peristimulus

time histogram), and it is identical to the estimated optimal stimulus for the cell (a spike triggered stimulus average) which would be in units of stimulus component probability, rather than neuronal firing rate.

Figure 4.2 panel *c* presents a second estimate of the neuron's optimal stimulus created using an entirely different stimulus set to show the very high consistency of the method. Data from this panel were collected in a second ten minute recording period during which stimuli were presented that had asynchronous onset times in each frequency band rather than chord-like structure across frequency bands (see methods). These stimuli correspond to independent Poisson trains of tonal stimuli in each of 84 frequency bands, which allows a greater range of relative time lags between stimuli at different frequencies. Additional examples showing the consistency of this method across different recording epochs and using different stimulus sets are shown in figure 4.3.

A minority of neurons in the primary auditory cortex have spectrotemporal receptive fields that show only a single region of increased rate (5%, n=206 isolated single units), which corresponds to simple selectivity for a particular frequency region, with no additional feature processing structure. We have found that cells of this type (not shown) are much less common than cells with complex and multimodal receptive field structure (see below). Neurons typically have regions of both increased and decreased firing rate within their receptive fields (>93.3%, n=206). For terminological convenience, these will be referred to as excitatory and inhibitory regions, although these changes in rate are not necessarily diagnostic of an underlying mechanism. Responses are all measured as deviations in firing rate from the ongoing firing rate during the presentation of these stimuli (see methods).

Neurons with receptive fields of this type can serve as detectors of stimulus edges in both frequency space, and in time. The neuron shown in figure 4.2d has a receptive field structure within its frequency response region indicative of lateral inhibition in frequency space, making it a detector of spectral edges. The neuron shown in figure 4.2e shows strong inhibition both above and below its optimal frequency, with the dominant feature being its lateral inhibitory components, which also show time structure. The neuron shown in figure 4.2f shows a decrease in firing rate caused by a stimulus frequency which at a later time caused an increase in rate. This receptive field structure is ideally suited

to detect stimulus transients, making this cell a detector of temporal edges. Neurons in the auditory cortex often prefer a stimulus onset transition within their frequency responsive area, rather than sustained stimuli. Neurons were also recorded that responded with increased rate to one frequency range at one time, and a different frequency range at a later time, with regions of decreased firing rate showing a similar pattern. The neuron shown in figure 4.2g is an example of this type. This pattern of response within the receptive field is strongly analogous to motion energy detectors, which detect a stimulus edge moving in space through their receptive field, and these cells are indeed selective for sweeps in frequency (see below). (Adelson & Bergen, 1985; Suga, 1988; Suga, 1992)

The neurons shown in figures 4.2b, h, and i show examples that have complex, multimodal receptive field structure, with multiple excitatory or inhibitory regions. It should be noted that these cells had action potential waveforms that were well isolated from the action potentials of other neurons. Response areas of this type are indicative of selectivity for stimulus feature conjunctions. They are sometimes quite complex, and perhaps related to sounds that the animal must process within its learned environment.

Single Tone Response Areas and the Spectrotemporal Receptive Field

Examples of single neuron tuning curves from the primary auditory cortex of the awake primate are shown in figure 4.4. Although a quantitative comparison of tuning properties in the awake and anesthetized animal will not be presented here, the response tuning areas of these neurons are similar to those found in the primary auditory cortex of anesthetized cats and monkeys. (Abeles & Goldstein, 1972; Brugge & Merzenich, 1973a; Pelleg-Toiba & Wollberg, 1989; Schreiner & Mendelson, 1990) These example neurons include (from top to bottom) a weakly multi-peaked profile, two profiles with differing frequency selectivity at different intensity levels, and a neuron with a non-monotonic response magnitude with stimulus intensity. We have observed a wide range of tuning curves shapes and widths in this preparation, as in previous studies of the anesthetized animal. As can be seen in the corresponding spectrotemporal receptive fields shown in *b* at right, the pattern of excitation and inhibition computed with our method is similar to the that computed using isolated pure tones, but the

spectrotemporal receptive field contains more information about the detailed temporal relationships between excitatory and inhibitory regions.

Spatiotemporal Receptive Field Structure in the Primary Visual Cortex

To allow for direct comparison, an example spatiotemporal receptive field recorded from a single neuron in the primary visual cortex of the anesthetized cat is presented in figure 4.5. This neuron has a receptive field with similarly sized excitatory and inhibitory components, a combined excitatory/inhibitory response which lasts for approximately 60 milliseconds, and a pattern indicative of selectivity for a horizontally oriented narrow bar. This pattern is comparable in duration, strength, and excitatory/inhibitory structure to response areas observed in the primary auditory cortex like those shown above.

Neuronal Responses to Optimized Stimuli

Stimuli were created that were designed to be exactly matched to the spectral and temporal selectivity of individual neurons, and then these stimuli, variants of these stimuli, and other stimulus types were presented back to the same neurons to measure driven responses. Figure 4.6 shows a diagram of the methods used to compute these stimuli (see methods). A stimulus was created with spectral and temporal properties matched to those predicted to be optimal for each given neuron, as shown in the top two panels of figure 4.6. This stimulus corresponds to the average stimulus preceding a spike from the neuron concatenated end on end to produce one second of total sound length. Variants of this stimulus were also created with slightly differing separations between spectrotemporal receptive field components. Stimuli were also generated that contained the same average envelope, but random frequency composition (central two panels), and that contained the same average spectral composition, but random envelope.

Figure 4.7 shows the responses of one neuron in the primary auditory cortex to stimuli of this type, as well as conventional stimuli. Panel *a* shows the responses of the neuron to a one second long stimulus with a temporal envelope optimized to match that predicted from the cell's spectrotemporal receptive field, but with random positions of individual frequency components. In this case the

stimulus with optimized envelope structure alone did not drive strong activity in the neuron. A stimulus with exactly matched spectral properties but a randomized envelope drove a dramatic response in this cell, with the neurons' sustained rate exceeding 40 spikes/second. The response of this neuron to the optimized stimulus which was best matched to the neuon's true selectivity, and hence drove the best response, is shown in panel *c*. This was the best response from several optimized stimuli which were presented using different repeat rates of the individual stimulus components. In this case the neuron achieved a sustained rate of 57 spikes/second. For this neuron, continuous tonal stimuli and natural vocalizations were also presented. In this example, the neuron's best sustained response to a tonal stimulus (of 20 tones spanning two octaves around the neurons center frequency) is shown in *d*. The neuron's best response to any of five natural vocalization stimuli is shown in panel *e* (note different timescale).

The average responses of ten individual neurons and ten multi-neuron cluster recordings to these stimuli, from which we have made quantitative measurements, are shown in figure 4.8. The average response of these cells to a stimulus with an exactly matched frequency spectrum, but random envelope, is shown at left. These stimuli drove sustained rates in single neurons averaging 14 spikes/second. The average response to stimuli with matched temporal pattern but random spectral composition were significantly smaller in magnitude (standard errors of the mean are shown), although a significant sustained response was still generated. Stimuli with matched spectral and temporal characteristics also drove significant sustained responses from this population, both for single neurons and multi-unit cluster recordings. There was no significant difference for this small neuronal sample in the average rate driven by the stimuli with matched spectrotemporal characteristics compared with stimuli with matched spectral properties alone. Responses to stimuli matched to the selectivity of a different neuron, recorded on the same day, are shown at right. Neurons were weakly driven by interleaved stimuli that were presented at the same sound level but matched to the response characteristics a different cell in the same recorded population.

Magnitude of Neuronal Responses to Optimized Stimuli

Forty isolated neurons were carried through the extended protocol of recording the STRF, generating linearly predicted optimal stimuli, and presenting these stimuli back to the animal in the same recording sesssion. The full distribution of firing rate responses from this population is plotted along the vertical axis in figure 4.9. As can be seen, many neurons were driven to rates above 20 spikes/second using this method, a substantial sustained rate for neurons in the primary auditory cortex. The excitatory volume of the neuron's STRF, in units of firing rate, is plotted along the horizontal axis for comparison. This is the integral of the statistically significant excitatory area of the STRF, divided by the total time which it contains, to yield a measure in spikes/second. The neurons which were not strongly driven by the linearly estimated optimal stimulus all had weakly modulated STRFs. These two parameters were significantly correlated, $r = .69$, Pearson correlation coefficient, $p<.001$.

In order to determine the relationship between the rate driven by the linearly predicted stimulus for a neuron and the 'linarity' for that neuron, we developed a simple measure of response linearity during our noise stimuli. After presenting 30,000 separate stimuli during our noise protocol, we calculated the STRF for the neuron which is the best linear fit using a restricted number of parameters between this large response space and the neuron's output rate. We assessed the quality of this fit for individual neurons by computing the correlation coefficient between the observed firing rate, and the firing rate predicted by convolving the STRF with the progression of 30,000 stimuli, binned at 5ms, and then smoothed with a 5 bin wide gaussian to yield a time resolution of 25ms. The correlation coefficients between the predicted and observed rates varied from 0 to .38, partly reflecting the very large single-trial variability of cortical responses. The range of correlation coefficients (r) is plotted on the horizontal axis of figure 4.10, vs. the observed rate driven by the predicted optimal stimulus ($r = .61$, $p<.001$), indicating that more linear neurons had greater responses to linearly predicted optimal stimuli. In addition, figure 4.11 plots the same correlation coefficients vs. the magnitude of the STRF, as described above and these two parameters were highly correlated ($r=.89, p<.001$), indicating that neurons with more significantly modulated STRFs had a higher measure of linearity (r).

Number of Sub-Regions in Response Areas of AI neurons

To calculate the number, size, and strength of sub-regions of the spectrotemporal receptive fields of these neurons, we developed a thresholding method shown diagramatically in figure 4.12. For each recorded spectrotemporal receptive field (example shown in *a*), the recorded data was smoothed with a 1 pixel wide radial gaussian (shown in *b*), and a measure of the statistical reliability of each pixel was computed. The total recording session, typically 10 minutes, was divided into ten equal segments and individual spectrotemporal receptive fields were calculated for each segment. The standard error of the mean value at each pixel over this sample was then computed. Any pixel which achieved a value of 3 standard errors above or below the mean response rate was judged to be a statistically significant portion of the response area (shown in *c*). Isolated pixels, typically originating from noise, were removed from the response area. Finally, the portion of the original spectrotemporal receptive field falling within this selected area (shown in *d*) was used for further calculations. The number and properties of the various receptive field parameters were estimated using this very conservative receptive field area criterion.

The distribution of the number of excitatory and inhibitory sub-regions for all single neurons is presented in figure 4.10. Of 206 single units recorded, 13.1% did not yield a statistically significant STRF in 10 minutes of recording time, suggesting that these cells were not responsive to the noise stimuli or were strongly non-linear. Of cells with a significant STRF, 46.4% had multiple excitatory sub-regions, and 48.6% had multiple inhibitory sub-regions. Figure 4.13 shows the distribution of numbers of statistically significant excitatory and inhibitory sub-regions for this population.

Response Bandwidths

The bandwidth of response areas of these neurons were computed by taking the extreme upper and lower frequency positions of the statistically significant extent of the receptive field, according to the criteria described above. The distribution of total response bandwidths from this population is shown in figure 4.14 panel *a*. The mean total bandwidth of both excitatory and inhibitory components of the receptive field of these neurons was 1.87 octaves. The excitatory area of the neurons usually

encompassed a sub-range of frequencies, and the distribution of excitatory bandwidths in presented in figure 4.14 panel *b*. The mean excitatory bandwidth from this sample was .85 octaves, less than one half of the total response area bandwidth. The distribution of bandwidths of inhibitory regions is plotted in figure 4.14 panel *c*, with a mean of 1.0 octaves. The average total bandwidth, average excitatory bandwidth, and average inhibitory bandwidth from this sample are plotted in figure 4.15, with standard errors shown. The inhibitory bandwidth is significantly larger than the excitatory bandwidth ($p<1*10^{-9}$, two-tailed t-test), and the total bandwidth is significantly larger than either excitatory or inhibitory alone ($p<.1*10^{-8}$, two-tailed t-test).

Response Durations

The distribution of total response durations is shown in figure 4.16. Primary cortical neurons show a response to stimuli which is limited in temporal extent, with a mean response duration of 66.2 milliseconds. The longest responses observed to a single stimulus component in this paradigm were approximately 130 milliseconds. The distribution of durations of excitatory components of the responses of these neurons is shown in figure 4.11 panel *b*. The mean duration of excitatory response was 41.8msec, and the maximum temporal extent was approximately 100msec. The distribution of the extent of the total inhibitory response is plotted in panel *c*, with a mean extent of 47msec, and a maximum of approximately 100msec. The inhibitory component of these responses was usually longer in duration.

Response Areas and Volumes

A measure of area was computed for the excitatory and inhibitory sub-regions of the receptive fields, and these data are presented in figure 4.17, in units of octave seconds. There was a wide distribution of excitatory and inhibitory areas up to .1 octave seconds, with neurons usually showing a greater total inhibitory area than excitatory area. Excitatory and inhibitory response volume measures were also calculated by separately computing a weighted average of the response rates in each pixel within the excitatory and inhibitory sub-regions of the spectrotemporal receptive field, and multiplying this by the area of the sub-regions to give a total volume measure is spikes. These data, presented in figure 4.18,

showed that there was considerable dispersion of excitatory and inhibitory receptive field volumes, with maxima of about 3 spikes. Total excitatory and total inhibitory volumes were comparable across this sample.

DISCUSSION

This study addresses the question of the feature processing of sounds by single neurons in the primary auditory cortex. Using a new method of receptive field characterization based on reverse correlation with a new class of random stimuli, it was discovered that it is possible to construct detailed characterizations of neuronal response selectivity in the awake primary auditory cortex, in contrast with previous reverse correlation methods which have not succeeded for cortical neurons. Cortical neurons show varied and complex patterns of selectivity within the frequency range to which they respond, and these patterns typically contain combinations of both excitatory and inhibitory sub-regions. These spectrotemporal receptive field calculations present in a single measure the combined spectral and temporal selectivity of auditory cortical cells.

Relevance of Sound Processing in the Auditory Cortex

The auditory cortex has long been recognized as playing an important role in the processing of time-varying acoustic stimuli as a result of lesion experiments. As cortical sound processing of any single sound source is largely bilateral, human lesion studies addressing the role of the auditory cortex have been hampered by the lack of selective bilateral lesions encompassing both primary cortical areas. In animals, the cortex has been directly implicated in the performance of a number of auditory perceptual tasks. Bilateral ablation of large segments of the temporal lobe auditory cortex leads to significant impairment in discriminating patters of tone sequences(Diamond & Neff, 1957), and tone durations (Scharlock, Neff, & Strominger, 1965). In addition, auditory cortical lesions in animals also lead to a disruption in the capacity to discriminate species-specific vocalizations (Heffner & Heffner, 1984; Heffner & Heffner, 1989). Finally, lesions in discrete regions of the primary auditory cortex in animals lead to frequency-specific deficits in the ability to precisely localize contralateral sounds (Jenkins &

Masterton, 1982; Jenkins & Merzenich, 1984). These lesion data define a clear role for the auditory cortex in the processing of the time structure of perceived sound.

Previous Studies of Inhibition in the Primary Auditory Cortex

The ability of cortical neurons to process successive stimuli has primarily been studied in the anesthetized animal, and primarily using either pairs of two stimuli or repetitively modulated single stimuli. The latter approach has been used to generate modulation transfer functions, which characterize the stimulus following characteristics of neurons. Modulation transfer functions have been generated using amplitude modulations of pure tone carriers, typically presented at the best frequency of a studied neuron (Phillips, Hall, & Hollett, 1989; Schreiner & Urbas, 1988b), or using amplitude modulated white noise (Eggermont, 1994), or using trains of broad-band clicks (Eggermont, 1991; Eggermont, 1993; Eggermont, 1994). The most salient finding of these studies has been that cortical neurons in anesthetized animals typically show a band-pass character for modulation rates, following modulation rates up to around 15Hz, and typically showing the strongest responses to rates of about 8-10Hz. These modulation rates correspond reasonably with the durations of the spectrotemporal receptive fields presented here, although these spectrotemporal receptive fields suggest neuronal following to somewhat higher rates in the awake animal. The mean duration of the spectrotemporal receptive fields shown here was 66ms, which would correspond to a repetition rate of 16Hz. This suggests that these neurons would be predicted to show little interaction to repetitive stimuli presented up to this rate, although this does not necessarily indicate that this would be the preferred repetition rate. There is only one study of modulation following which has recently been conducted in the awake animal using pure tones, which documents a distribution of best modulation rates that is in agreement with our findings. (Bieser & Muller-Preuss, 1996)

A second class of experiments have investigated two-tone or inhibitory interactions in the primary auditory cortex of both awake and anesthetized animals. Early studies by Phillips, et.al. demonstrated that the responses of an auditory cortical neuron to pure tones can be decreased by the presence of a simultaneous broad-band noise stimulus (Phillips, 1985; Phillips & Cynader, 1985; Phillips, Orman, Musicant, & Wilson, 1985). As all neurons in the auditory nerve show monotonic

rate-level functions, this is a clear indication of central inhibition at some stage or stages of auditory processing. This initial finding has been extended by the use of two-tone paradigms which have studied the effect of a masker tone on the neural response to a probe tone, which can be presented either simultaneously or following the masker. (Brosch & Schreiner, 1997; Calford & Semple, 1995) These studies have demonstrated frequency and time specific inhibitory effects on the firing of primary cortical neurons. It has been demonstrated that a tonal stimulus can lead to a decreased response to a second simultaneous stimulus of nearby or identical frequency. A preceding stimulus can also diminish the response to a second presentation of the same stimulus (habituation), or to the closely following presentation of other stimuli of slightly different frequency. The temporal extent of this effect has been shown to extend to durations up to about 300msec in Pentobarbital or Ketamine anesthetized cats, and the bandwidth of the inhibitory effect has been reported to span an extent from .5 to about 4 octaves. There has been only one study which has directly addressed the issue of inhibition in the awake animal, and this study also found that a single masking tone can diminish the response to a following probe stimulus, but the distribution of bandwidths and durations of this effect were not presented (Shamma & Symmes, 1985). Our own experiments found a narrower spectral range of inhibition (mean of 1.0 octaves, range up to approximately 3 octaves), and a shorter duration of inhibition (mean 47msec, extent 100msec). These differences may be accounted for by anesthetic effects in the previous studies, or by the fact that the previous studies presented isolated pure tones in silence as masking stimuli.

Although previous studies have often found complex patterns of facilitation or inhibition derived from a single masking tone, they have not been able to assess the full spectrotemporal pattern of inhibitory and facilitatory effects on neuronal firing. The method presented here confirms and greatly extends previous work by showing the full pattern of excitation and inhibition of these neurons in spectral structure and time, which is a generalization from inhibition caused by one single tone onto another single tone.

Previous Studies of Single Neuron Responses in the Primary Auditory Cortex of the Awake Animal

In comparison with other cortical areas, there have been surprisingly few studies of neurons in the primary auditory cortex of awake animals to date, (Bieser & Muller-Preuss, 1996; Caan, 1977; Funkenstein & Winter, 1973; Glaser, 1971; Glass & Wollberg, 1979; Glass & Wollberg, 1983a; Glass & Wollberg, 1983b; Manley & Muller-Preuss, 1978; McKenna, Ashe, & Weinberger, 1989; Miller, Dobie, Pfingst, & Hienz, 1980a; Miller, Dobie, Pfingst, & Hienz, 1980b; Pelleg-Toiba & Wollberg, 1989; Pelleg-Toiba & Wollberg, 1991; Pfingst & O'Connor, 1981; Pfingst, TA, & Miller, 1977a; Pfingst et al., 1977b; Shamma & Symmes, 1985; Steinschneider, Arezzo, & Vaughan, 1982; Steinschneider, Arezzo, & Vaughan, 1990; Steinschneider, Reser, Schroeder, & Arezzo, 1995a; Steinschneider, Schroeder, Arezzo, & Vaughan, 1994; Steinschneider, Schroeder, Arezzo, & Vaughan, 1995b; Vaadia & Abeles, 1987; Vaadia, Benson, Hienz, & Goldstein, 1986a; Vaadia, Benson, Hienz, & Goldstein, 1986b; Winter & Funkenstein, 1973; Zurita, Villa, de Ribaupierre, de Ribaupierre, & Rouiller, 1994). In addition, the majority of work performed on the awake primary auditory cortex was done before modern methods of data acquisition and neuronal spike separation were available. There is, however, a body of evidence demonstrating the selectivity of neurons in the awake primary auditory cortex to a number of individual sound features, some of which have been mentioned above.

The earliest studies of the awake primary auditory cortex investigated both the stimulus selectivity and behavioral lability of neuronal responses. The studies of Whitfield et.al. and others (Evans, Ross, & Whitfield, 1965; Glaser, 1971; Pfingst et al., 1977b; Swarbrick & Whitfield, 1972; Whitfield, 1967) demonstrated that neurons in the primary auditory cortex of the awake animal are highly selective to stimulus frequency, showing tuning bandwidths equal to those of some fibers in the auditory nerve, as well as being selective for additional parameters, such as spectral envelope. Early experiments also demonstrated the responses of these neurons to sinusoidally modulated FM stimuli. (Glaser, 1971; Whitfield & Evans, 1965) Other early experiments demonstrated that neurons in the awake primate auditory cortex can be highly selective for species-specific natural vocalizations. (Glass & Wollberg, 1979; Winter & Funkenstein, 1973; Wollberg & Newman, 1972) Early studies also

documented effects of behavioral context on neuronal responsiveness in the primary auditory cortex. (Benson & Hienz, 1978; Hocherman, Benson, Goldstein, Heffner, & Heinz, 1976; Hubel et al., 1959; Miller et al., 1980a; Miller, Sutton, Pfingst, Ryan, & Beaton, 1972)

Two of the very few contemporary studies of the awake primary auditory cortex addressing the issue of parametric stimulus tuning of individual neurons have shown that using single pure tone stimuli presented in silence, neurons have excitatory bandwidths spanning .4 octaves to 1.4 octaves, compared with our mean excitatory bandwidth of .7 octaves, (Pelleg-Toiba & Wollberg, 1989) and that neurons can show a decrease in firing rate from the response driven by a preferred pure tone stimulus if a second tone is presented as well (see above). (Shamma & Symmes, 1985)

Parameter Extraction in the Auditory System

These studies of the primary auditory cortex in awake non-specialist animal species, together with a more extensive literature of responses in the anesthetized animal, (Brugge & Merzenich, 1973a; Brugge, 1985; Diamond & Neff, 1957; Eggermont, 1991; Eggermont, 1994; Heil, 1997a; Heil, 1997b; Mendelson, Schreiner, Grasse, & Sutter, 1988; Mendelson & Cynader, 1985; Schreiner, 1992; Schreiner & Langner, 1988; Schreiner & Mendelson, 1990; Schreiner & Urbas, 1988b; Sutter & Schreiner, 1991; Sutter & Schreiner, 1995) have thoroughly documented primary auditory cortical selectivity to a number of individual stimulus parameters. Neurons in the primary auditory cortex can show significant stimulus selectivity for sound frequency, (Brugge, 1985) location, (Middlebrooks et al., 1994; Vaadia et al., 1986a) intensity, (Pfingst et al., 1977b) amplitude modulation, (Eggermont, 1994; Schreiner & Urbas, 1988b; Sutter & Schreiner, 1995) frequency modulation, (Mendelson et al., 1988) onset rate, (Heil, 1997a; Heil, 1997b) binaural structure, (Brugge & Merzenich, 1973a) spacing between stimulus frequency components, (Kowalski et al., 1996a; Kowalski et al., 1996b; Schreiner & Calhoun, 1994) as well as other parameters. The central remaining issue pointed to by these many studies of individual parameter tuning and two-stimulus interactions is how the activity of auditory cortical neurons integrates the components of these individual parameters to form a full pattern of stimulus feature selectivity. This can also be addressed as a search for the multiple parameters that

form an idealized stimulus for a particular neuron. (Nelken et al., 1994a; Nelken et al., 1994b; Nelken et al., 1994c)

Previous Spectrotemporal Receptive Field Measurements in the Central Auditory System

Previous methods of reverse correlation have not been successful in the auditory cortex because they have relied on the locking of cortical action potentials to the fine structure of auditory stimuli (DeBoer & deJongh, 1978; DeBoer & Kuyper, 1968), which is typically weak or absent, or because they have used other classes of stimuli which are ineffective in driving cortical neurons (Jos Eggermont, personal communication). Our method for characterizing the response properties of auditory cortical neurons is similar in concept to a method developed almost two decades ago by Eggermont, et.al., for the study of neurons in the auditory periphery and first central auditory processing station of the anesthetized grass frog using white noise. (Eggermont et al., 1983a; Eggermont et al., 1983b; Hermes et al., 1981; Hermes et al., 1982) These authors demonstrated the importance of measuring the non-separable spectral and temporal response properties of central auditory neurons using a method based on reverse correlation, although their method used a very different stimulus set designed for neurons closer to the auditory periphery that was inefficient for studying cortical neuronal responses (Jos Eggermont, personal communication). Unfortunately, despite the elegance of these early papers, this conception for studying central auditory processing has remained largely unexplored from that time.

Recently Kim, et.al. have explored spectrotemporal receptive fields of neurons in the auditory nerve (Kim & Young, 1994) and determined that STRF analysis using white noise can give information which is similar to that derived from frequency tuning curves but can capture additional features, such as two-two suppression effects (although there is no inhibition *per se* in auditory nerve fibers). Kao,et.al. have explored the spectrotemporal receptive fields of neurons in the anesthetized rat inferior colliculus, (Kao, Poon, & Sun, 1997) and] and more recently in a limited number of neurons (nine) in the dorsal cochclear nucleus (Nelken, Kim, & Young, 1997). These authors document that the STRF of neurons can be computed using white noise as the stimulus in these low-order auditory structures, although this method is not successful in the auditory cortex. Nonetheless, some of the features which

we observe in the cortex, such as regions of suppression surrounding excitation, are clearly present in lower-level structures as well. Additional studies will be required to fully elucidate the differences in spectrotemporal processing between different stations in the auditory pathway.

Validity and Significance of the Spectrotemporal Receptive Field Method

It is important to assess the extent to which the spectrotemporal receptive fields measured here reflect the true feature selectivity of auditory cortical neurons, and whether they are statistically reliable. Using this reverse correlation method, it was found that the response areas measured for auditory cortical neurons are highly reproducible, as shown in figures 4.2 and 4.3. Much of the detailed spectral and temporal structure of responses is closely reproduced using successive applications of the method, even when completely different stimulus sets and different recording epochs are compared. This indicates that many of the precise details of the receptive fields that were measured do in fact reveal the auditory response properties of cortical neurons, as opposed to arising from noise in the measurement method. In addition, receptive field components were quantified using a highly conservative threshold value of three standard errors above the mean neuronal rate, ensuring that measured peaks were extremely statistically reliable.

The question remains of the extent to which this characterization method truly captures the basic feature processing characteristics of auditory cortical neurons. Any characterization of a neuronal response, from conventional pure tone tuning curves and modulation transfer functions to the reverse correlation method presented here, suffers from the question of the extent to which the characterization reflects the general processing character of the neuron being measure, or is primarily due to the nature of the stimuli chosen. The most straightforward means to measure the extent to which these noise stimuli capture essential features of the processing character of auditory cortical cells is to determine whether they generalize to other types of stimuli. The first indication of this generalization using these stimuli is that extremely similar spectrotemporal receptive fields were derived using different sets of pure tone stimuli with either synchronous or asynchronous onset.

As understanding of cortical processing progresses, it may become possible to predict the responses of cortical neurons to arbitrarily complex stimuli, such as natural vocalizations or localized

sounds in the environment, based upon a detailed characterization of neuronal properties. This goal has not yet been satisfactorily accomplished in any cortical system. An intermediate goal, and one which is being investigated, is the extent to which responses to an independent class of simple stimuli can be predicted by a simple characterization (Kowalski et al., 1996b; McLean & Palmer, 1989). It is possible to use spectrotemporal receptive fields as linear filters to predict the neuronal responses to complex stimuli by a convolution method. The spectrotemporal receptive field of a neuron can be considered as a sum of linear filters in different frequency bands, which can be convolved with the energy of an arbitrary stimulus in each corresponding frequency band at each time point. The spectrotemporal content of a stimulus, which is convolved with the neuronal spectrotemporal receptive field in this method, is derived by applying a bank of constant bandwidth filters to an input stimulus and then taking the timecourse of the power in each frequency band by squaring the corresponding filter output, or by taking a Hilbert transform of the filter output. We are in the process of applying this method to the responses of neurons measured in the primary auditory cortex using amplitude and frequency modulated tones, and natural vocalizations.

While predictions based upon this method can be made, they would not be expected to significantly capture the responses of these cells to complex stimuli. The stimuli used here measure the linear component of cortical responses to stimulus frequency content and time, but they do not capture all aspects of the information processing nature of these neurons. Particularly, this response characterization method does not capture the details of any systematic non-linear feature processing of these cells, and it does not capture their responses to different amplitudes of stimulation. Natural stimuli contain considerable information in the amplitude envelopes of separate frequency bands, and cortical neurons clearly capture this information (Eggermont, 1994; Heil, 1997a; Heil, 1997b; Phillips & Hall, 1987; Phillips et al., 1994; Schreiner & Urbas, 1988a; Schreiner & Urbas, 1988b; Sutter & Schreiner, 1995). For this reason, predictions of neural responses based upon the spectrotemporal receptive fields of cortical neurons should be expected to produce only a crude first approximation of the full responses to stimuli which contain information that is different in kind to that which was used to create these measures, particularly amplitude fluctuations.

Despite these significant limitations, these data suggest that the this simple method for computing spectrotemporal receptive fields of auditory cortical neurons is capturing essential features of the processing modes of these cells. This method is not able to predict responses to arbitrary stimuli just as tuning curves or other characterizations cannot. The method is nonetheless a valuable and valid overall characterization of neuronal response feature selectivity. This can be justified with the empirically useful finding that using stimuli predicted to be optimal based upon this method, we are able to drive firing rates higher than have typically been encountered in the primary auditory cortex. For the reasons just presented, it would not be expected that this method would allow us to predict the ideal stimulus for every neuron, and in fact we are not always able to predict optimal stimuli. Nonetheless, the fact that stimuli derived here often drive these neurons to very high sustained rates of firing (see figure 4.9) is a strong argument that this method has captured essential features of the processing nature of these cells.

Feature Selectivity and High Rate Responses in the Primary Auditory Cortex

These data demonstrate that auditory cortical neurons have complex selectivity within their best frequency region for patterns of stimulus features. Unlike many studies using individual stimulus tuning to probe neuronal selectivity, this work has allowed us to compute the full spectrotemporal selectivity of these cells, which brings together the influences of many individual features of auditory stimuli, such as frequency and amplitude changes, inhibitory interactions, and others. Previous studies of the primary auditory cortex have typically found that cells produce precisely timed transient responses, at rates up to several hundred spikes per second for a few tens of milliseconds, but sustained rates are typically dramatically lower than those recorded in other cortical areas, (deCharms & Merzenich, 1996b) leading to the idea that auditory cortical representation might be special in its reliance upon temporal coding. The data reported here present a cohesive picture of the response selectivity for these neurons, and demonstrate that given appropriate stimuli, neurons in the primary auditory cortex can fire at relatively high rates of action potential discharge.

Similarity of Responses in the Primary Auditory and Visual Cortices

Reverse correlation techniques have been used in the visual system since the studies of Jones and Palmer, (Jones & Palmer, 1987a; Jones & Palmer, 1987b; Jones, Stepnoski, & Palmer, 1987; McLean & Palmer, 1989) which demonstrated selectivity for well-defined regions of visual space, as well as tightly constrained response selectivities in time. This work has been extended by Reid and colleagues. (Alonso, Usrey, & Reid, 1996; Reid & Alonso, 1995; Reid & Shapley, 1992; Reid et al., 1991) An example of a visual cortical receptive field, shown in figure 4.4, shows a clear similarity to the pattern of responses that we have obtained in the auditory cortex in several respects. Spatiotemporal response areas in the primary visual cortex are typically constrained to a temporal window of a few tens up to about 100 milliseconds, they typically contain a balance of excitatory and inhibitory components, and they often show selectivity for stimulus edges, transients, or movement. This is reflected in the selectivity of most visual cortical neurons to stimuli which change in time, (Adelson & Bergen, 1985; McLean & Palmer, 1989) and to drifting bar (Hubel & Wiesel, 1962) and grating stimuli in particular. (Shapley & Lennie, 1985)

Implications for Cortical Stimulus Decomposition

These data demonstrate that the cortical processing of sounds is based upon a decomposition into small and well-defined but often complex spectral and temporal features within a limited receptive field area, and thus that early cortical processing may share a similar logic across sensory modalities. In decomposing visual forms or auditory scenes, cortical neurons are often detectors within their response area of stimulus edges along the sensory receptor surface, or edges in time, or stimulus movement, or feature conjunctions. This decomposition is similar to that found in other cortical areas, supporting the possibility of somewhat general mechanisms of feature processing across differing cortical areas and even modalities.

In addition, these data indicate for the first time that by using optimized stimuli it is possible to drive auditory cortical cells to high rates of sustained firing. The most relevant and often defining physiological discovery for many cortical areas has been the discovery of the class of stimuli that can

drive neurons in that area effectively and with specificity. This has been true for color sensitive neurons in area V4 (Zeki, 1980; Zeki, 1978), velocity selective neurons in area MT (Allman & Kaas, 1971; Maunsell & Van Essen, 1983), face cells and cells responsive to complex learned patterns in area IT (Miyashita & Chang, 1988; Perrett, Rolls, & Caan, 1982), and drifting bar stimuli in area V1 (Hubel & Wiesel, 1962). In each area, the discovery of the stimulus set which is effective in driving tuned responses in these neurons has led to a much more detailed understanding of that areas properties, and led to a great opening for further experiments.

The method presented here allows neurons in the primary auditory cortex to be driven at rates more comparable to those found in these other cortical areas to optimal stimuli, and may open up avenues to considerable further exploration. This method should allow a number of specific future questions to be addressed, including the pattern of response mapping of the primary auditory cortex, how these cortical maps develop or are changed with learning, and how the detailed response selectivity of these cells is altered by stimulus or behavioral context. In addition, these data give data on the feature decomposition of sound taking place in the auditory cortex, which suggests how artificial model systems might decompose sounds.

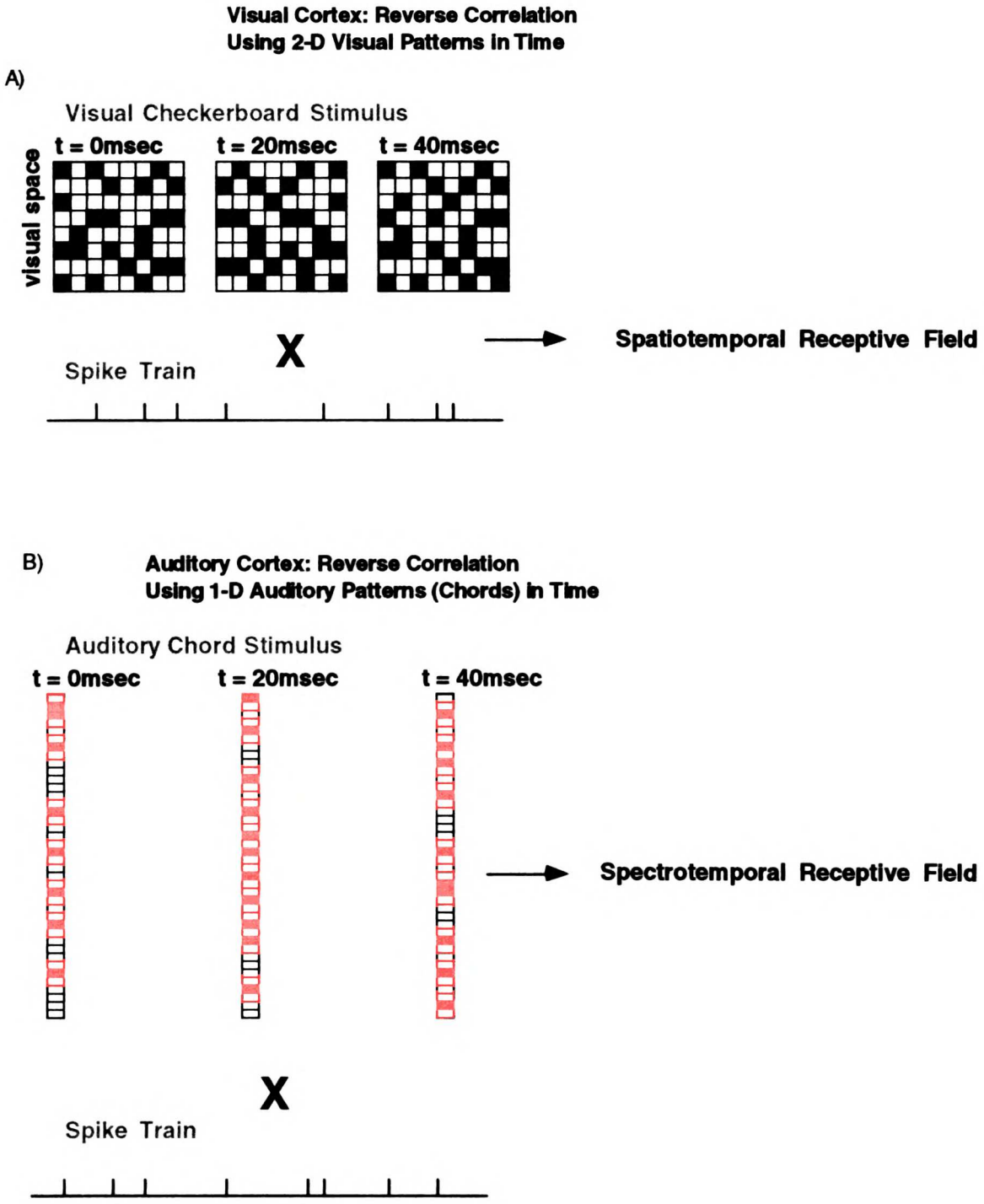

Figure 4.1: Schematic of stimuli used for reverse correlation in the visual and auditory systems.

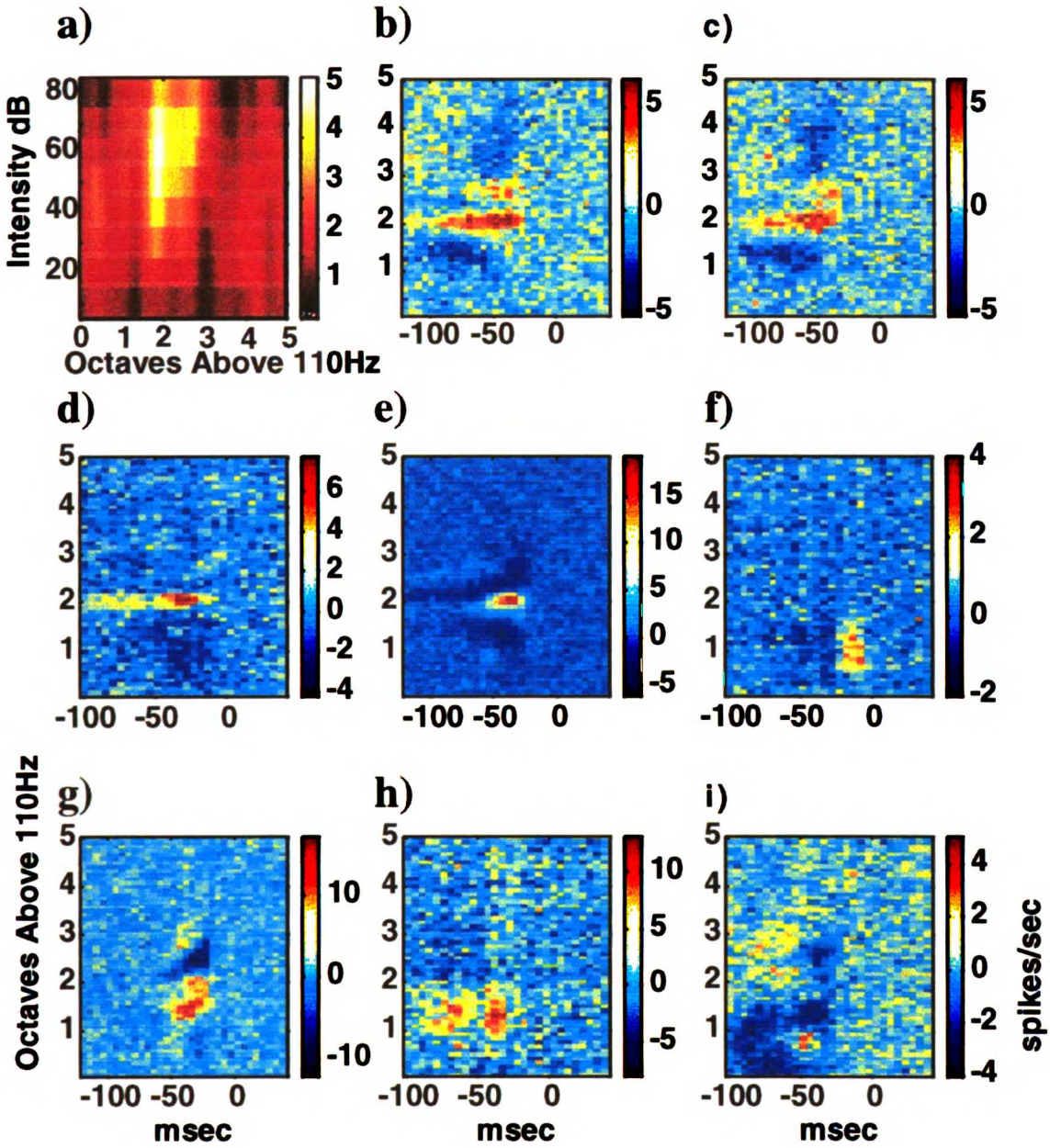

Figure 4.2: Spectrotemporal receptive fields of neurons in the primary auditory cortex of the awake primate show the pattern of sound features selected for by particular neurons. The tuning curve shown in *a* was computed by counting the number of spikes elicited from a single auditory cortex neuron by 100msec pure tone pips presented at 84 frequencies and 8 intensities, smoothed by 1 pixel. The spectrotemporal receptive field presented in *b* shows the full time/frequency structure of the same neuron's sound feature selectivity, its estimated optimal stimulus, including multiple excitatory and inhibitory regions, in units of mean spikes/second. For all spectrotemporal receptive fields, raw average data are presented with no smoothing. Spectrotemporal receptive fields shown in *b-i*, were computed as described in *methods*. The spectrotemporal receptive field shown in *c* was computed for the same neuron using a completely different stimulus set (in *b* the stimuli were made up of random chords with synchronous onset times for each component in the chord, in *c* all frequency components

presented at completely random and asynchronous times). Receptive fields in *a-g* are all from well isolated single neuron recordings. Receptive field structures correspond to the average rate of spikes from the neuron at time zero driven by each stimulus component frequency at the lag time shown (this is the standard peristimulus spike rate value triggered on each stimulus component). Formally equivalent, the spectrotemporal receptive field is also the average stimulus preceding each neuronal spike at time zero (an average of the stimulus components triggered on the spike occurrence). Therefore, scale bars shown (in spikes/stimulus) are directly proportional to the probability of occurrence of each stimulus component (in stimuli/spike).

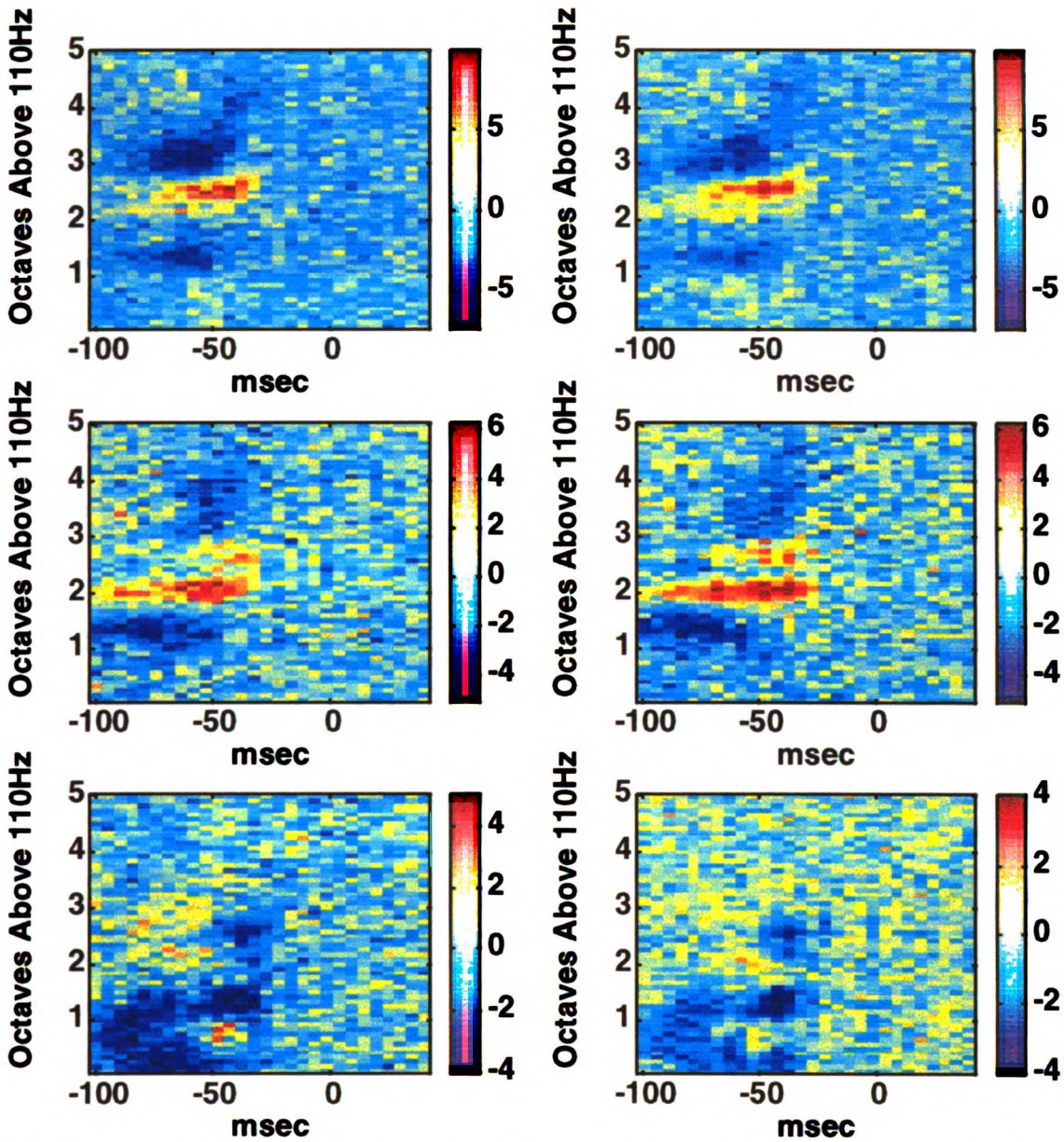

Figure 4.3. Correspondence of spectrotemporal receptive fields computed using different stimulus sets, and taken from separate time epochs. Responses in *a* show spectrotemporal receptive fields for neurons in the primary auditory cortex computed using chord-like stimuli, having stimulus onsets in each frequency channel randomly occur on fixed 20msec intervals. The spectrotemporal receptive fields presented in *b* show the full time/frequency structure of the same neurons' sound feature selectivity computed using a second stimulus set with asynchronous component onsets (see methods).

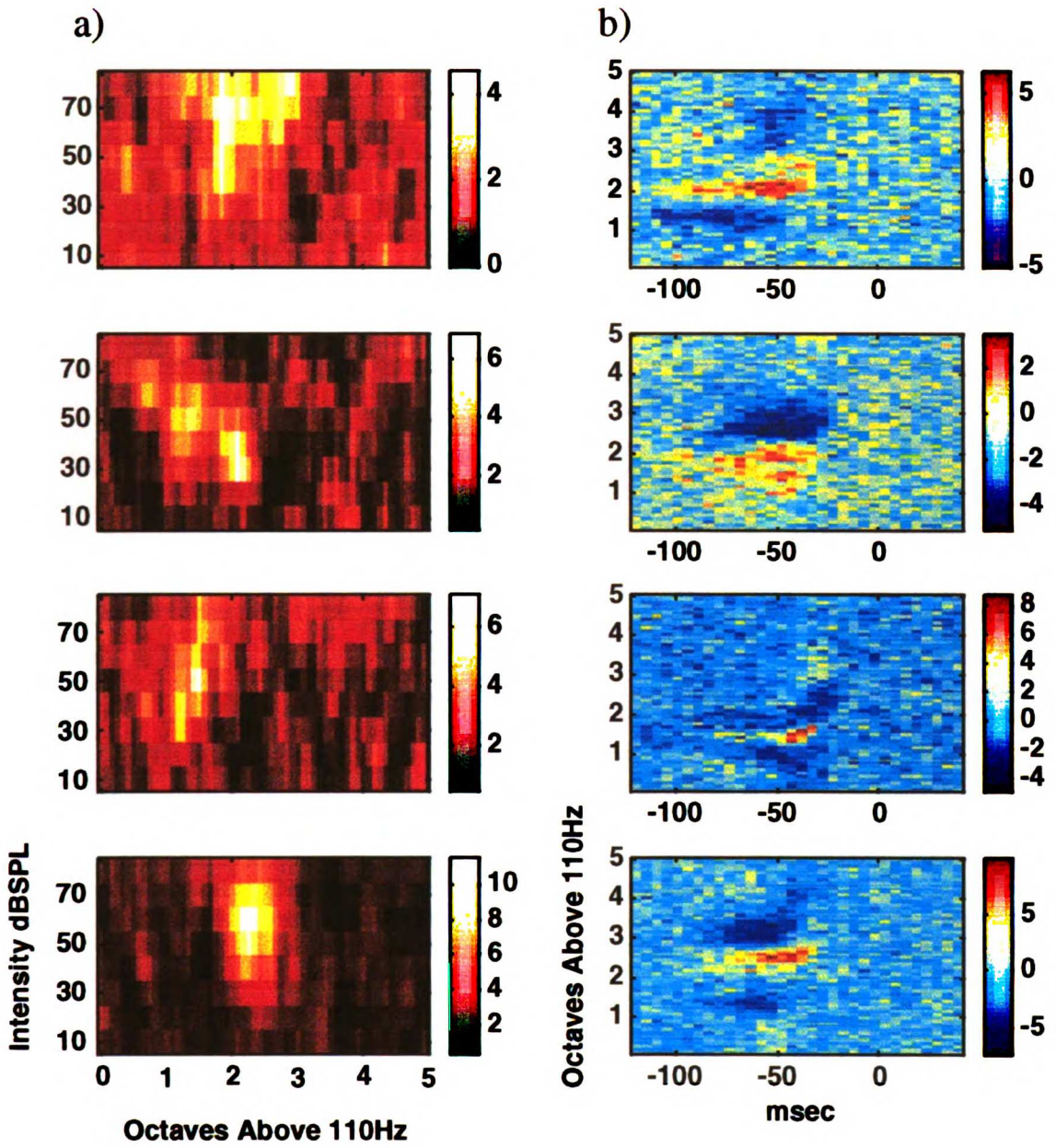

Figure 4.4. Comparison of traditional response areas with spectrotemporal receptive fields from four neurons in the awake primary auditory cortex. Tuning curves were computed by individually presenting stimuli at 84 frequencies and 8 intensities and counting the number of spikes evoked by each stimulus. Spectrotemporal receptive fields revealing the full spectral and temporal selectivity of these neurons were computed from an identical time period using noise stimuli (see methods).

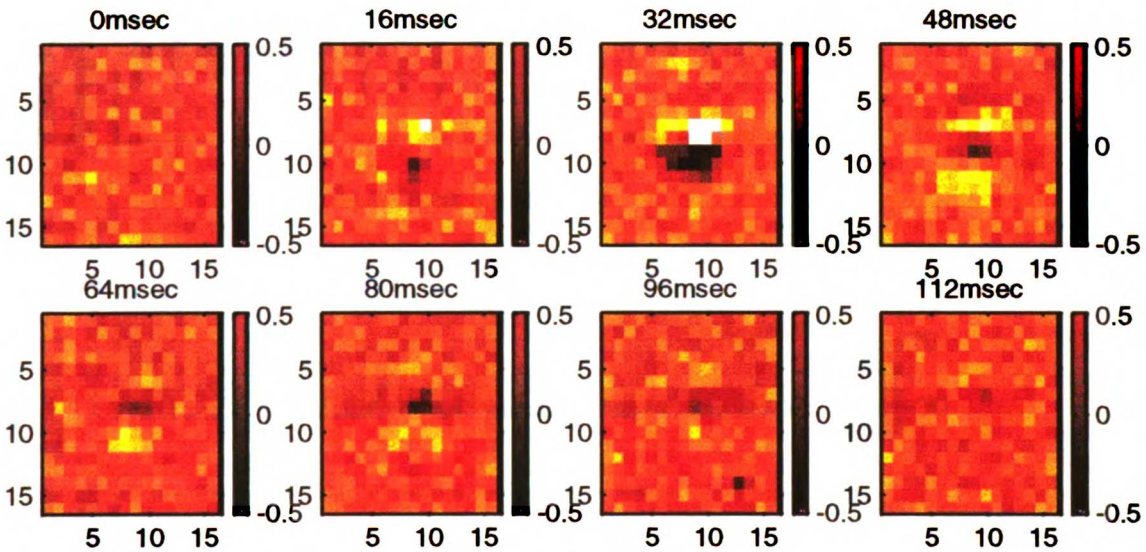

Figure 4.5. Example spatiotemporal receptive field of a neuron recording in the primary visual cortex of the anesthetized cat. Stimuli were black and white checkerboards presented at 62.5 Hz. This neurons receptive field covers approximately 2 degrees of arc, has similarly sized excitatory and inhibitory regions, and lasts approximately 60msec. (Data courtesy of Clay Reid, Jose-Manuel Alonso and Martin Usrey).

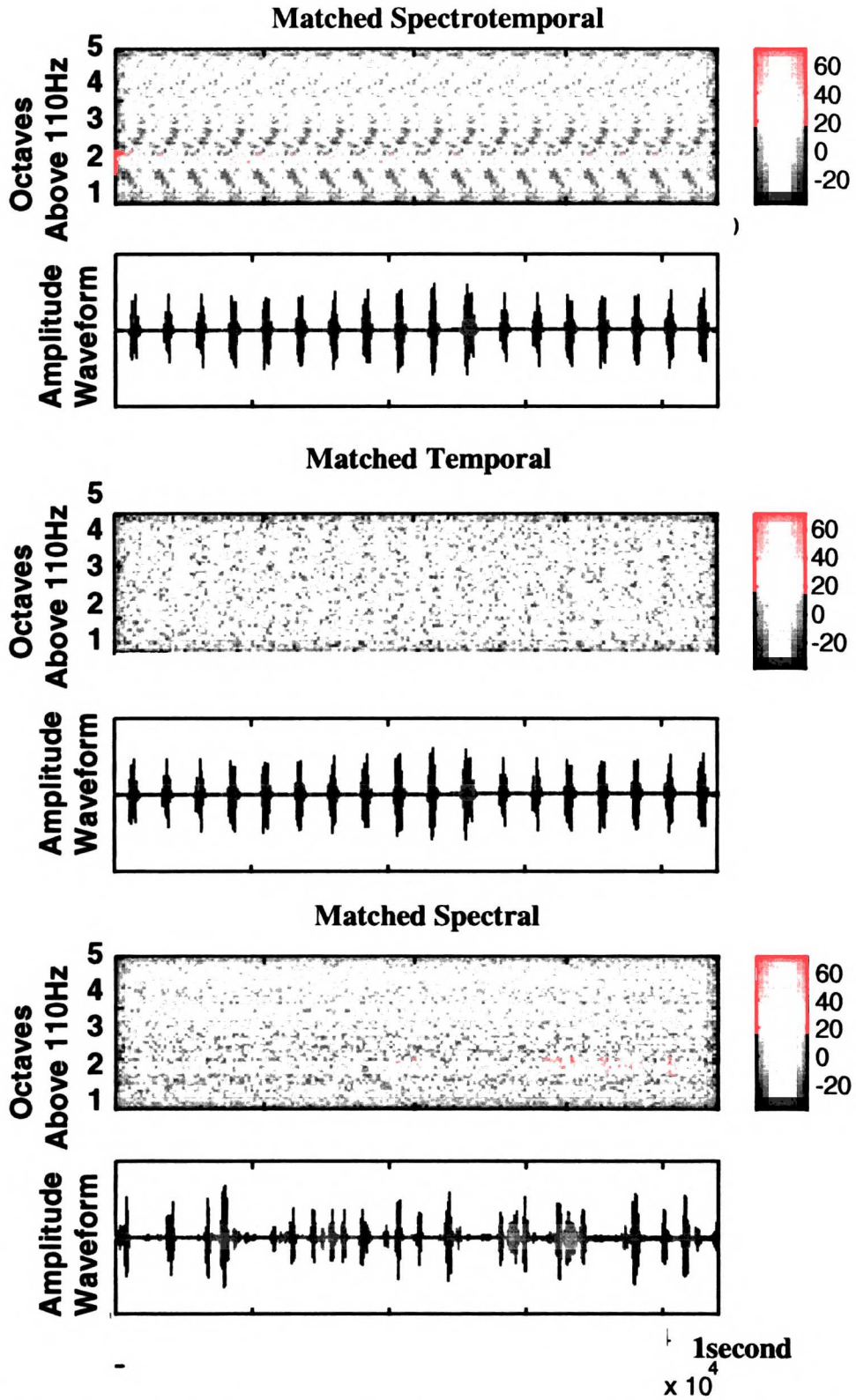

Figure 4.6. Creation of optimized stimuli matched to the spectrotemporal properties of individual neurons (see text).

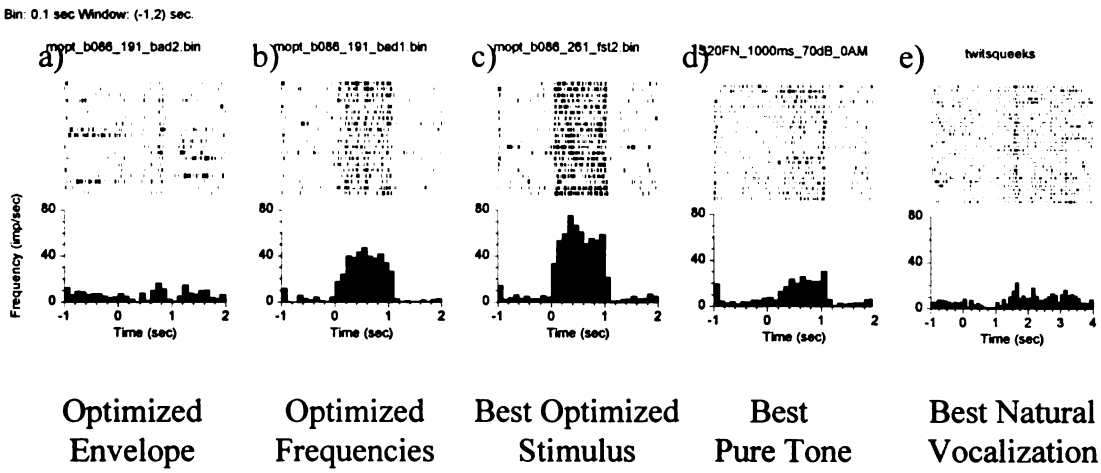

Figure 4.7. Responses of a single neuron in the primary auditory cortex of the awake primate to optimized and other stimuli. In each panel, the average response rate histogram in spikes per second is shown below rastergrams showing the individual action potentials elicited on each of twenty trials. The one second long stimulus presented in panel a was generated with a temporal enveloped matched to the cell's strf, panel b stimulus was matched to the excitatory and inhibitory spectral profile of the cell, panel c the was the best response to any of our selection of optimized stimuli, matching the spectral and temporal profile of the cell, panel d was the response to the best single tone from a selection of 20 pure tones near the unit's characteristic frequency, and panel e was the best response to a selection of 5 natural vocalizations made by the animal (note different timescale for e). Optimized stimuli were created by taking the average stimulus intensity at each 5msec time and frequency bin before an action potential (the STRF in units of stimulus intensity), convolving this intensity pattern with 5msec onset and offset ramps, multiplying each component by a sin wave component for its frequency channel, summing, and concatenating the stimulus to produce 1 second of total length. The alternate stimulus shown in a was computed by randomly shuffling frequency components within each time column, maintaining the overall envelope, and the stimulus shown in b was computed by randomly shuffling time components within each frequency row, maintaining the average spectral structure.

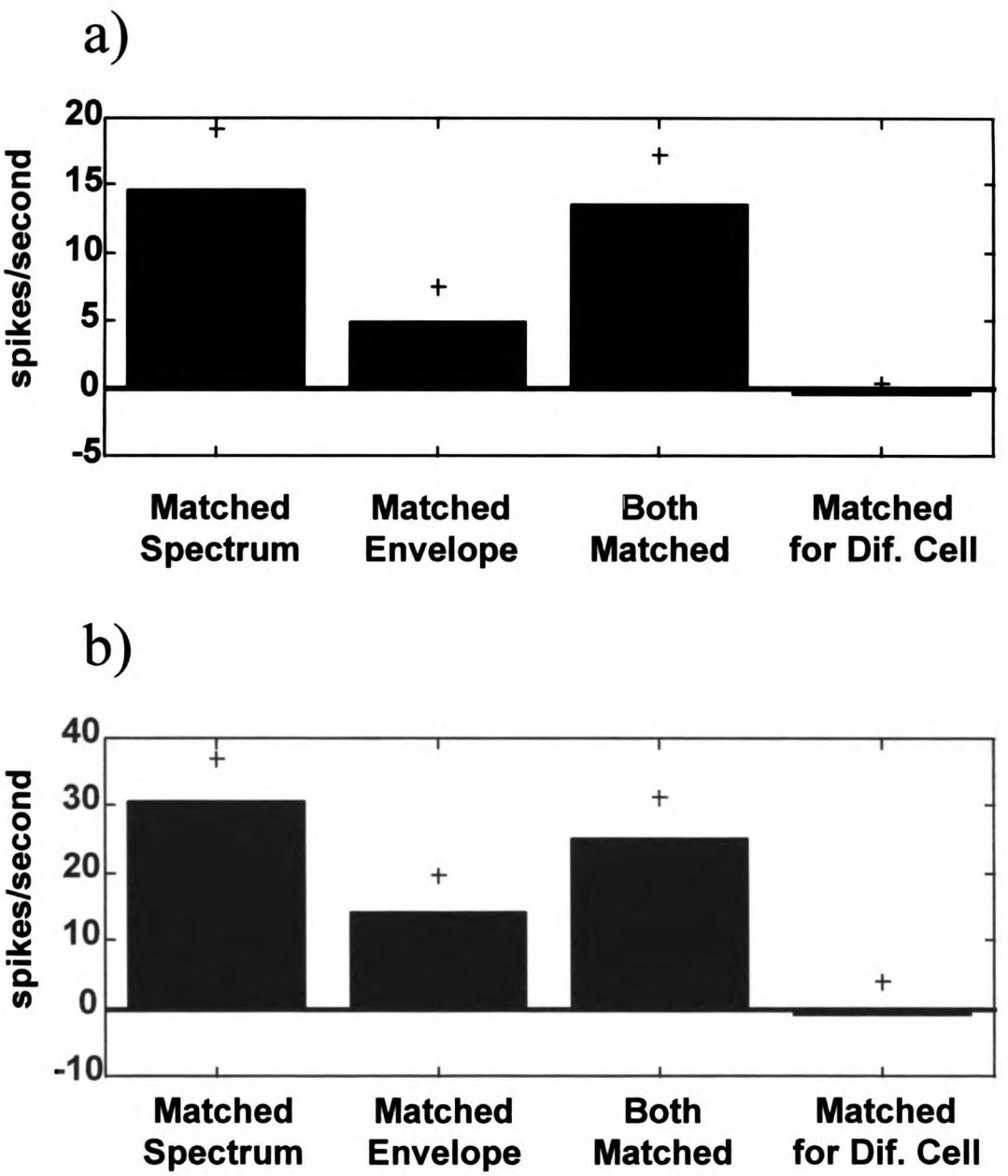

Figure 4.8. Mean responses to stimuli with matched spectrum, matched envelope, or matched spectral and temporal properties for the recorded cell, or a different cell. Responses shown in *a* are for single neuron recordings, and responses shown in *b* are for multiple neuron recordings.

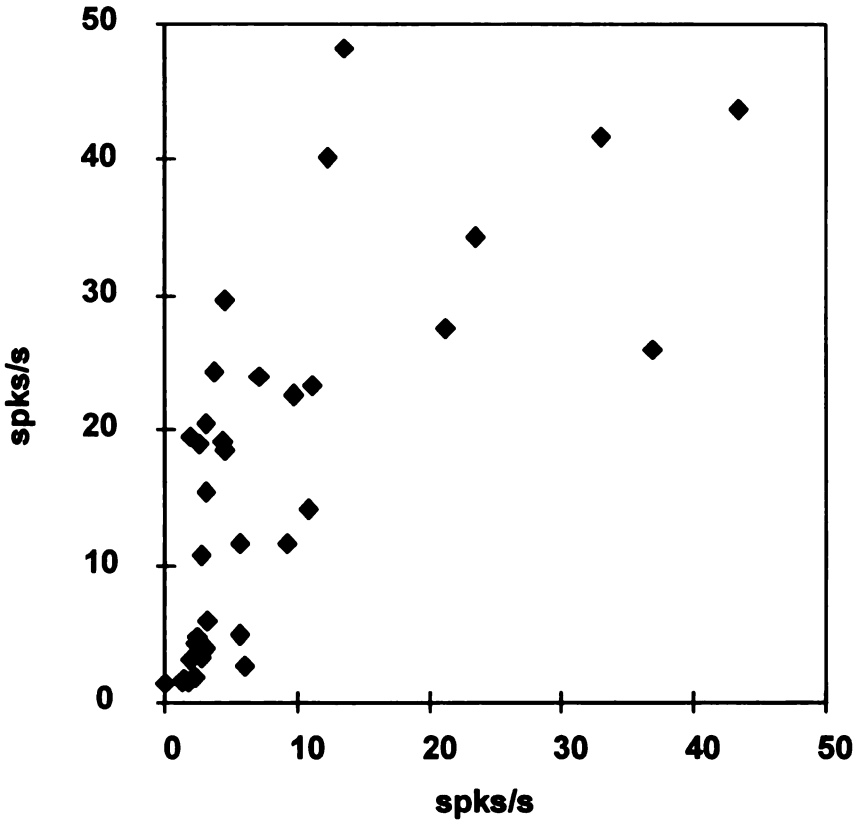

Figure 4.9. Distribution of responses of neurons to optimized stimuli vs. STRF excitatory volumes (in units of spikes/second). The mean firing rate response of each neuron is plotted vs. the sum of the statistically significant excitatory area of the STRF, divided by the total time of that area to give firing rate units.

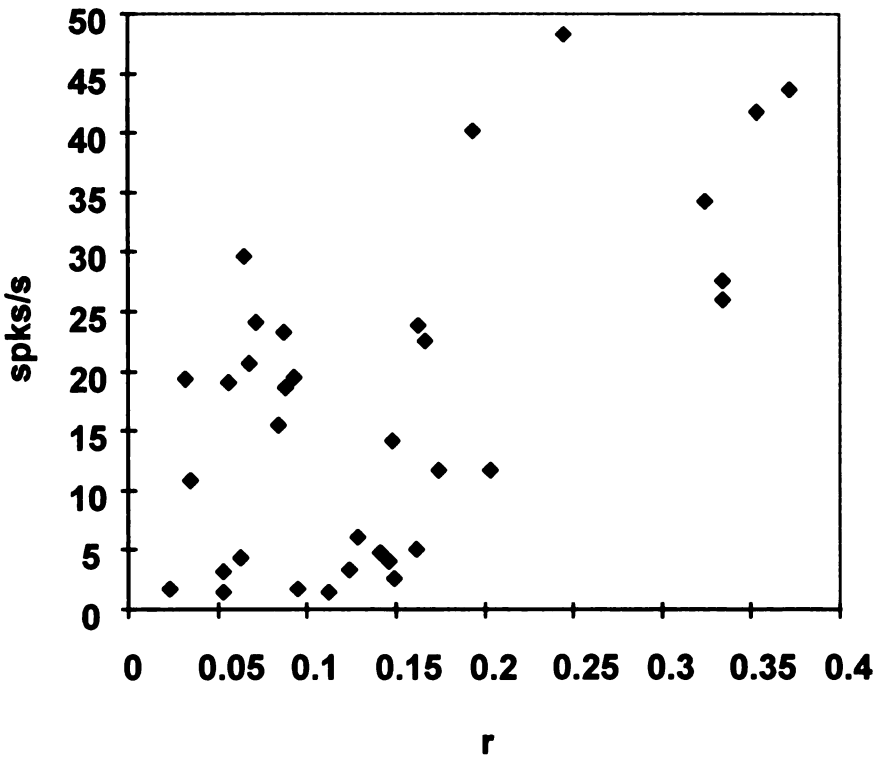

Figure 4.10. Distribution of responses of neurons to optimized stimuli vs. the 'linearity' of the neuron. Linearity was measured as the correlation coefficient between the observed responses during the noise stimuli and the fit to these responses based upon the STRF as a filter (see text).

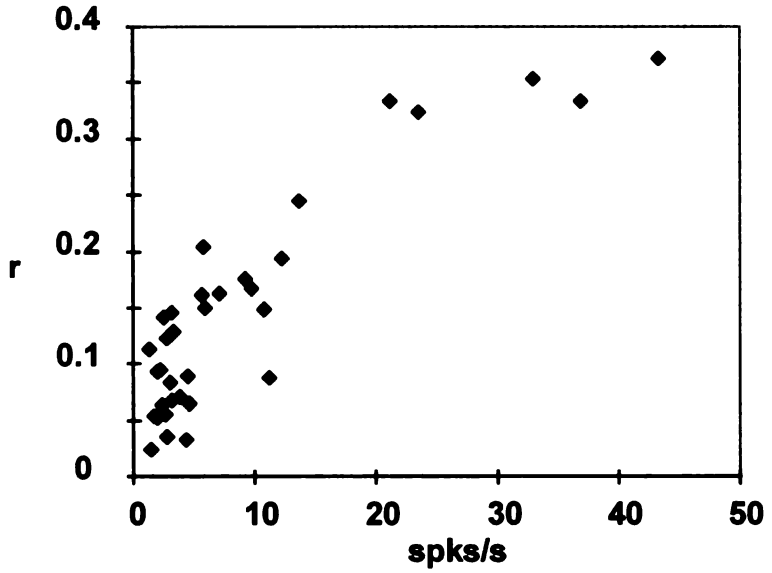

Figure 4.11. Relationship between STRF excitatory magnitude and the 'linearity' of neurons. Linearity was measured as the correlation coefficient between the observed responses during the noise stimuli and the fit to these responses based upon the STRF as a filter (see text), and the STRF volume is the sum of the statistically significant excitatory area of the STRF, divided by the total time of that area to give firing rate units

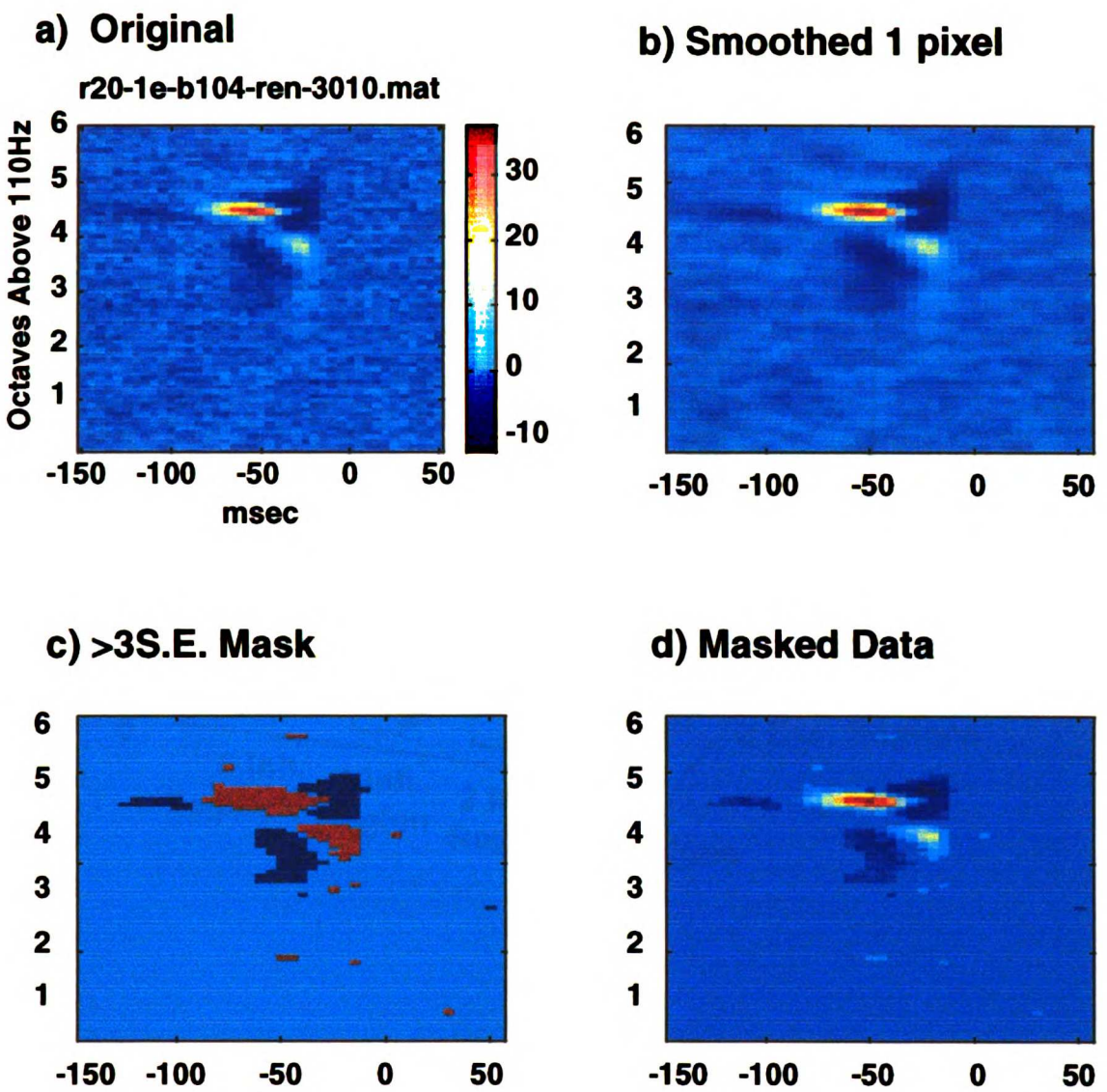

Figure 4.12. Method for computing spectrotemporal receptive field parameters (see *methods*).

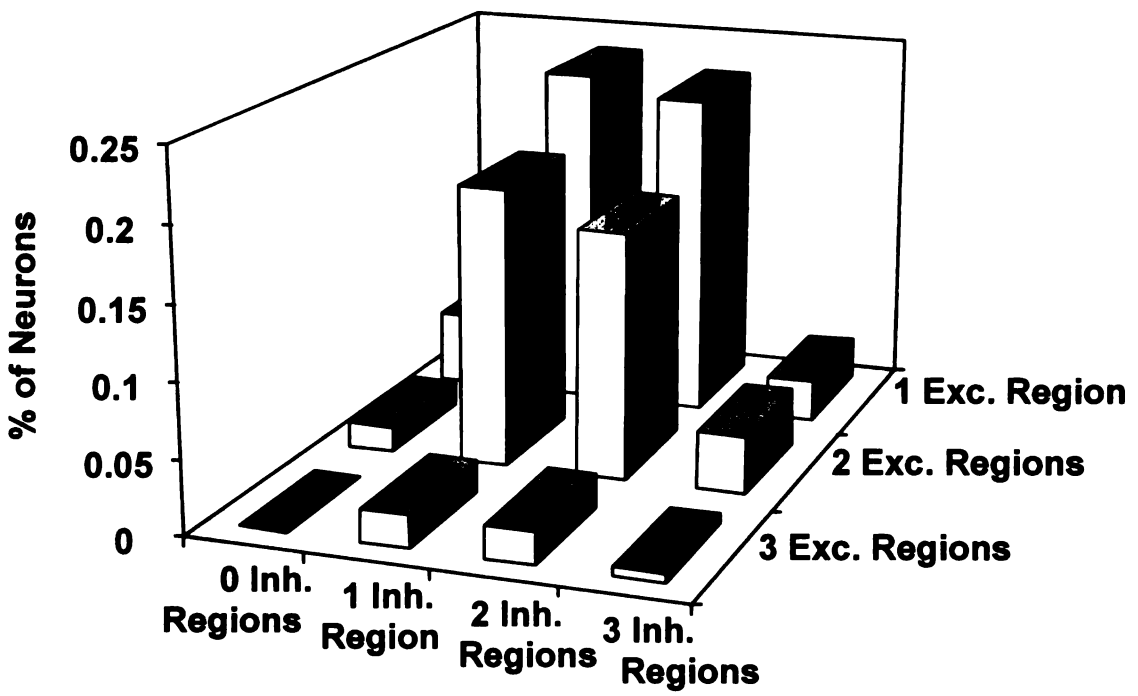

Figure 4.13. Number of sub-regions in response area of primary cortical neurons. The number of neurons recorded in each category is plotted against the configuration of the receptive field properties of the cells (number of excitatory and inhibitory sub-regions).

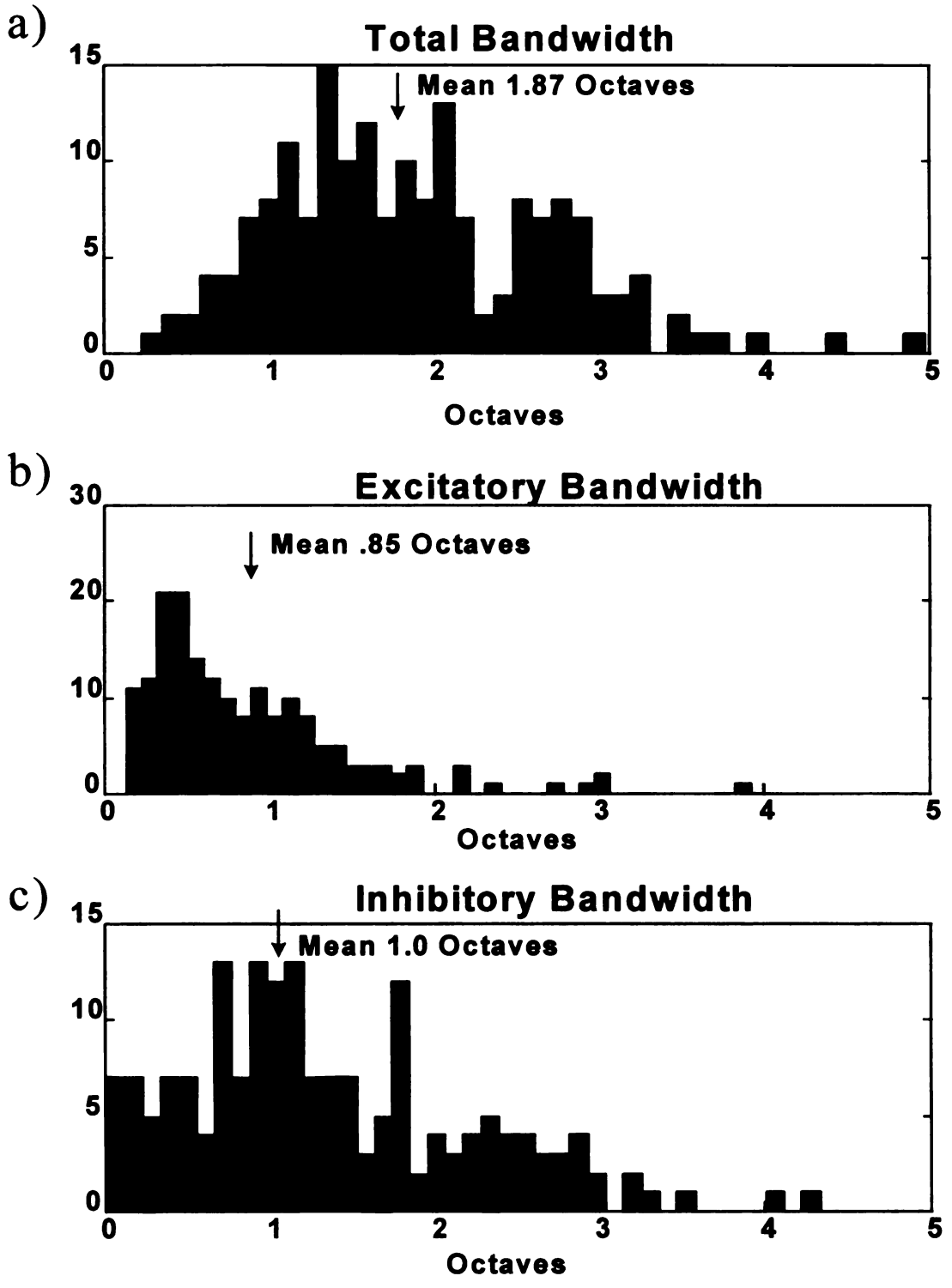

Figure 4.14. Distributions of response bandwidth of neurons in the primary auditory cortex. The distribution of total response bandwidths is shown in *a*, excitatory bandwidths are shown in *b*, and inhibitory bandwidths are shown in *c*.

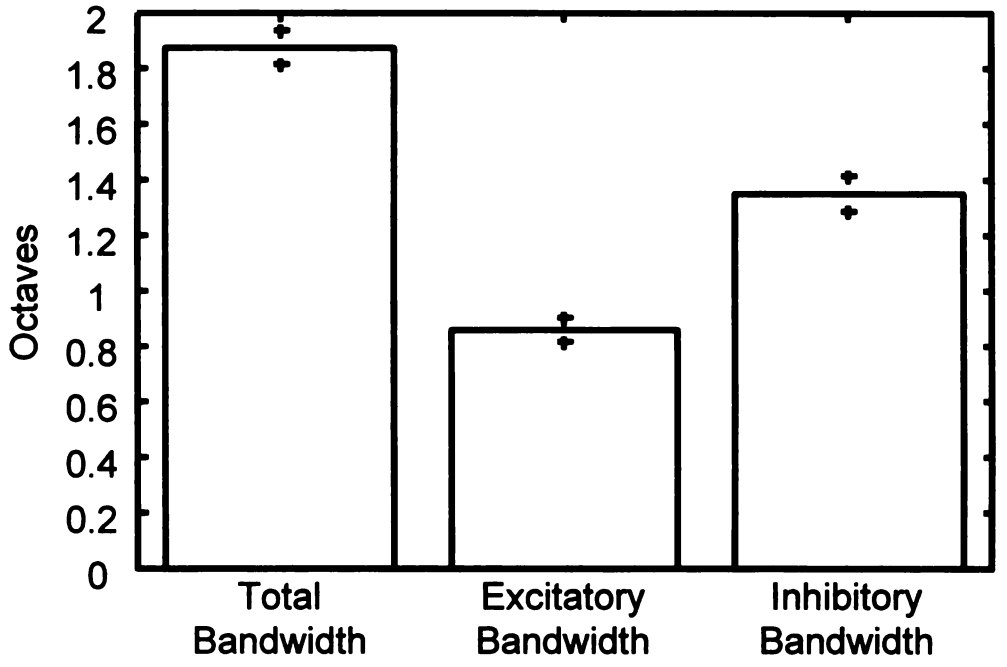

Figure 4.15. Comparison of excitatory, inhibitory, and total bandwidth of AI neurons (n=206). Means of population (n=206), and means +/- standard errors are shown.

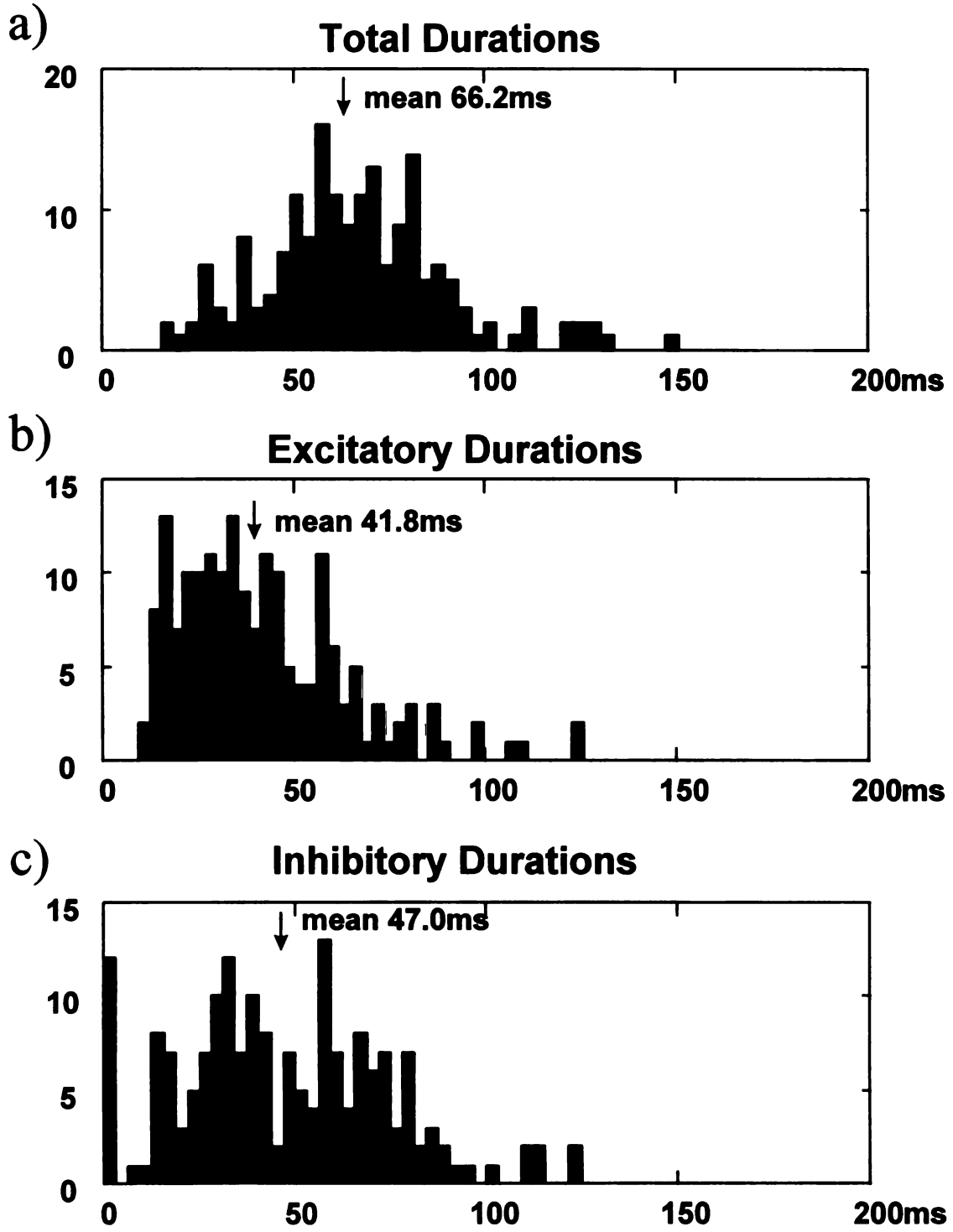

Figure 4.16. Distributions of response duration of neurons in the primary auditory cortex (n=206). The distribution of total response duration is shown in *a*, excitatory durations are shown in *b*, and inhibitory durations are shown in *c*.

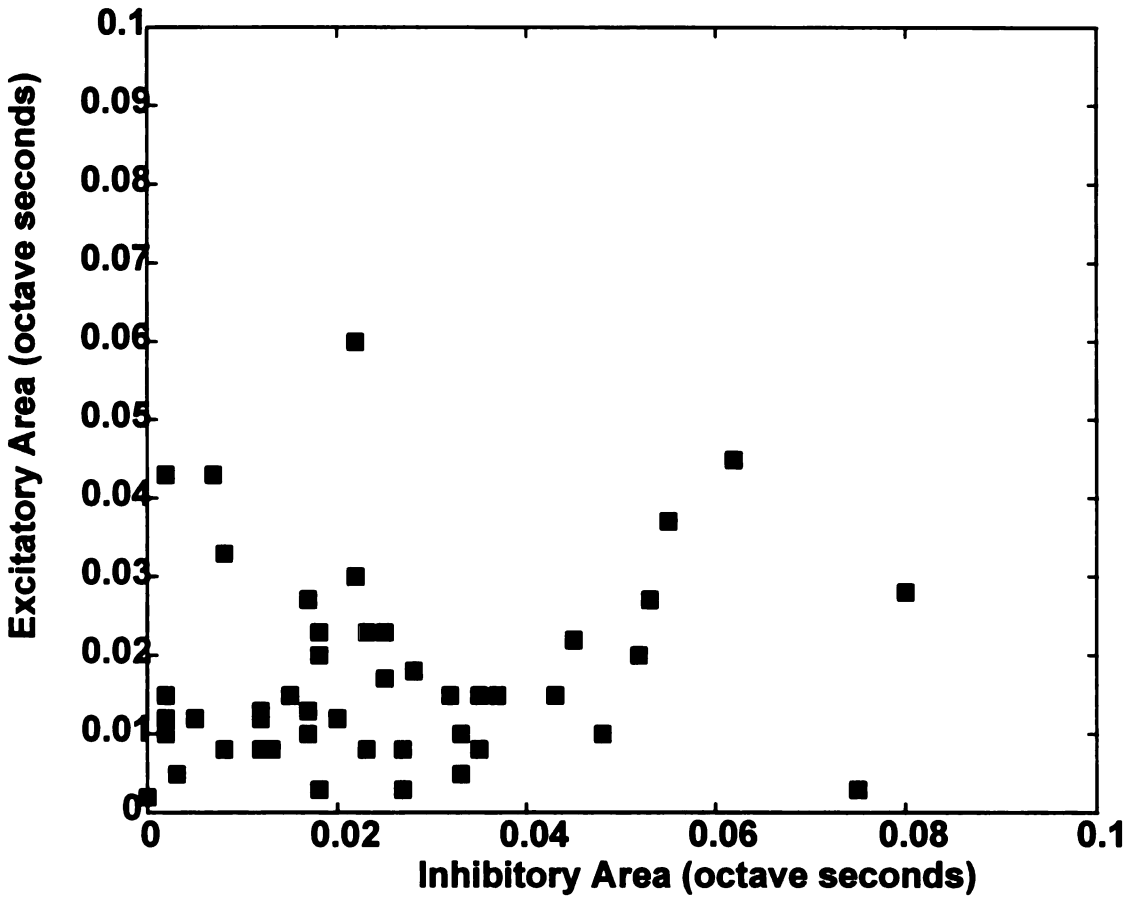

Figure 4.17. Excitatory and inhibitory response areas of the spectrotemporal receptive fields of AI neurons (n=54). The area of excitation is plotted against the area of inhibition for individual neurons studied.

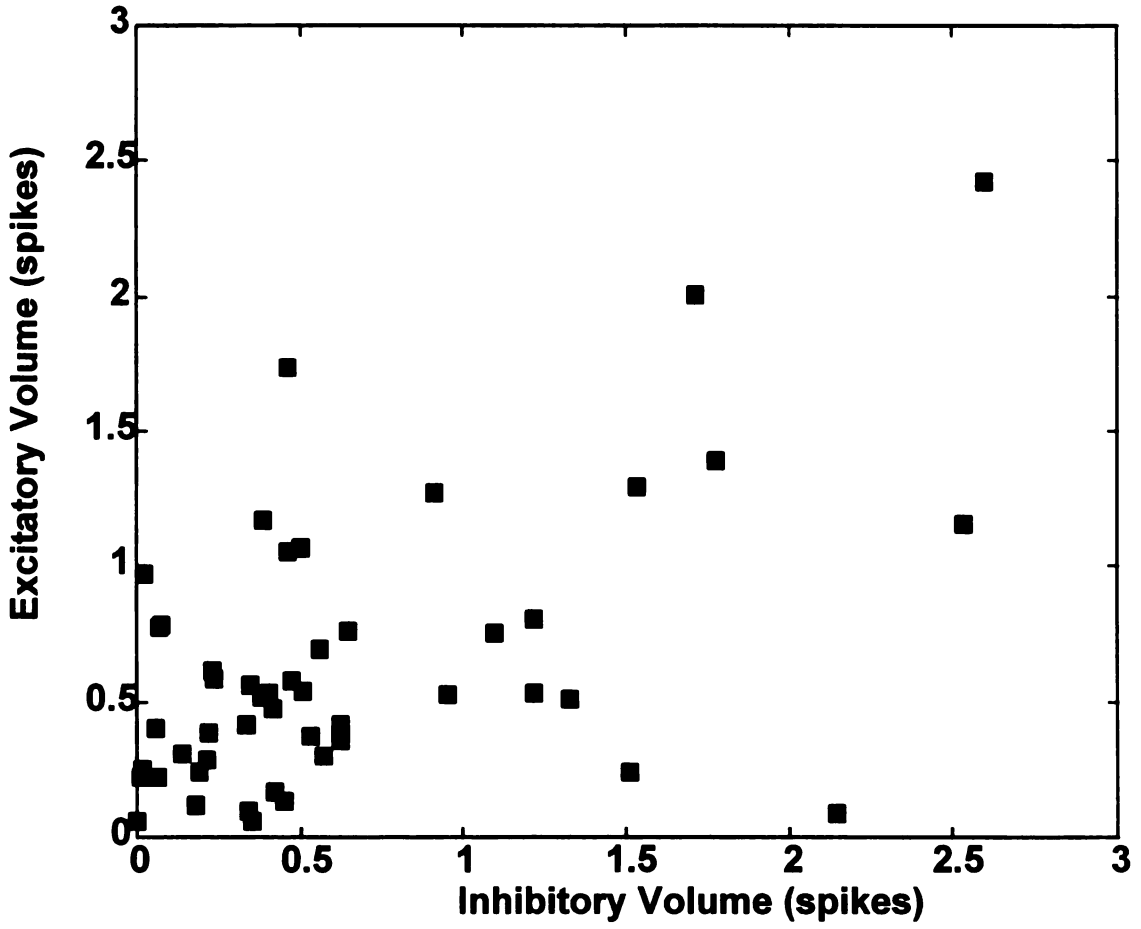

Figure 4.18. Excitatory and inhibitory volumes of receptive field sub-regions from spectrotemporal receptive fields of neurons in the primary auditory cortex (n=54). The volume of excitation is plotted against the volume of inhibition for individual neurons studied.

Chapter 5. Future Directions

Population Coding

As these data have made clear, sounds are represented in the primary auditory cortex by the activity of large populations of neurons; on the order of 10^6 neurons respond to any behaviorally meaningful acoustic stimulus. It is also clear that the activity from neurons within the densely interconnected cortical circuitry are not independent, so that recording from neurons individually, or analyzing data from neurons individually, is almost certainly missing fundamental aspects of cortical coding. One of the primary remaining challenges for understanding the cortical processing of stimuli in general is to discover the logic of how cortical populations function, and particularly how the timing of spikes within populations carries information and is decoded.

We have collected data from populations of neurons in the awake animal under psychophysical control, and these data will serve as a test bed for ideas about cortical population coding. Analyses will be carried out both using such standard measures and cross correlation and burst statistics, and also measures which capture the activity of larger populations of cells. Ultimately, all information in the cortical code is thought to be carried by the pattern of activity in the component neurons. By applying a non-linear pattern-recognition algorithm to this problem, (deSa, deCharms, & Merzenich, in press) we hope that we will be able to extract stochastic patterns from neural activity which are important in the representation of acoustic stimuli. Given the tremendous variability of neuronal responses, it appears very likely that relevant patterns of cortical activity would encompass many neurons and be inherently stochastic. Despite reports of very precise patterns over a small number of neurons, (Abeles, 1991; Abeles, Bergman, Gat, Meilijson, Seidemann, Tishby, & Vaadia, 1995; Abeles et al., 1993) the cortex very likely uses patterns of activity to represent stimuli in which the precise timing or number of spikes that any one neuron produces is less important than the overall structure of activity within the population. For this reason, the algorithm which we are developing searches for patterns that are stochastic in nature and can in principle involve large numbers of cells. Any single neuron need not

participate in a particular time epoch for an activity pattern across the population as a whole to be recognized. This work is still in its preliminary stages, but we hope that this approach will give us new insights into this challenging problem.

Pragmatic Applications

As a scientist, I see a tremendous importance in maintaining a focus on the ultimate utility of the scientific enterprise for society in general. In privately conducted work not directly related to this thesis I have performed experiments towards a number of pragmatic applications of this work that will be continued in the future. In particular, in work conducted outside of the laboratory and separately from my dissertation studies, I have developed working prototype methods for an auditory/visual localization prosthesis in people based upon bat echolocation, for the lessening or remediation of tinnitus based upon perceptual plasticity and remapping following training with appropriate stimuli, and for assaying and potentially altering the degree of awareness or attention of auditory percepts. Future work will continue to elucidate the extent to which any of these methods can be pragmatically applied on a wide scale.

Neural Correlates of Awareness

The understanding of the neural correlates of awareness has been hindered both by the lack of a clear operational definition of how awareness functions, as well as a lack of experiments searching for its neural correlates. It is my hypothesis that awareness has an essential biological and evolutionary function, which is to allow spontaneous intentional choice about how to act in any particular circumstance. I believe that this definition, in elaboration, can be fully operationalized in terms of cognitive and psychophysical performance and decision making, allowing a quantitative estimate of subjective awareness to be produced, and can also be expressed in neurophysiological terms, allowing a direct and quantitative correlation between the psychological phenomenon of awareness, measured psychophysically, and neuronal activity, measured neurophysiologically.

References

Abeles, M. (1991). *Corticonics : neural circuits of the cerebral cortex.* Cambridge ; New York: Cambridge University Press,.

Abeles, M., Bergman, H., Gat, I., Meilijson, I., Seidemann, E., Tishby, N., & Vaadia, E., "Cortical activity flips among quasi-stationary states," *Proc Natl Acad Sci U S A* **92**(1995): 8616-20.

Abeles, M., Bergman, H., Margalit, E., & Vaadia, E., "Spatiotemporal firing patterns in the frontal cortex of behaving monkeys," *J Neurophysiol* **70**(1993): 1629-38.

Abeles, M., & Goldstein, M. J., "Responses of single units in the primary auditory cortex of the cat to tones and to tone pairs," *Brain Res* **42**(1972): 337-52.

Adelson, E. H., & Bergen, J. R., "Spatiotemporal energy models for the perception of motion," *J. Opt. Soc. Am. A* **2**(1985): 284-299.

Allman, J. M., & Kaas, J. H., "Representation of the visual field in striate and adjoining cortex of the owl monkey (Aotus trivirgatus)," *Brain Res* **35**(1971): 89-106.

Alonso, J. M., Usrey, W. M., & Reid, R. C., "Precisely correlated firing in cells of the lateral geniculate nucleus," *Nature* **383**(1996): 815-9.

Bach, M., & Kruger, J., "Correlated neuronal variability in monkey visual cortex revealed by a multi-microelectrode," *Exp Brain Res* **61**(1986): 451-6.

Benson, D. A., & Hienz, R. D., "Single-unit activity in the auditory cortex of monkeys selectively attending left vs. right ear stimuli," *Brain Res.* **159**(1978): 307-320.

Bieser, A., & Muller-Preuss, P., "Auditory responsive cortex in the squirrel monkey: neural responses to amplitude-modulated sounds," *Exp Brain Res* **108**(1996): 273-84.

Brosch, M., & Schreiner, C. E., "Time course of forward masking tuning curves in cat primary auditory cortex," *J Neurophysiol* 77(1997): 923-43.

Brugge, & Merzenich, M. M., "Responses of neurons in auditory cortex of the macaque monkey to monaural and binaural stimulation," *J. Neurophysiol.* **36**(1973a): 1138-1158.

Brugge, J. F., "Patterns of organization in auditory cortex," *J. Acoust. Soc. Am.* **78**(1985): 353-359.

Brugge, J. F., Dubrovsky, N. A., Aitkin, L. M., & Anderson, D. J., "Sensitivity of single neurons in auditory cortex of cat to binaural tonal stimulation; effects of varying interaural time and intensity," *J Neurophysiol* **32**(1969): 1005-24.

Brugge, J. F., & Merzenich, M. M., "Responses of neurons in auditory cortex of the macaque monkey to monaural and binaural stimulation," *J Neurophysiol* **36**(1973b): 1138-58.

Buzsaki, G., Horvath, Z., Urioste, R., Hetke, J., & Wise, K., "High-frequency network oscillation in the hippocampus," *Science* **256**(1992): 1025-7.

Caan, W., "Recording from the auditory system in the awake monkey [proceedings]," *J Physiol (Lond)* **272**(1977): 87P-88P.

Calford, M. B., & Semple, M. N., "Monaural inhibition in cat auditory cortex," *J Neurophysiol* **73**(1995): 1876-91.

Colby, C. L., "The neuroanatomy and neurophysiology of attention," *J. Child Neurol.* **6, Supplement**(1991): S90-S118.

DeBoer, E., & deJongh, H. R., "On cochlear encoding: potentialities and limitations of the reverse correlation technique," *J Acoust Soc Am* **63**(1978): 115-135.

DeBoer, E., & Kuyper, P., "Triggered correlation," *IEEE Transact. Biomed Eng* **15**(1968): 169-179.

deCharms, R. C., & Merzenich, M. M., "Primary cortical representation of sounds by the coordination of action-potential timing," *Nature* **381**(1996a): 610-613.

deCharms, R. C., & Merzenich, M. M., "Primary cortical representation of sounds by the coordination of action-potential timing," *Nature* **381**(1996b): 610-3.

deSa, V. R., deCharms, R. C., & Merzenich, M. M., "Using Helmholtz machines to analyze multi-channel neuronal recordings," *Neural Information Processing Systems, 1997*(in press): .

Desimone, R., & Duncan, J., "Neural mechanisms of selective visual attention," *Annu Rev Neurosci* **18**(1995): 193-222.

Desimone, R., Wessinger, M., Thomas, L., & Schneider, W., "Attentional control of visual perception: cortical and subcortical mechanisms," *Cld. Spr. Hrbr. Symp. Quant. Biol.* **LV**(1990): 963-971.

Diamond, I. T., & Neff, W. D., "Ablation of temporal cortex and discrimination of auditory patterns," *J. Neurophysiol.* **20**(1957): 300-315.

Eggermont, J. J., "Rate and synchronization measures of periodicity coding in cat primary auditory cortex," *Hear Res* **56**(1991): 153-67.

Eggermont, J. J., "Differential effects of age on click-rate and amplitude modulation-frequency coding in primary auditory cortex of the cat," *Hear Res* **65**(1993): 175-92.

Eggermont, J. J., "Temporal modulation transfer functions for AM and FM stimuli in cat auditory cortex. Effects of carrier type, modulating waveform and intensity," *Hear Res* **74**(1994): 51-66.

Eggermont, J. J., Aertsen, A. M., & Johannesma, P. I., "Quantitative characterisation procedure for auditory neurons based on the spectro-temporal receptive field," *Hear Res* **10**(1983a): 167-90.

Eggermont, J. J., Johannesma, P. M., & Aertsen, A. M., "Reverse-correlation methods in auditory research," *Q Rev Biophys* **16**(1983b): 341-414.

Evans, E. F., Ross, H. F., & Whitfield, I. C., "The spatial distribution of unit characteristic frequency in the primary auditory cortex of the cat," *J Physiol (Lond)* **179**(1965): 238-47.

Farah, M. J., "Is visual imagery really visual? Overlooked evidence from neuropsychology," *Psychol Rev* **95**(1988): 307-17.

Farah, M. J., "Mechanisms of imagery-perception interaction," *J Exp Psychol [Hum Percept]* **15**(1989a): 203-11.

Farah, M. J., "The neural basis of mental imagery," *Trends Neurosci* **12**(1989b): 395-9.

Farah, M. J., Peronnet, F., Gonon, M. A., & Giard, M. H., "Electrophysiological evidence for a shared representational medium for visual images and visual percepts," *J Exp Psychol [Gen]* **117**(1988): 248-57.

Funkenstein, H. H., & Winter, P., "Responses to acoustic stimuli of units in the auditory cortex of awake squirrel monkeys," *Exp Brain Res* **18**(1973): 464-88.

Fuster, J. M., "Unit activity in prefrontal cortex during delayed-response performance: Neuronal correlates of transient memory," *J. Neurophysiol.* **36**(1973): 61-78.

Fuster, J. M., "Inferotemporal units in selective visual attention and short-term memory," *J Neurophysiol* **64**(1990): 681-97.

Glaser, E. M., "Cortical responses of awake cat to narrow-band FM noise stimuli," *J Acoust Soc Am* **50**(1971): 490-501.

Glass, I., & Wollberg, Z., "Lability in the responses of cells in the auditory cortex of squirrel monkeys to species-specific vocalizations," *Exp Brain Res* **34**(1979): 489-98.

Glass, I., & Wollberg, Z., "Auditory cortex responses to sequences of normal and reversed squirrel monkey vocalizations," *Brain Behav Evol* **22**(1983a): 13-21.

Glass, I., & Wollberg, Z., "Responses of cells in the auditory cortex of awake squirrel monkeys to normal and reversed species-specific vocalizations," *Hear Res* **9**(1983b): 27-33.

Goldberg, M. E., & Wurtz, R. H., "Activity of the superior colliculus in behaving monkey: II. The effect of attention on neuronal responses," *J. Neurophysiol.* **35**(1972): 560-574.

Gray, C. M., Maldonado, P. E., Wilson, M., & McNaughton, B., "Tetrodes markedly improve the reliability and yield of multiple single-unit isolation from multi-unit recordings in cat striate cortex," *J Neurosci Methods* **63**(1995): 43-54.

Haenny, P. E., Maunsell, J. H., & Schiller, P. H., "State dependent activity in monkey visual cortex. II. Retinal and extraretinal factors in V4," *Exp Brain Res* **69**(1988): 245-59.

Heffner, H. E., & Heffner, R. S., "Temporal lobe lesions and perception of species-specific vocalizations by macaques," *Science* **226**(1984): 75-6.

Heffner, H. E., & Heffner, R. S., "Effect of restricted cortical lesions on absolute thresholds and aphasia-like deficits in Japanese macaques," *Behav Neurosci* **103**(1989): 158-69.

Heil, P., "Auditory cortical onset responses revisited. I. First-spike timing," *J Neurophysiol* 77(1997a): 2616-41.

Heil, P., "Auditory cortical onset responses revisited. II. Response strength," *J Neurophysiol* 77(1997b): 2642-60.

Hermes, D. J., Aertsen, A. M., Johannesma, P. I., & Eggermont, J. J., "Spectro-temporal characteristics of single units in the auditory midbrain of the lightly anaesthetised grass frog (Rana temporaria L) investigated with noise stimuli," *Hear Res* **5**(1981): 147-78.

Hermes, D. J., Eggermont, J. J., Aertsen, A. M., & Johannesma, P. I., "Spectro-temporal characteristics of single units in the auditory midbrain of the lightly anaesthetised grass frog (Rana temporaria L.) investigated with tonal stimuli," *Hear Res* **6**(1982): 103-26.

Hocherman, S., Benson, D. A., Goldstein, J. M. H., Heffner, H. E., & Heinz, R. D., "Evoked unit activity in auditory cortex of monkeys performing a selective attention task," *Brain Res.* **117**(1976): 51-68.

Hsiao, S. S., DM, O. S., & Johnson, K. O., "Effects of selective attention on spatial form processing in monkey primary and secondary somatosensory cortex," *J Neurophysiol* **70**(1993): 444-7.

Hubel, D. H., Henson, C. O., Rupert, A., & Galambos, R., ""Attention" units in the auditory cortex," *Science* **129**(1959): 1279-1280.

Hubel, D. H., & Wiesel, T. N., "Receptive fields, binocular interaction and functional archtecture in the cat's visual cortex," *J. Physiol.* **160**(1962): 106-154.

Jenkins, W. M., & Masterton, R. B., "Sound localization: effects of unilateral lesions in central auditory system," *J Neurophysiol* **47**(1982): 987-1016.

Jenkins, W. M., & Merzenich, M. M., "Role of cat primary auditory cortex for sound-localization behavior," *J Neurophysiol* **52**(1984): 819-47.

Jones, J. P., & Palmer, L. A., "An evaluation of the two-dimensional Gabor filter model of simple receptive fields in cat striate cortex," *J Neurophysiol* **58**(1987a): 1233-58.

Jones, J. P., & Palmer, L. A., "The two-dimensional spatial structure of simple receptive fields in cat striate cortex," *J Neurophysiol* **58**(1987b): 1187-211.

Jones, J. P., Stepnoski, A., & Palmer, L. A., "The two-dimensional spectral structure of simple receptive fields in cat striate cortex," *J Neurophysiol* **58**(1987): 1212-32.

Jones, K. E., Campbell, P. K., & Normann, R. A., "A glass/silicon composite intracortical electrode array," *Ann Biomed Eng* **20**(1992): 423-37.

Kao, M. C., Poon, P. W., & Sun, X., "Modeling of the response of midbrain auditory neurons in the rat to their vocalization sounds based on FM sensitivities," *Biosystems* **40**(1997): 103-9.

Kim, P. J., & Young, E. D., "Comparative analysis of spectro-temporal receptive fields, reverse correlation functions, and frequency tuning curves of auditory-nerve fibers," *J Acoust Soc Am* **95**(1994): 410-22.

Kinchla, R. A., "Attention," *Annu Rev Psychol* **43**(1992): 711-42.

Knudsen, E. I., & Brainard, M. S., "Creating a unified representation of visual and auditory space in the brain," *Annu Rev Neurosci* **18**(1995): 19-43.

Konishi, M., "An outline of recent advances in birdsong neurobiology," *Brain Behav Evol* **44**(1994): 279-85.

Kowalski, N., Depireux, D. A., & Shamma, S. A., "Analysis of dynamic spectra in ferret primary auditory cortex. I. Characteristics of single-unit responses to moving ripple spectra," *J Neurophysiol* **76**(1996a): 3503-23.

Kowalski, N., Depireux, D. A., & Shamma, S. A., "Analysis of dynamic spectra in ferret primary auditory cortex. II. Prediction of unit responses to arbitrary dynamic spectra," *J Neurophysiol* **76**(1996b): 3524-34.

Kruger, J., & Bach, M., "Simultaneous recording with 30 microelectrodes in monkey visual cortex," *Exp Brain Res* **41**(1981): 191-4.

Lashley, K. S. (1960). *The neuropsychology of Lashley*. New York: McGraw-Hill.

Loeb, G. E., Peck, R. A., & Martyniuk, J., "Toward the ultimate metal microelectrode," *J Neurosci Methods* **63**(1995): 175-83.

Manley, J. A., & Muller-Preuss, P., "Response variability of auditory cortex cells in the squirrel monkey to constant acoustic stimuli," *Exp Brain Res* **32**(1978): 171-80.

Maunsell, J. H., & Van Essen, D. C., "Functional properties of neurons in middle temporal visual area of the macaque monkey. I. Selectivity for stimulus direction, speed, and orientation," *J Neurophysiol* **49**(1983): 1127-47.

McKenna, T. M., Ashe, J. H., & Weinberger, N. M., "Cholinergic modulation of frequency receptive fields in auditory cortex: I. Frequency-specific effects of muscarinic agonists," *Synapse* **4**(1989): 30-43.

McLean, J., & Palmer, L. A., "Contribution of linear spatiotemporal receptive field structure to velocity selectivity of simple cells in area 17 of cat," *Vision Res* **29**(1989): 675-9.

Mendelson, J., Schreiner, C. E., Grasse, K., & Sutter, M., "Spatial distribution of responses to FM sweeps in cat primary auditory cortex," *Assoc. Res. Otolaryngol. Abstr.* **11**(1988): 36.

Mendelson, J. R., & Cynader, M. S., "Sensitivity of cat primary auditory cortex (AI) neurons to the direction and rate of frequency modulation," *Brain Res.* **327**(1985): 331-335.

Mendelson, J. R., Schreiner, C. E., Sutter, M. L., & Grasse, K. (1992). Functional topography of cat primary auditory cortex: responses to frequency sweeps, *in press*.

Merzenich, M. M., Knight, P. L., & Roth, G. L., "Cochleotopic organization of primary auditory cortex in the cat," *Brain Res* **63**(1973): 343-6.

Middlebrooks, J. C., Clock, A. E., Xu, L., & Green, D. M., "A panoramic code for sound location by cortical neurons," *Science* **264**(1994): 842-4.

Miller, J. M., Dobie, R. A., Pfingst, B. E., & Hienz, R. D., "Electrophysiologic studies of the auditory cortex in the awake monkey," *Am. J. Otolaryng.* **1**(1980a): 119-129.

Miller, J. M., Dobie, R. A., Pfingst, B. E., & Hienz, R. D., "Electrophysiologic studies of the auditory cortex in the awake monkey," *Am J Otolaryngol* **1**(1980b): 119-30.

Miller, J. M., Sutton, D., Pfingst, B., Ryan, A., & Beaton, R., "Single cell activity in the auditory cortex of Rhesus monkeys: behavioral dependency," *Science* **177**(1972): 449-451.

Miyashita, Y., & Chang, H. S., "Neuronal correlate of pictorial short-term memory in the primate temporal cortex," *Nature* **331**(1988): 68-70.

Motter, B. C., "Focal attention produces spatially selective processing in visual cortical areas V1, V2, and V4 in the presence of competing stimuli," *J Neurophysiol* **70**(1993): 909-19.

Naatanen, R., "Implications of ERP data for psychological theories of attention," *Biol Psychol* **26**(1988): 117-63.

Najafi, K., & Hetke, J. F., "Strength characterization of silicon microprobes in neurophysiological tissues," *IEEE Trans Biomed Eng* **37**(1990): 474-81.

Najafi, K., Ji, J., & Wise, K. D., "Scaling limitations of silicon multichannel recording probes," *IEEE Trans Biomed Eng* **37**(1990): 1-11.

Nelken, I., Kim, P. J., & Young, E. D., "Linear and nonlinear spectral integration in type IV neurons of the dorsal cochlear nucleus. II. Predicting responses with the use of nonlinear models," *J Neurophysiol* **78**(1997): 800-11.

Nelken, I., Prut, Y., Vaadia, E., & Abeles, M., "In search of the best stimulus: an optimization procedure for finding efficient stimuli in the cat auditory cortex," *Hear Res* **72**(1994a): 237-53.

Nelken, I., Prut, Y., Vaadia, E., & Abeles, M., "Population responses to multifrequency sounds in the cat auditory cortex: one- and two-parameter families of sounds," *Hear Res* **72**(1994b): 206-22.

Nelken, I., Prut, Y., Vaddia, E., & Abeles, M., "Population responses to multifrequency sounds in the cat auditory cortex: four-tone complexes," *Hear Res* **72**(1994c): 223-36.

Nicolelis, M. A., Baccala, L. A., Lin, R. C., & Chapin, J. K., "Sensorimotor encoding by synchronous neural ensemble activity at multiple levels of the somatosensory system," *Science* **268**(1995): 1353-8.

Nicolelis, M. A., Ghazanfar, A. A., Faggin, B. M., Votaw, S., & Oliveira, L. M., "Reconstructing the engram: simultaneous, multisite, many single neuron recordings," *Neuron* **18**(1997): 529-37.

Nicolelis, M. A., Lin, R. C., Woodward, D. J., & Chapin, J. K., "Dynamic and distributed properties of many-neuron ensembles in the ventral posterior medial thalamus of awake rats," *Proc Natl Acad Sci U S A* **90**(1993): 2212-6.

Pelleg-Toiba, R., & Wollberg, Z., "Tuning properties of auditory cortex cells in the awake squirrel monkey," *Exp Brain Res* **74**(1989): 353-64.

Pelleg-Toiba, R., & Wollberg, Z., "Discrimination of communication calls in the squirrel monkey: "call detectors" or "cell ensembles"?," *J Basic Clin Physiol Pharmacol* **2**(1991): 257-72.

Perrett, D. I., Rolls, E. T., & Caan, W., "Visual neurons responsive to faces in the monkey temporal cortex," *Exp. Brain Res.* **47**(1982): 329-342.

Pfingst, B. E., & O'Connor, T. A., "Characteristics of neurons in auditory cortex of monkeys performing a simple auditory task," *J. Neurophys.* **45**(1981): 16-34.

Pfingst, B. E., TA, O. C., & Miller, J. M., "Response plasticity of neurons in auditory cortex of the rhesus monkey," *Exp Brain Res* **29**(1977a): 393-404.

Pfingst, B. E., TA, O. C., & Miller, J. M., "Single cell activity in the awake monkey cortex: intensity encoding," *Trans Am Acad Ophthalmol Otolaryngol* **84**(1977b): 217-22.

Phillips, D. P., "Temporal response features of cat auditory cortex neurons contributing to sensitivity to tones delivered in the presence of continuous noise," *Hear Res* **19**(1985): 253-68.

Phillips, D. P., & Cynader, M. S., "Some neural mechanisms in the cat's auditory cortex underlying sensitivity to combined tone and wide-spectrum noise stimuli," *Hear Res* **18**(1985): 87-102.

Phillips, D. P., & Hall, S. E., "Responses of single neurons in cat auditory cortex to time-varying stimuli: linear amplitude modulations," *Exp Brain Res* **67**(1987): 479-92.

Phillips, D. P., Hall, S. E., & Hollett, J. L., "Repetition rate and signal level effects on neuronal responses to brief tone pulses in cat auditory cortex," *J Acoust Soc Am* **85**(1989): 2537-49.

Phillips, D. P., Orman, S. S., Musicant, A. D., & Wilson, G. F., "Neurons in the cat's primary auditory cortex distinguished by their responses to tones and wide-spectrum noise," *Hear Res* **18**(1985): 73-86.

Phillips, D. P., Semple, M. N., Calford, M. B., & Kitzes, L. M., "Level-dependent representation of stimulus frequency in cat primary auditory cortex," *Exp Brain Res* **102**(1994): 210-26.

Posner, M. I., & Petersen, S. E., "The attention system of the human brain," *Annu Rev Neurosci* **13**(1990): 25-42.

Reid, R. C., & Alonso, J. M., "Specificity of monosynaptic connections from thalamus to visual cortex," *Nature* **378**(1995): 281-4.

Reid, R. C., & Shapley, R. M., "Spatial structure of cone inputs to receptive fields in primate lateral geniculate nucleus," *Nature* **356**(1992): 716-8.

Reid, R. C., Soodak, R. E., & Shapley, R. M., "Directional selectivity and spatiotemporal structure of receptive fields of simple cells in cat striate cortex," *J Neurophysiol* **66**(1991): 505-29.

Riquimaroux, H., Gaioni, S. J., & Suga, N., "Cortical computational maps control auditory perception," *Science* **251**(1991): 565-8.

Rousche, P. J., & Normann, R. A., "A method for pneumatically inserting an array of penetrating electrodes into cortical tissue," *Ann Biomed Eng* **20**(1992): 413-22.

Scharlock, D. P., Neff, W. D., & Strominger, N. L., "Discrimination of tone duration after bilateral ablation of cortical auditory areas," *J Neurophysiol.* **28**(1965): 673-681.

Schreiner, C. E., "Functional organization of the auditory cortex: maps and mechanisms," *Curr Opin Neurobiol* **2**(1992): 516-21.

Schreiner, C. E., & Calhoun, B. M., "Spectral envelope coding in cat primary auditory cortex: properties of ripple transfer functions," *Auditory Neuroscience* **1**(1994): 39-61.

Schreiner, C. E., & Langner, G. (1988). *Coding of Temporal Patterns in the Central Auditory Nervous System*. New York: J. Wiley.

Schreiner, C. E., & Mendelson, J. R., "Functional topography of cat primary auditory cortex: distribution of integrated excitation," *J Neurophysiol* **64**(1990): 1442-59.

Schreiner, C. E., & Urbas, J. V., "Representation of amplitude in the auditory cortex of the cat. II. Comparison between cortical fields.," *Hear. Res.* **32**(1988a): 49-64.

Schreiner, C. E., & Urbas, J. V., "Representation of amplitude modulation in the auditory cortex of the cat. II. Comparison between cortical fields," *Hear Res* **32**(1988b): 49-63.

Semple, M. N., & Kitzes, L. M., "Binaural processing of sound pressure level in cat primary auditory cortex: evidence for a representation based on absolute levels rather than interaural level differences," *J Neurophysiol* **69**(1993a): 449-61.

Semple, M. N., & Kitzes, L. M., "Focal selectivity for binaural sound pressure level in cat primary auditory cortex: two-way intensity network tuning," *J Neurophysiol* **69**(1993b): 462-73.

Shamma, S. A., & Symmes, D., "Patterns of inhibition in auditory cortical cells in awake squirrel monkeys," *Hear Res* **19**(1985): 1-13.

Shapley, R., & Lennie, P., "Spatial frequency analysis in the visual system," *Ann. Rev. Neurosci.* **8**(1985): 547-583.

Shepard, R. N., & Metzler, J., "Mental rotation of three-dimensional objects," *Science* **171**(1971): 701-703.

Steinschneider, M., Arezzo, J., & Vaughan, H. G., Jr., "Speech evoked activity in the auditory radiations and cortex of the awake monkey," *Brain Res* **252**(1982): 353-65.

Steinschneider, M., Arezzo, J. C., & Vaughan, H. G., Jr., "Tonotopic features of speech-evoked activity in primate auditory cortex," *Brain Res* **519**(1990): 158-68.

Steinschneider, M., Reser, D., Schroeder, C. E., & Arezzo, J. C., "Tonotopic organization of responses reflecting stop consonant place of articulation in primary auditory cortex (A1) of the monkey," *Brain Res* **674**(1995a): 147-52.

Steinschneider, M., Schroeder, C. E., Arezzo, J. C., & Vaughan, H. G., Jr., "Speech-evoked activity in primary auditory cortex: effects of voice onset time," *Electroencephalogr Clin Neurophysiol* **92**(1994): 30-43.

Steinschneider, M., Schroeder, C. E., Arezzo, J. C., & Vaughan, H. G., Jr., "Physiologic correlates of the voice onset time boundary in primary auditory cortex (A1) of the awake monkey: temporal response patterns," *Brain Lang* **48**(1995b): 326-40.

Suga, N. (1988). *Auditory neuroethology and speech processing: complex-sound processing by combination-sensitive neurons*. New York: J. Wiley.

Suga, N., "Philosophy and stimulus design for neuroethology of complex-sound processing," *Philos Trans R Soc Lond B Biol Sci* **336**(1992): 423-8.

Sutter, M. L., & Schreiner, C. E., "Physiology and topography of neurons with multipeaked tuning curves in cat primary auditory cortex," *J Neurophysiol* **65**(1991): 1207-26.

Sutter, M. L., & Schreiner, C. E., "Topography of intensity tuning in cat primary auditory cortex: single-neuron versus multiple-neuron recordings," *J Neurophysiol* **73**(1995): 190-204.

Swarbrick, L., & Whitfield, I. C., "Auditory cortical units selectively responsive to stimulus 'shape'," *J Physiol (Lond)* **224**(1972): 68P-69P.

Vaadia, E., & Abeles, M., "Temporal firing patterns of single units, pairs and triplets of units in the auditory cortex," *Isr J Med Sci* **23**(1987): 75-83.

Vaadia, E., Benson, D. A., Hienz, R. D., & Goldstein, M. H., Jr., "Unit study of monkey frontal cortex: active localization of auditory and of visual stimuli," *J Neurophysiol* **56**(1986a): 934-52.

Vaadia, E., Benson, D. A., Hienz, R. D., & Goldstein, M. J., "Unit study of monkey frontal cortex: active localization of auditory and of visual stimuli," *J Neurophysiol* **56**(1986b): 934-52.

Vaadia, E., Haalman, I., Abeles, M., Bergman, H., Prut, Y., Slovin, H., & Aertsen, A., "Dynamics of neuronal interactions in monkey cortex in relation to behavioural events," *Nature* **373**(1995): 515-8.

Wang, X., Merzenich, M. M., Beitel, R., & Schreiner, C. E., "Representation of a species-specific vocalization in the primary auditory cortex of the common marmoset: temporal and spectral characteristics," *J Neurophysiol* **74**(1995): 2685-706.

Whitfield, I. C., "Coding in the auditory nervous system," *Nature* **213**(1967): 756-60.

Whitfield, I. C., & Evans, E. F., "Responses of auditory cortical neurons to stimuli of changing frequency," *J. Neurophysiol.* **28**(1965): 655-672.

Wilson, M. A., & McNaughton, B. L., "Dynamics of the hippocampal ensemble code for space [see comments] [published erratum appears in Science 1994 Apr 1;264(5155):16]," *Science* **261**(1993): 1055-8.

Wilson, M. A., & McNaughton, B. L., "Reactivation of hippocampal ensemble memories during sleep [see comments]," *Science* **265**(1994): 676-9.

Winter, P., & Funkenstein, H. H., "The effect of species-specific vocalization on the discharge of auditory cortical cells in the awake squirrel monkey. (Saimiri sciureus)," *Exp Brain Res* **18**(1973): 489-504.

Wollberg, Z., & Newman, J. D., "Auditory cortex of squirrel monkey: response patterns of single cells to species-specific vocalizations," *Science* **175**(1972): 212-214.

Wurtz, R. H., & Mohler, C. W., "Enhancement of visual responses in monkey striate cortex and frontal eye fields," *J. Neurophysiol.* **39**(1976): 766-772.

Zeki, S., "The representation of colours in the cerebral cortex," *Nature* **284**(1980): 412-8.

Zeki, S. M., "Uniformity and diversity of structure and function in rhesus monkey prestriate visual cortex," *J Physiol (Lond)* **277**(1978): 273-90.

Zurita, P., Villa, A. E., de Ribaupierre, Y., de Ribaupierre, F., & Rouiller, E. M., "Changes of single unit activity in the cat's auditory thalamus and cortex associated to different anesthetic conditions," *Neurosci Res* **19**(1994): 303-16.